

THE EVALUATION OF MINIMA IN TOTAL NEUTRON CROSS-SECTION
BY TRANSMISSION OF FISSION SPECTRA THROUGH THICK SAMPLES

by 6791

WILLIAM HOWARD MILLER

B.S., Kansas State University, 1970

A MASTER'S THESIS

submitted in partial fulfillment of the
requirements for the degree

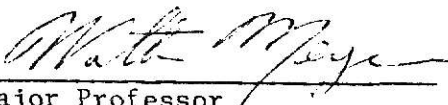
MASTER OF SCIENCE

Department of Nuclear Engineering

KANSAS STATE UNIVERSITY
Manhattan, Kansas

1971

Approved by:


Major Professor

LD
2668
T4
1971
M54
C.2

CONTENTS

1.0	Introduction	1
2.0	Theory	2
3.0	Experimental Facilities & Equipment	8
3.1	Neutron Source	8
3.2	Neutron Detection System	8
3.3	Multiparameter Analyzer	12
3.4	Sample Containers	12
3.5	Collimator and Shadow Shield	15
4.0	Experimental Procedure	17
4.1	Equipment Calibration	17
4.1.1	Calibration of the detection system	17
4.1.2	Maximum total flux at the detector	17
4.1.3	Integrated flux monitor	17
4.2	Neutron Spectrum Measurements	18
5.0	Data Analysis	23
5.1	Data Handling	23
5.2	Calculated Transmitted Spectra	23
5.3	System Resolution Analysis	23
6.0	Results	25
7.0	Conclusions	39
7.1	Detector Resolution	39
7.2	Energy Calibration	40
7.3	Consistency of Experimental Results	40
7.4	Forward Scattering Assumptions	40
7.5	Multiple Scattering Assumptions	45
7.6	Evaluation of Published Data	45

7.6.1	Iron	46
7.6.2	Lead	46
7.6.3	Oxygen	46
7.6.4	Sodium	46
8.0	Suggestions for Further Study	48
9.0	Acknowledgements	50
10.0	References	51
11.0	Appendices	53
Appendix A:	Computer Codes - CALFLUX	54
	NE213RES	74
	POLYFIT	80
Appendix B:	Derivations - Transmitted Flux Integral	86
	Gaussian Fitting Analysis	91
	Polynomial Fitting Analysis	97
Appendix C:	Sample Container Design - Liquid O ₂	100
	Liquid Sodium	103

1.0 INTRODUCTION

Total neutron cross-section data is available from many sources and reasonable agreement is found between independently determined cross-section tables. However, small discrepancies in the minima of integral cross-section data lead to large errors in transport calculations involving deep penetration. An error of a few percent in the cross-section data can approach an order of magnitude error in transmitted spectrum through a thick sample (ten or more mean free paths). To determine the reliability of literature data the neutron cross-section has been experimentally evaluated by measuring the uncollided neutron spectra transmitted through thick samples. Experimental data were compared to a calculated transmitted spectrum determined as a function of the spectrum, the resolution of the detector, and the particular cross-section data being tested. Since thick samples (three or more mean free paths) were used, the experimental versus calculated analysis is very sensitive to minima in the cross-section.

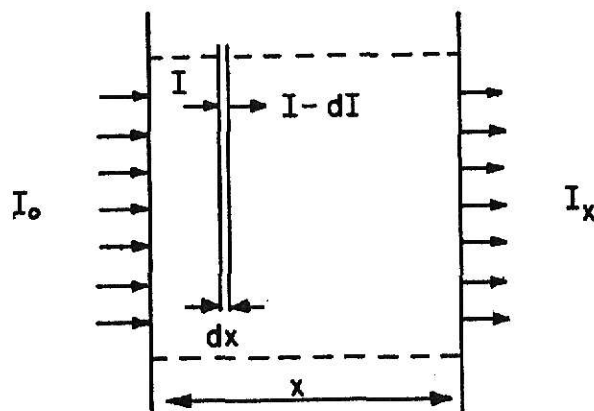
In this work, total neutron cross-sections were evaluated for iron, lead, liquid oxygen, solid sodium and liquid sodium. The incident neutron spectra for these measurements were obtained from the fast (northeast) beam port of the K.S.U. Triga Mark II reactor and the transmitted neutron spectra were detected with an NE-213 fast neutron spectrometer system. Data were collected with a TMC 4096 Multiparameter Analyzer and the results were unfolded with a suitable computer code.

**THIS BOOK
CONTAINS
NUMEROUS PAGES
WITH DIAGRAMS
THAT ARE CROOKED
COMPARED TO THE
REST OF THE
INFORMATION ON
THE PAGE.**

**THIS IS AS
RECEIVED FROM
CUSTOMER.**

2.0 THEORY

The theoretical basis for this experiment is similar to that applied in the transmission method⁹ of cross-section determination. A collimated beam of neutrons striking, perpendicularly, a specified area of a material of thickness x will be attenuated. Considering a thin layer of thickness dx parallel to the surface and recalling the definition of cross-section, it follows that $\Sigma_t dx$ is the fraction of neutrons that will interact with the material. This fraction may be set equal to $-dI/I$ which is the fractional decrease in the neutron beam as the result of passing through thickness dx .



Thus,

$$-\frac{dI}{I} = \Sigma_t dx \quad (1)$$

Integration over the thickness x of the material gives,

$$I_x = I_0 \exp(-\Sigma_t x) \quad (2)$$

where I_0 = number of incident neutrons/cm²

I_x = number of neutrons/cm² left at thickness x

Σ_t = total neutron cross-section

Recalling that this experiment dealt with neutron fluxes as a function of energy, equation 2 can be rewritten as:

$$\phi_{\text{trans}}(E) = \phi_I(E) \exp[-\Sigma_t(E)t] \quad (3)$$

where ϕ_I = incident flux($\text{n/cm}^2 \cdot \text{min} \cdot \text{MeV}$)

ϕ_{trans} = transmitted flux($\text{n/cm}^2 \cdot \text{min} \cdot \text{MeV}$)

Σ_t = total cross-section

The quantities ϕ and Σ_t are now functions of energy.

In this experiment very large thicknesses (three or more mean free paths) were used causing the argument of the exponential term in equation 3 to be large. Any variation in the total cross-section, Σ_t , would produce an exponential variation in the transmitted flux. This becomes especially apparent for minima in the cross-section. For a given material of thickness t and some mean cross-section $\bar{\Sigma}_t$, equation 3 becomes:

$$\phi_{\text{trans}}/\phi_I = \exp(-\bar{\Sigma}_t t) \quad (4)$$

Now, if there is a minima in the cross-section at some energy such that the cross-section is reduced by some fraction k ($k < 1$) of the mean value, then:

$$[\phi_{\text{trans}}/\phi_I]_{\text{minima}} = \exp[-(1-k)\bar{\Sigma}_t t] \quad (5)$$

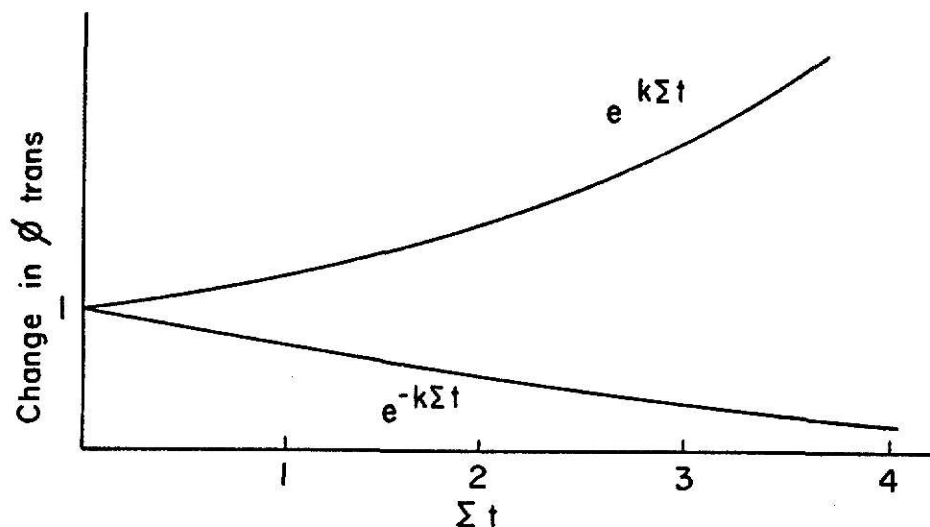
Likewise, for a maxima in the cross-section resulting in an increase in the cross-section by the same fraction k of the mean value, then:

$$[\phi_{\text{trans}}/\phi_I]_{\text{maxima}} = \exp[-(1+k)\bar{\Sigma}_t t] \quad (6)$$

The fractional change in the transmitted flux, obtained by dividing equation 5 and equation 6 by equation 4, is given by:

$$\begin{aligned}\text{fractional change for minima} &= \exp(k\bar{\Sigma}_t t) \\ \text{fractional change for maxima} &= \exp(-k\bar{\Sigma}_t t)\end{aligned}\tag{7}$$

These two functions are plotted in Fig. 2 and, as can be seen, the resultant change in the transmitted flux at a minima increases greatly for large thicknesses whereas the corresponding change in the transmitted flux at a maxima is small. Therefore, by using large thicknesses in the experiment, the sensitivity to minima becomes great. When the experimental results are compared to the corresponding calculated results, large errors in the transmitted spectrum will appear for small errors in the minima of total cross-section.



If a detection system with infinite resolution was used, the experimentally measured transmitted spectrum could be directly compared to the transmitted spectrum calculated by equation 3. However, the actual resolution of the spectrometer system must be included to "smooth" the calculated spectrum as the experimentally measured spectrum is "smoothed" by the measuring system. The transmitted spectrum can be calculated as:

$$\phi_{\text{trans}}(E) = \int_0^{\infty} \phi_I(E') \exp[-\Sigma_t(E')t] R(E, E') dE' \tag{8}$$

where $\phi_I(E')$ = incident flux at energy E'

Σ_t = total neutron cross-section at E'

$R(E, E')$ = probability of a neutron of energy E' being detected at energy E .

Based upon the unfolded responses of the detection system to mono-energetic neutrons, it can be seen that the resolution function $R(E, E')$ is of the form of a gaussian:

$$R(E, E') = y_o(E) \exp\left[-\frac{(E-E')^2}{b_o(E)}\right] \quad (9)$$

where $y_o = \frac{1}{\sqrt{b_o \pi}}$, which normalizes the function $R(E, E')$

such that $\int R(E, E') dE' = 1$

E = neutron energy detected

E' = actual neutron energy

$b_o = (\text{FWHM})^2 / 4 \cdot \ln(2)$, where FWHM is the full width at half maximum of the gaussian.

Experimental measurements^{1,23} have been made to determine $R(E, E')$ at several energies E . These measurements actually give the probability of neutrons of energy E being detected at E' , but since the detection system cannot discriminate between neutrons of energy E and E' (within the probability given by this function) it is assumed that neutrons of E' have an equal probability of being detected at E .

If it is assumed that $\phi_I(E')$ and $\Sigma_t(E')$ have values at discrete energy points E_i , then the integral of equation 8 can be integrated piecewise from E_i to E_{i+1} , from E_{i+1} to E_{i+2} , etc. If it is also assumed that the $\log(\phi_I)$ is linear between energy points and that $\Sigma_t(E')$ is linear between energy points, then equation 8 can be integrated into the exact form:

$$\phi_{\text{trans}}(E) = \sum_{i=1}^{\infty} \left\{ \left\{ \frac{1}{2} \exp \left[\frac{b_o}{4} \left(\frac{\Sigma_{i+1} - \Sigma_i}{E_{i+1} - E_i} \right)^2 + \left(\frac{\Sigma_{i+1} - \Sigma_i}{E_{i+1} - E_i} \right) (E_i - E) - \Sigma_i \right] \right\} \cdot \right. \\ \left. \left\{ \phi_I^i [\text{erf}(y_{i+1}) - \text{erf}(y_i)] + [\text{erf}(z_{i+1}) - \text{erf}(z_i)] \exp \left[\left(\frac{\ln \phi_I^{i+1} - \ln \phi_I^i}{E_{i+1} - E_i} \right) \right. \right. \right. \\ \left. \left. \left(E - E_i - \frac{b_o}{2} \left(\frac{\Sigma_{i+1} - \Sigma_i}{E_{i+1} - E_i} \right) \right) - \frac{b_o}{4} \left(\frac{\ln \phi_I^{i+1} - \ln \phi_I^i}{E_{i+1} - E_i} \right)^2 \right] \right\} \right\} \quad (10)$$

where ϕ_I^i = the incident flux at E_i

Σ_i = cross-section at E_i

$$y_i = \frac{1}{\sqrt{b_o}} \left| E_i - E + \frac{b_o}{2} \left(\frac{\Sigma_{i+1} - \Sigma_i}{E_{i+1} - E_i} \right) \right|$$

$$z_i = \frac{1}{\sqrt{b_o}} \left| E_i - E + \frac{b_o}{2} \left(\frac{\Sigma_{i+1} - \Sigma_i}{E_{i+1} - E_i} \right) - \frac{b_o}{2} \left(\frac{\ln \phi_I^{i+1} - \ln \phi_I^i}{E_{i+1} - E_i} \right) \right|$$

The experiment was performed using several different experimental geometries. For the first condition the detector was placed as far from the beam port as possible (approximately 128 inches). In this case it was assumed that any interaction of a neutron with the sample would either result in absorption or in scattering at an angle larger than the solid angle subtended by the detector. If this assumption is true, only those neutrons that are uncollided will be detected resulting in a true measure of the total cross-section. However, two phenomenon can occur which will cause an error in this measurement. If there is a large probability for forward scattering in the sample, it is possible that neutrons scattering at small angles will reach the detector. To reduce this error a collimator was used directly in front of the detector to reduce its effective area. Thus, those neutrons scattered at shallow angles (solid angles greater than 7.5×10^{-4} steradians) were removed by the collimator. Neutrons scattered

at 0° to the solid angle subtended between sample and detector could be present. Finally, there is a probability that neutrons will be scattered several times in a thick sample and some of these will be scattered back into the solid angle subtended by the detector. In this case, the end of the sample nearest the detector will be fully "illuminated" with neutrons, some of which will be scattered toward the detector. To study this effect, the collimator was placed against the sample, with the detector in the same position as before. With this latter geometry the area of the end of the sample viewed by the detector was smaller than that viewed with the collimator positioned next to the detector and thus a smaller number of multiple scattered neutrons would be expected to be detected.

3.0 EXPERIMENTAL FACILITIES AND EQUIPMENT

3.1 Neutron Source

The northeast fast beam port ("C") of the 250 kW K.S.U. Triga Mark II reactor was used as the source of fast neutrons. This radial beam port is aligned with a cylindrical void in the core reflector graphite as shown in Fig. 3, and is nominally 8 inches in diameter at the reactor face. It is fitted with a lead and borated paraffin 1-1/4 inch square collimator (Fig. 4). The neutron beam from this beam port diverges slightly to approximately five inches by five inches at the reactor bay wall 146 inches from the face of the beam port and is well defined even at this distance.¹⁶ Since there is little material in the path of neutrons coming from the core, the spectrum is essentially a fission spectrum with sufficient neutrons for experimental measurement up to 12 MeV. A 2 inch long bismuth plug inserted in the end of the collimator reduces the gamma background while leaving the neutron spectrum essentially unaffected.

3.2 Neutron Detection System

Neutrons were detected with a proton recoil NE-213 liquid scintillator spectrometer. Fast neutrons produce both neutron-hydrogen and neutron-carbon interactions which are subsequently detected and amplified by a photomultiplier tube. Unfortunately NE-213 responses are not limited to neutron interactions; gamma rays produce electrons in the scintillator which are also detected and amplified. It is possible, however, to electronically distinguish between pulses caused by neutron and gamma ray interactions.

The K.S.U. NE-213 detector and tube base Forte gamma ray discrimination circuit²³ are shown in Fig. 5. The pulse shape discrimination (PSD) output from the Forte circuit is a timing pulse which makes it possible to eliminate the gamma ray pulses. After additional pulse shaping this pulse

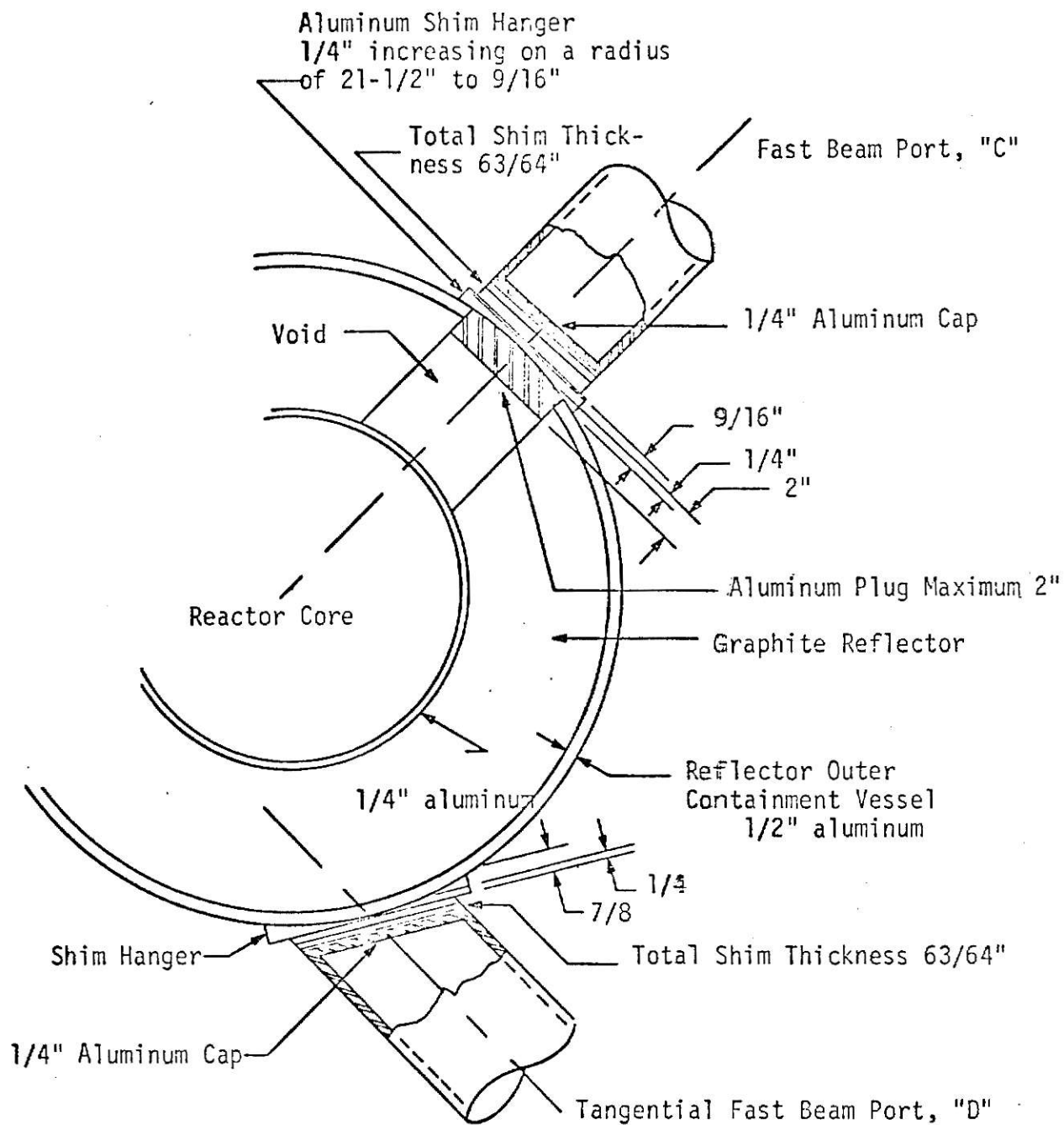


Figure 3 KSU TRIGA reactor core, reflector and beam port assembly.

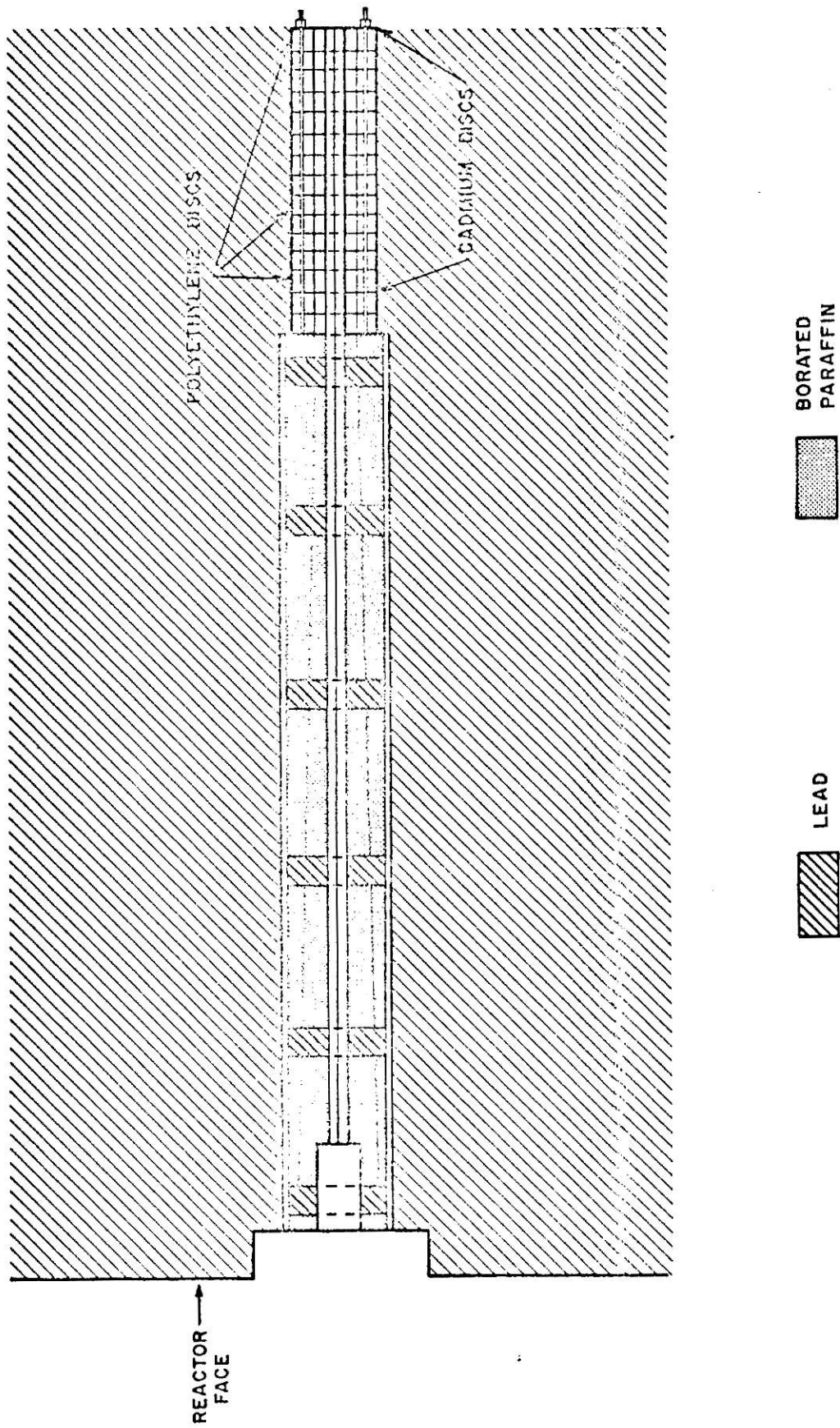


Figure 4 Internal construction of KSU TRIGA beam port collimator.

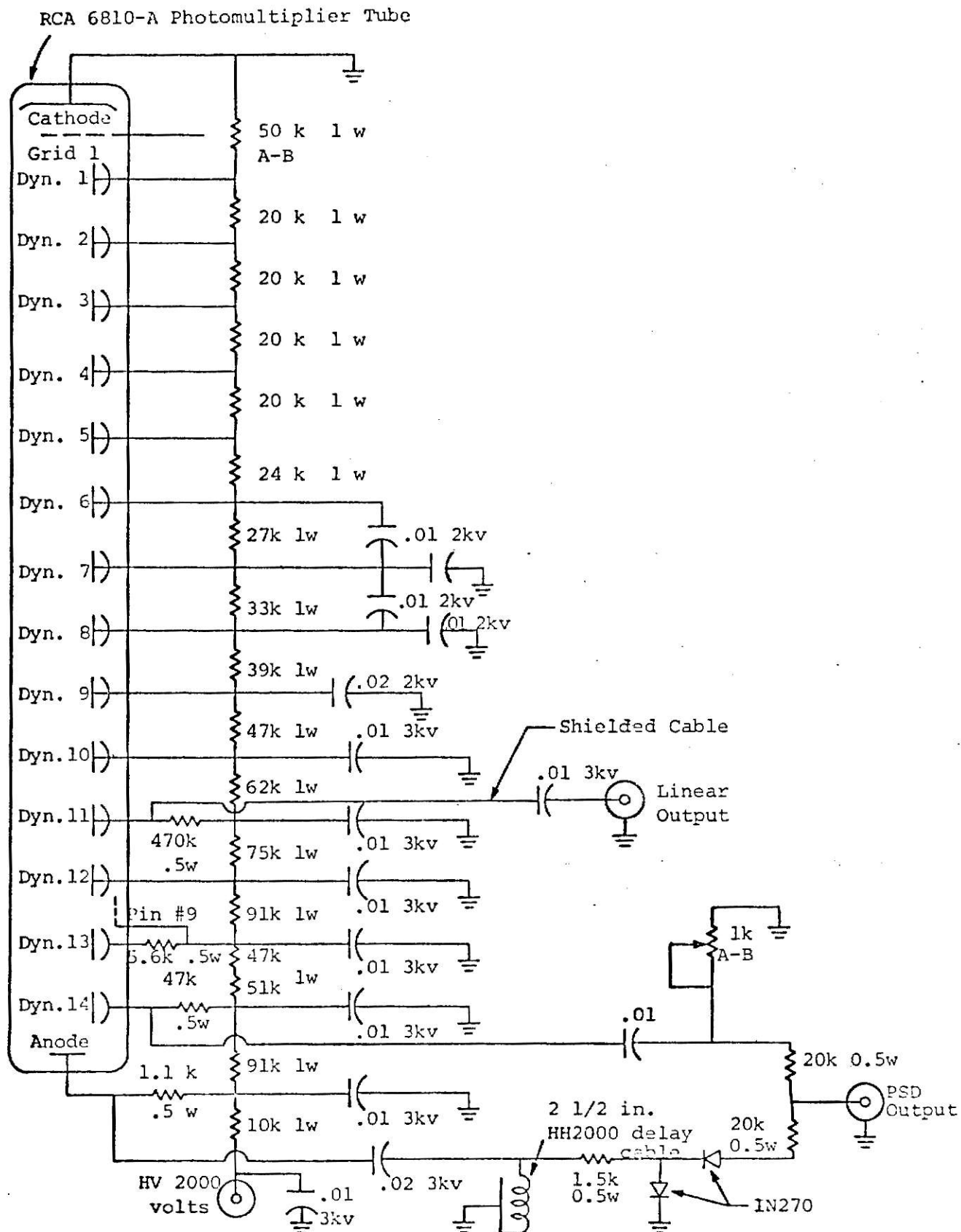


Figure 5 KSU Gamma Ray Pulse Shape Discrimination Circuit

**THIS BOOK
CONTAINS
NUMEROUS PAGES
WITH THE ORIGINAL
PRINTING BEING
SKEWED
DIFFERENTLY FROM
THE TOP OF THE
PAGE TO THE
BOTTOM.**

**THIS IS AS RECEIVED
FROM THE
CUSTOMER.**

is used in coincidence with the linear signal as shown in a block diagram of the NE-213 fast neutron spectrometer electronics in Fig. 6. (A description of the design and operating characteristics of the K.S.U. NE-213 fast neutron spectrometer system can be found in a report by Meyer, "Intercalibration of the K.S.U. Fast-Neutron Spectrometer System."¹⁶⁾

The resolution of the K.S.U. NE-213 system has been measured by Simons.²³ Verbinski made similar measurements on another NE-213 detection system at ORNL.¹ Both of these measurements were analyzed by unfolding the measured monoenergetic neutron response functions with the ORNL FERDOR code. The width of the approximately gaussian peak in the unfolded spectrum gave a measure of the resolution for that particular energy. This resolution was actually the resolution of the combined detection and unfolding processes at that energy.

3.3 Multiparameter Analyzer

A TMC-4096 Multiparameter Analyzer was used to measure the signals coming from the detection system with the resultant data stored in the memory. Readout options included paper tape, magnetic tape and omnigraphic plotter. The magnetic tape was converted directly to cards at the K.S.U. IBM 360-50 facility.

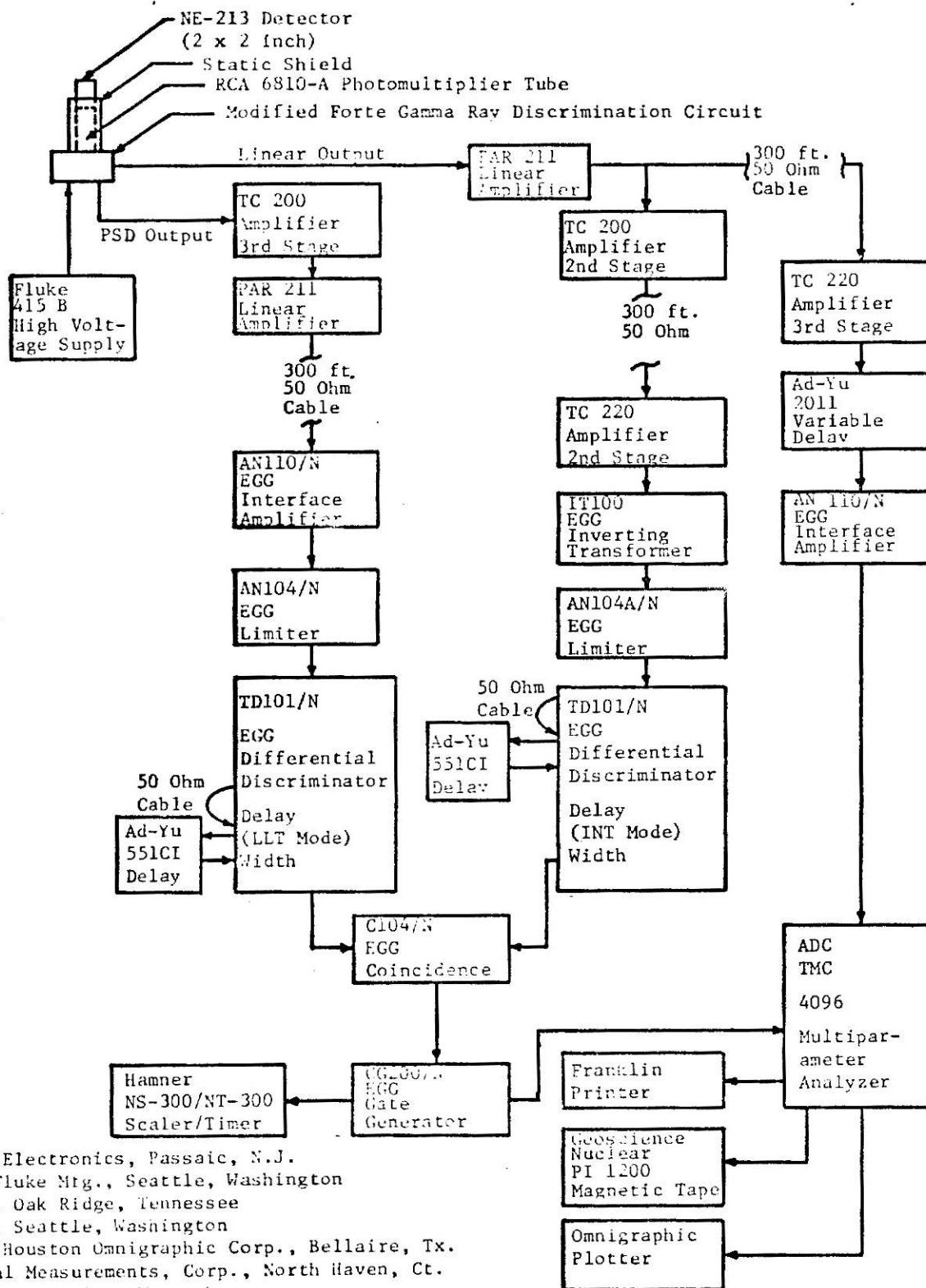
3.4 Sample Containers

For the experimental measurements involving liquid oxygen and sodium, special sample containers were fabricated in K.S.U. shops. The aluminum liquid oxygen container is shown in Fig. 7. It was of double-walled construction with the space between the inner and outer boxes filled with vermiculite insulation. Vermiculite is known for its inert, as well as insulating, properties. During an experiment the container was filled from the top to replace oxygen lost by evaporation.

ILLEGIBLE DOCUMENT

**THE FOLLOWING
DOCUMENT(S) IS OF
POOR LEGIBILITY IN
THE ORIGINAL**

**THIS IS THE BEST
COPY AVAILABLE**



Ad-Yu: Ad-Yu Electronics, Passaic, N.J.
 Fluke: John Fluke Mfg., Seattle, Washington
 TC: Tennelec, Oak Ridge, Tennessee
 Tally: Tally, Seattle, Washington
 Omnigraphic: Houston Omnigraphic Corp., Bellaire, Tx.
 TMC: Technical Measurements, Corp., North Haven, Ct.
 EGG: EG & G Inc., Salem, Massachusetts
 Hamner: Hamner Electronics, Princeton, N.J.
 Geoscience Nuclear: Geoscience Instruments Corp., Hamden, Conn.

Figure 6 Block Diagram of the KSU NE-213 Fast-Neutron Spectrometer System

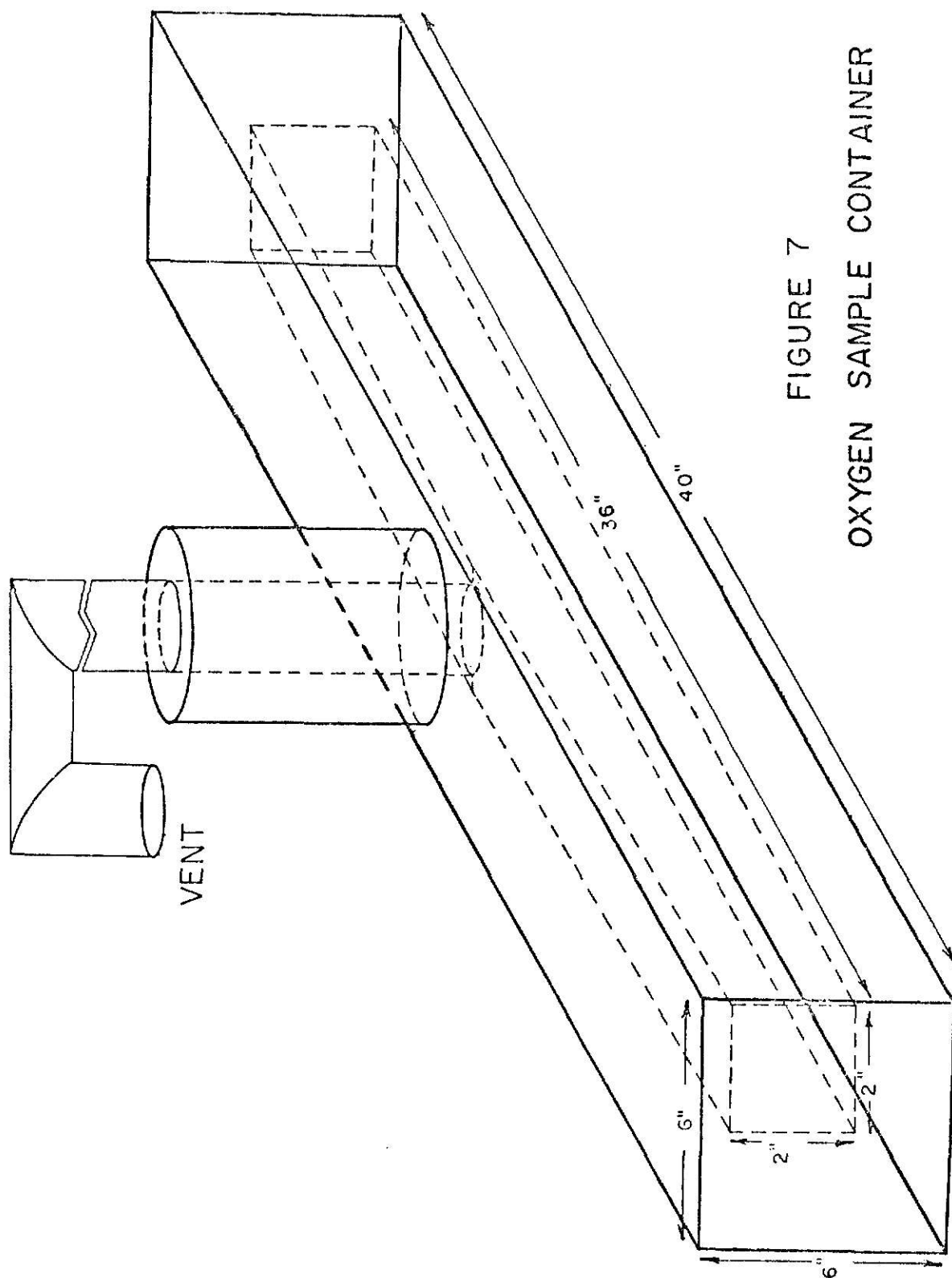


FIGURE 7
OXYGEN SAMPLE CONTAINER

The container for solid sodium was fabricated from stainless steel. The sodium was cast into this container under an inert atmosphere and then the container was sealed. After sealing there was no problem in handling the sodium. The liquid sodium container (Fig. 8) like the oxygen container was also double walled but in this case fabricated from stainless steel. The inner box was wrapped with resistance heating wire to permit heating the sodium sample above the melting point during an experiment. Thermocouples were welded to the container wall to monitor the sodium temperature. Vermiculite was again used as insulation. The inner box was vented into the outer container to allow for the expansion of the sodium during heating. When heated, an inert gas (nitrogen) was constantly passed through the container to reduce oxidation at the sodium-air interface.

3.5 Collimator and Shadow Shield

The neutron collimator was made of methyl methacrylate and was 3 inches by 3 inches by 24 inches long with a .318 inch square hole lengthwise through the center. By placing this collimator directly in front of the detector, the effective area of the detector was reduced to .101 square inches. This particularly sized collimator was used to duplicate the geometry used by Straker in a similar experiment at ORNL.²⁶ By using the collimator the solid angle subtended by the effective detector area was the same as the solid angle subtended by Straker's detector which was placed 50 feet from the sample.

When the collimator was not used directly in front of the detector, a shadow shield was used for background measurements. This shield is an aluminum cylinder approximately 2.5 inches I.D. and 24 inches long and is filled with water. For background measurements in experiments where the collimator was used, the ends were sealed and the void was filled with water.

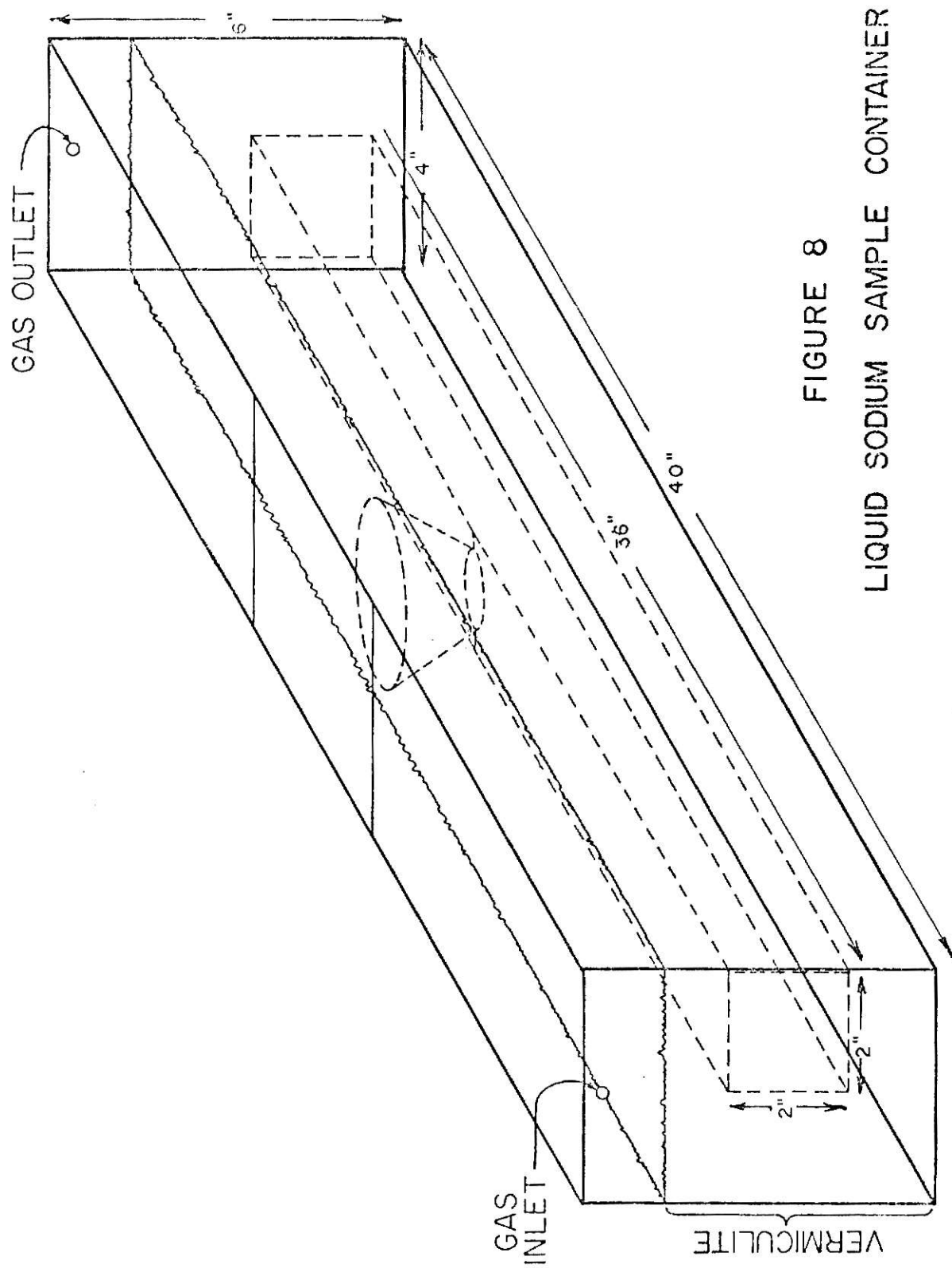


FIGURE 8
LIQUID SODIUM SAMPLE CONTAINER

4.0 EXPERIMENTAL PROCEDURE

4.1 Equipment Calibration

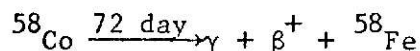
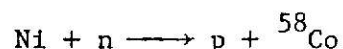
The basic procedure for obtaining a neutron spectrum was the same for all experimental runs. This basic procedure established the detection system parameters, the maximum reactor power and the integrated reactor flux.

4.1.1 Calibration of the detection system - After a twelve hour warm-up period for the NE-213 system, several parameters were checked and adjusted to insure proper response. First, a ^{60}Co gamma-ray spectrum was taken and the extrapolated Compton tail was used to set the energy gain. The gamma rejection ratio was set at >150:1 using the ^{60}Co source; that is, less than one gamma-ray in 150 was counted. The efficiency of the system was also checked using the ^{60}Co source. A one hour PuBe spectrum was measured with the gamma rejection circuit operative. This test spectrum was compared to a standard complex PuBe spectrum to insure that the system was working properly. A ^{60}Co spectrum was again taken immediately before or after each experimental spectrum to reestablish the gain and gamma rejection ratio.

4.1.2 Maximum total flux at the detector. - Due to the sensitivity of the Forte circuit and photomultiplier tube to radiation, the total radiation at the detector was kept below 3 mrem/hr. When the detection system is operative in the anticoincidence mode a 10% dead time on the TMC 4096 corresponds roughly to 3 mrem/hr at the detector. Thus, the 10% dead time was used to establish the maximum reactor power for all experimental runs.

4.1.3 Integrated flux monitor - Nickel foils were activated in the central thimble of the Triga to monitor the integrated flux during an experimental run. Nickel-neutron interactions produce ^{58}Co which decays,

emitting gamma-rays:



The total number of counts in the 0.811 MeV photoelectric peak of the ${}^{58}\text{Co}$ is directly proportional to the integrated flux. (It should be noted that one set of data reported in this work used sulfur as a flux monitor. However, all other experiments used nickel since it has proven to be a more accurate monitor.)

4.2 Neutron Spectrum Measurements

For all spectral measurements the detector, sample, shadow shield and collimator were placed on the centerline of the neutron beam. The detector was placed as far from the reactor as possible, or approximately 136 inches from the face of the beam port. All samples were placed so that the leading edge was flush with the beam port face except for the Pb sample which, because of its shape, could be placed inside the lip of the beam port collimator. When the shadow shield or collimator was used, it was placed as close to the detector as possible.

The experimental arrangement for collecting data without the collimator is shown in Fig. 9. To measure incident spectra the sample was removed or the empty sample container was placed in the beam. The background measurement for an incident spectrum measurement was obtained by placing the shadow shield directly in front of the detector. Foreground and background penetration (transmitted) spectra were collected in a manner similar to that described above except the sample was in place.

Figure 10 shows the geometry of the experimental measurements involving the use of the collimator at the detector. A surveyor's transit was used to insure proper alignment of the collimator and detector with the neutron

FIGURE 9
Experimental Geometry
No Collimator

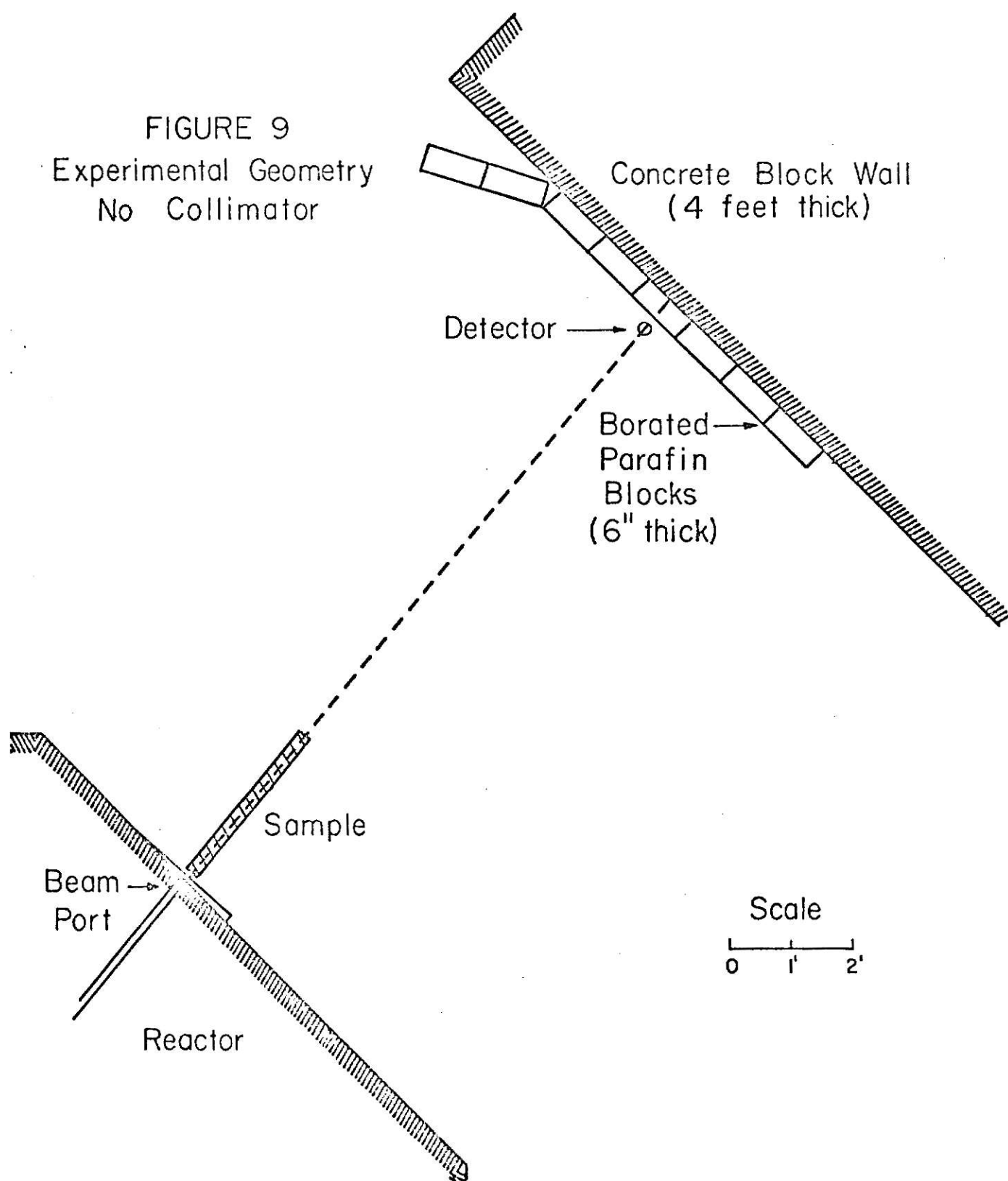
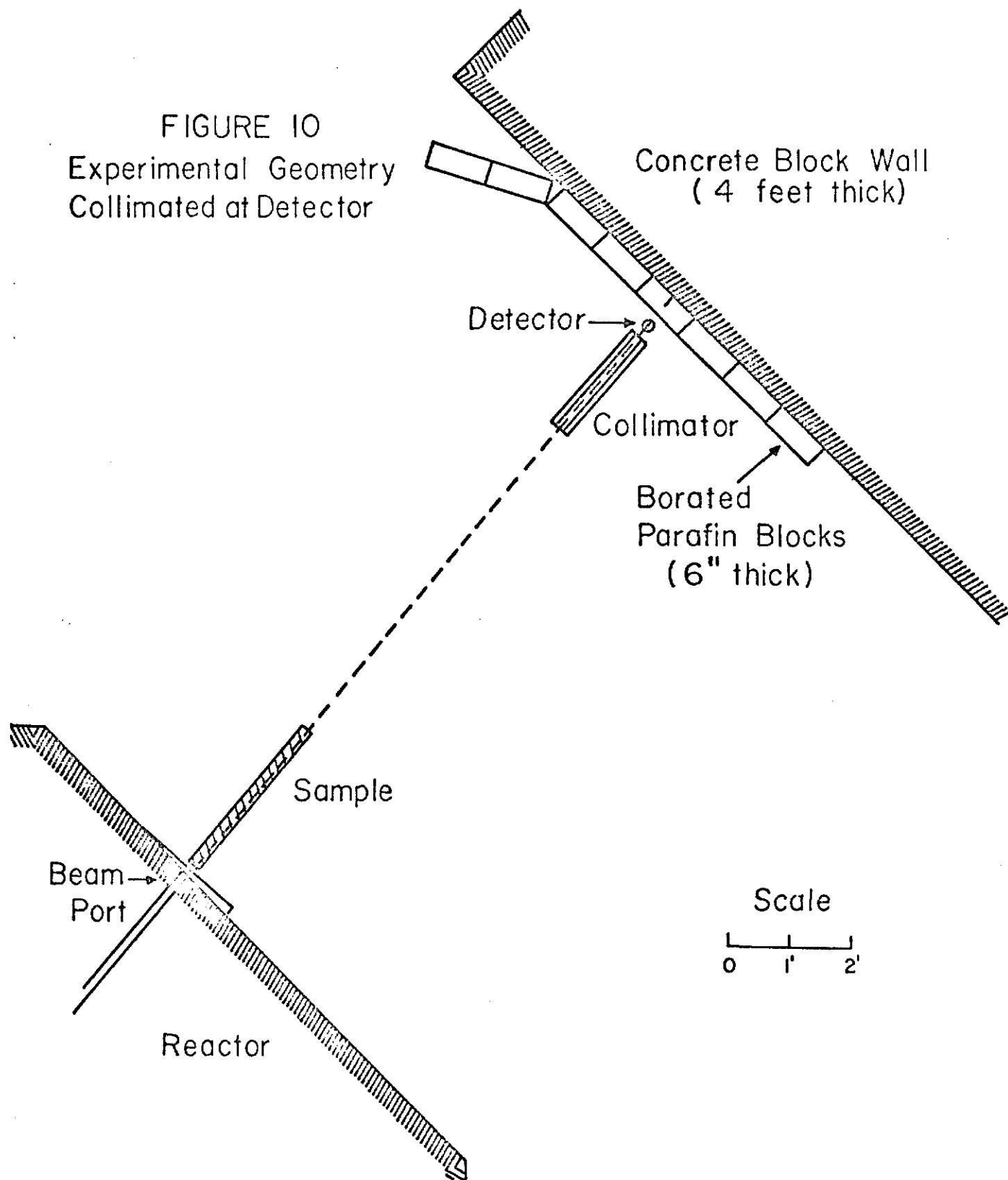


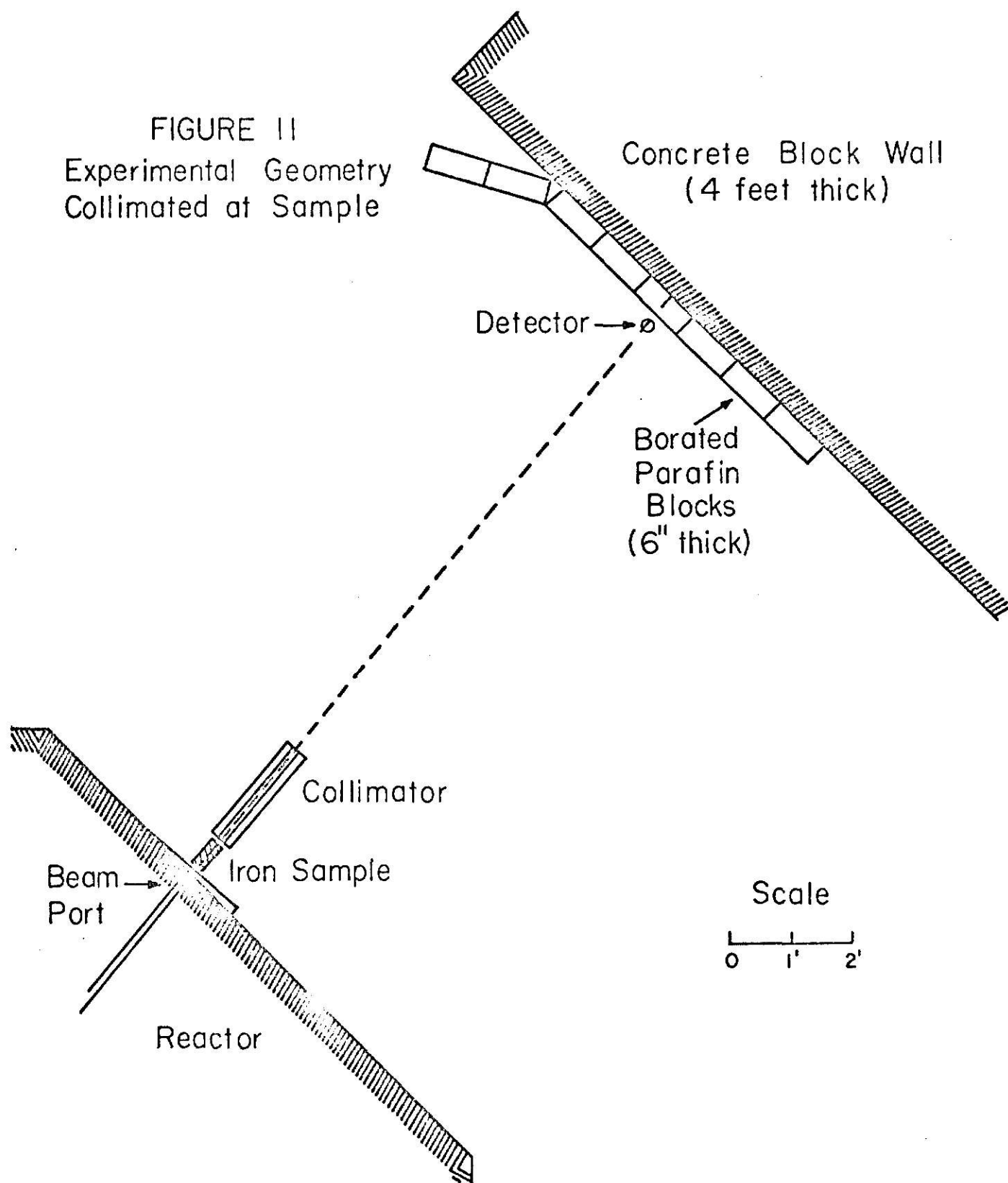
FIGURE 10
Experimental Geometry
Collimated at Detector



beam. Again both foreground and background measurements were made for both incident and penetration spectra, the background being obtained by sealing the end of the collimator and filling the collimator void with water.

One additional measurement was taken with the collimator next to the sample as shown in Fig. 11. The shadow shield was again used in front of the detector for background measurements.

FIGURE II
Experimental Geometry
Collimated at Sample



5.0 DATA ANALYSIS

5.1 Data Handling

After several spectra were measured, the raw data in the memory of the TMC 4096 were read onto magnetic tape; the tape was subsequently processed to obtain punched cards. A computer code, NUDASBIN, compiled this raw data using the ^{60}Co spectrum, the Ni foil data, and the foreground and background measurements. NUDASBIN treated the raw data using the ^{60}Co data to normalize the raw data with respect to energy. Background subtraction was performed after an integrated flux normalization of the background to the foreground using the Ni foil measurement. The resultant complex spectrum was binned for use by the unfolding code. For this work, the complex spectrum was unfolded with the ORNL code FERDOR.

5.2 Calculated Transmitted Spectra

A computer code, CALFLUX, was written to calculate the transmitted spectra using the measured incident spectra, cross-section data and the resolution of the detector as given in equation 8. Input to the code included the normalization factor between the incident and transmitted measurements based on the Ni data.

5.3 System Resolution Analysis

As stated earlier, the resolution of the detector system had been previously measured by two separate experimenters. To use this data in equation 8, the unfolded results of the mono-energetic neutron spectrum measurements of Verbinski were fitted to a gaussian curve by a KSU computer code, NE213RES. The NE213RES results gave the full width at one-half the maximum (FWHM) for each experimental energy. Simons' data had previously been analysed by a similar procedure. Both sets of resolution data were

then fitted to an nth order polynomial by another computer code, POLYFIT. This formulation gave resolution (FWHM) versus energy (MeV) for the entire system (which included both the detector and unfolding resolution).

6.0 RESULTS

The plots of resolution versus energy for the NE-213 spectrometer system are shown in Fig. 12, along with the polynomial fit for this data. Simons' data set is fitted to a 6th order polynomial and Verbinski's data set is fitted to a 7th order polynomial.

All neutron spectra taken for this work are shown in table 1. Table 2 lists some of the sample constants used.

Figure 13 demonstrates the effect of the resolution function on the transmitted spectra. The "unsmoothed" spectrum was calculated at discrete energies by Equation 3 and the "smoothed" spectrum was calculated at the same energies by Equation 8. The data set used was that for an oxygen penetration run. Figure 14 shows a comparison between two different resolution functions for the same oxygen data. In one case Verbinski's data set is used as the resolution function, and in the other case Verbinski's resolution is increased by 25%. The modified resolution function (the one with FWHM decreased by 25%) shows better agreement with the experimental measurements and was therefore used for all subsequent calculations.

A plot of all the incident spectra taken is shown in Fig. 15. Figures 16 and 17 show the comparison between experimental and calculated transmitted (penetration) spectra for Fe and O_2 measured without the collimator present. Figures 18, 19, 20, and 21 show experimental and calculated results for Fe, Pb, O_2 and Na, respectively, measured with the collimator. For the Fe measurement the collimator was placed next to the sample while for all other measurements the collimator was placed next to the detector. Finally, Fig. 22 shows a comparison between the collimated and uncollimated experimental Fe penetration spectra.

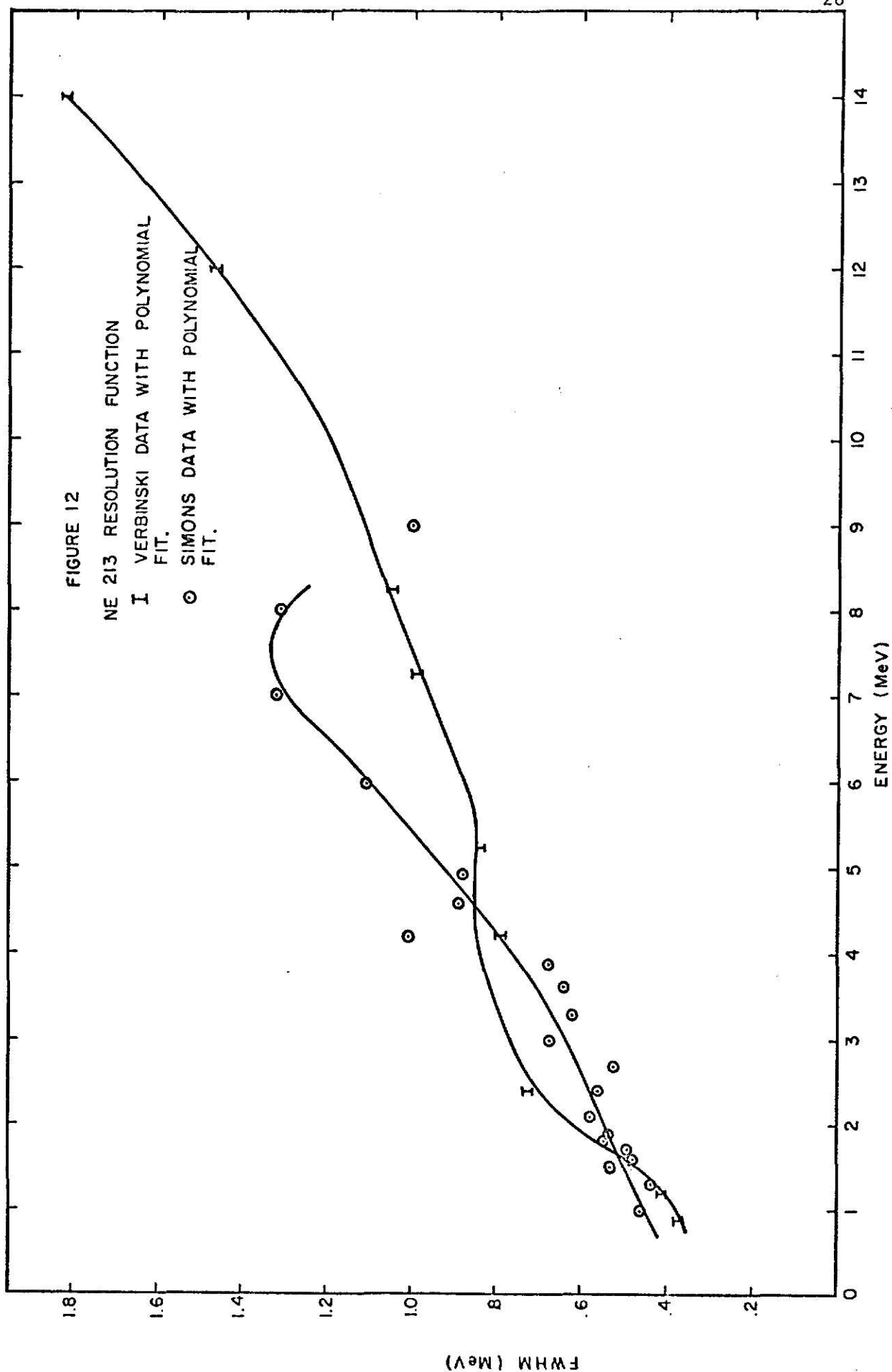


Table 1

EXPERIMENTAL NEUTRON SPECTRA

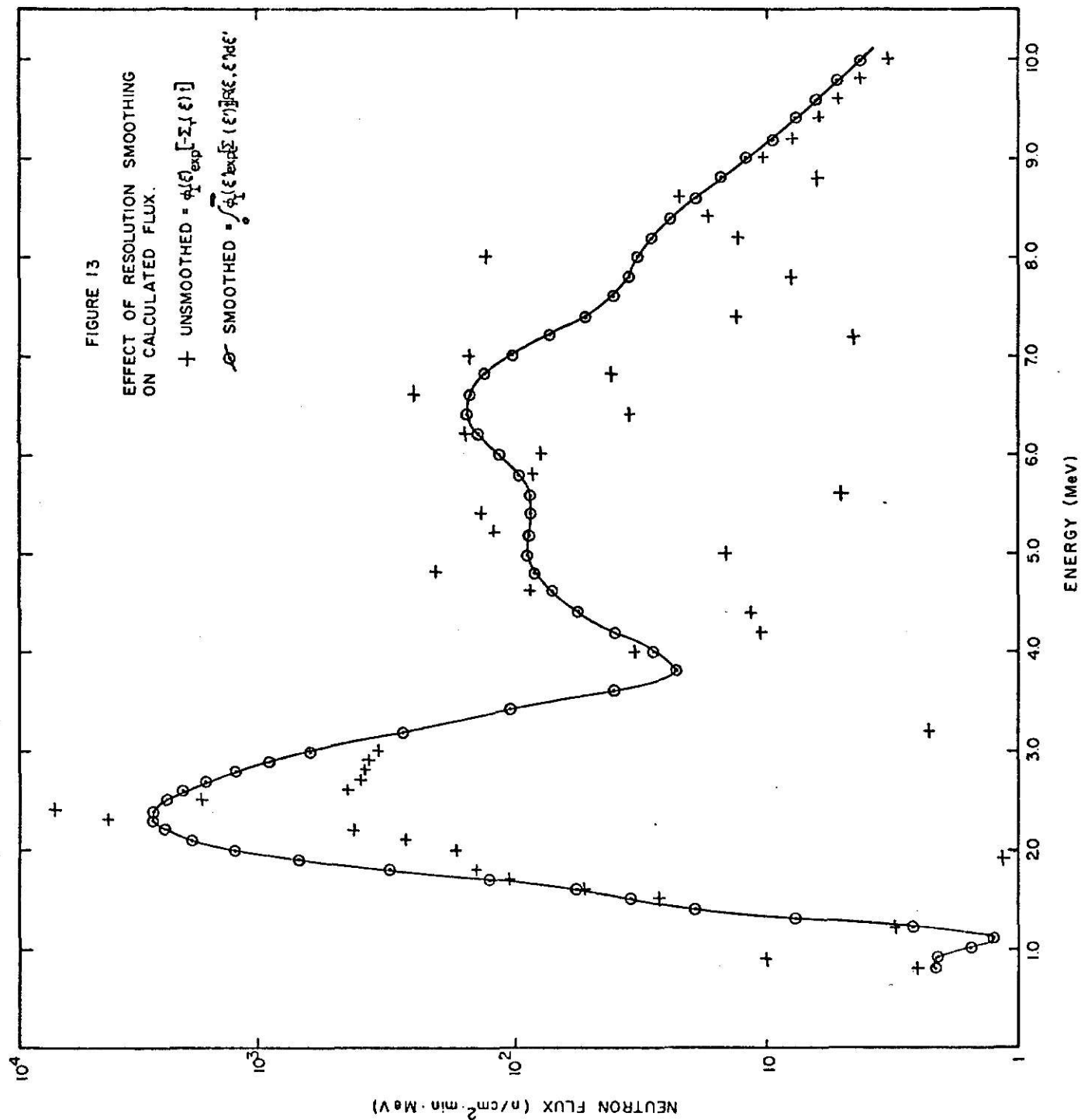
Run Number	Description	Geometry Used	Nominal Reactor Power Fluence (Ni Foil Data)
9-30-70- 4	O ₂ Incident	Uncollimated	40 W 52.914 (Sulfur Data)
10-14-71- 4	Fe Incident	Uncollimated	50 W -
10-23-70- 4	O ₂ Penetration #1	Uncollimated	1 kW 1728.8 (Sulfur Data)
10-23-70- 8	O ₂ Penetration #2	Uncollimated	1 kW 1412.1 (Sulfur Data)
1-18-71- 4	Incident	Collimator at Detector	135 W .1528 x 10 ⁵
1-27-71- 6	Pb Pene	Collimated at Detector	50 kW .616326 x 10 ⁷
2-19-71- 7	O ₂ Incident	"	750 W .94199 x 10 ⁵
2-22-71- 4	Na (Solid) Incident	"	750 W .2563 x 10 ⁵
2-23-71- 4	O ₂ Pene	"	20 kW .242035 x 10 ⁷
3-16-71- 4	Fe Incident	Collimator at Sample	500 W .55465 x 10 ⁵
3-16-71- 6	Na (liquid) Incident	Collimator at Detector	1.25 kW .16989 x 10 ⁶
3-16-71- 9	Fe Pene	Collimator at Sample	16 kW .22089 x 10 ⁷
3-23-71-13	Fe Pene	Uncollimated	2 kW .25849 x 10 ⁶
3-24-71- 4	Na (liquid) Pene	Collimated at Detector	30 kW .37835 x 10 ⁷
3-24-71- 8	Na (solid) Incident	"	30 kW .40028 x 10 ⁷
3-30-71- 4	Na (solid) Incident	"	1.2 kW .1707 x 10 ⁶

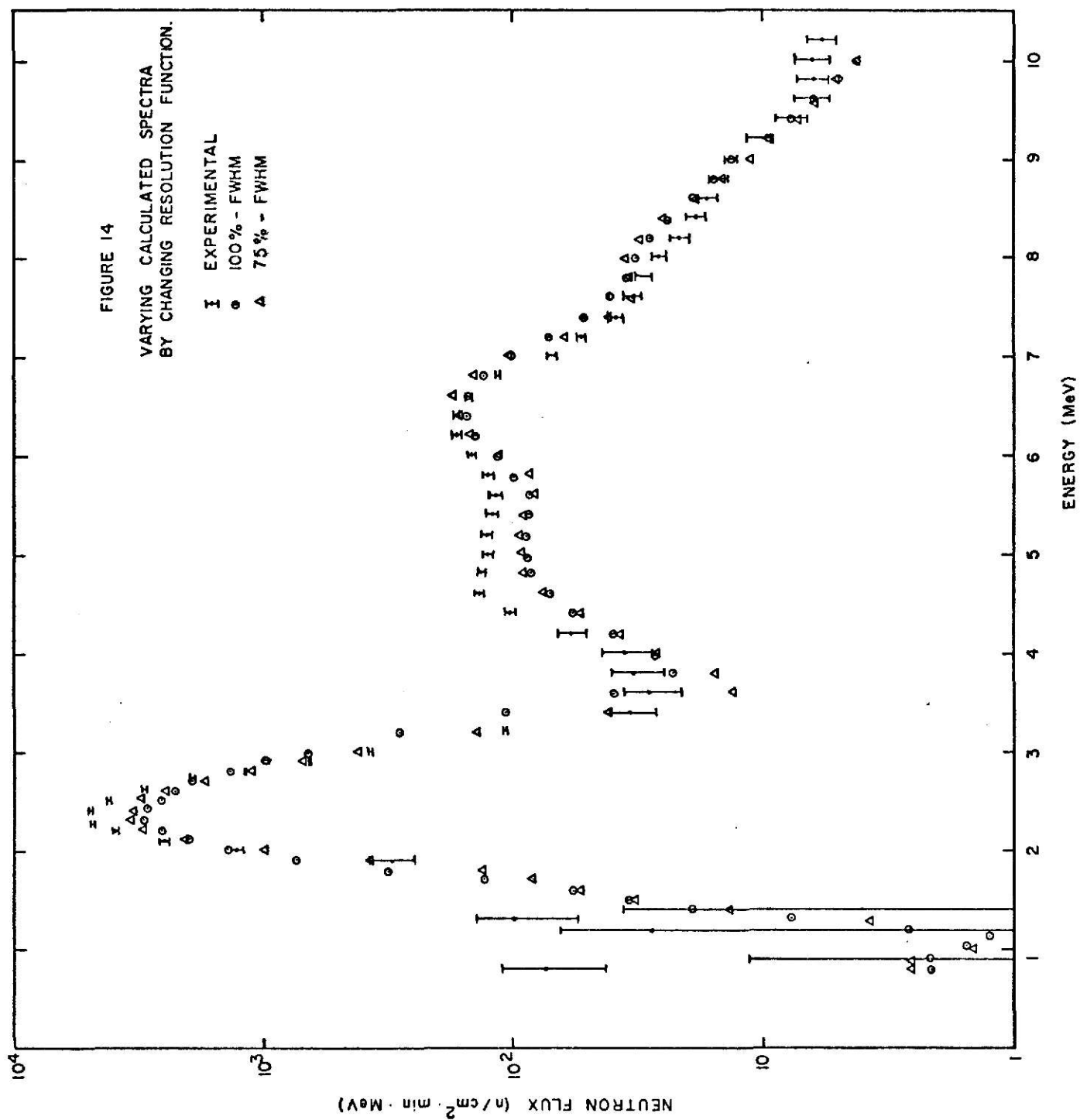
Table 2
Sample Descriptions

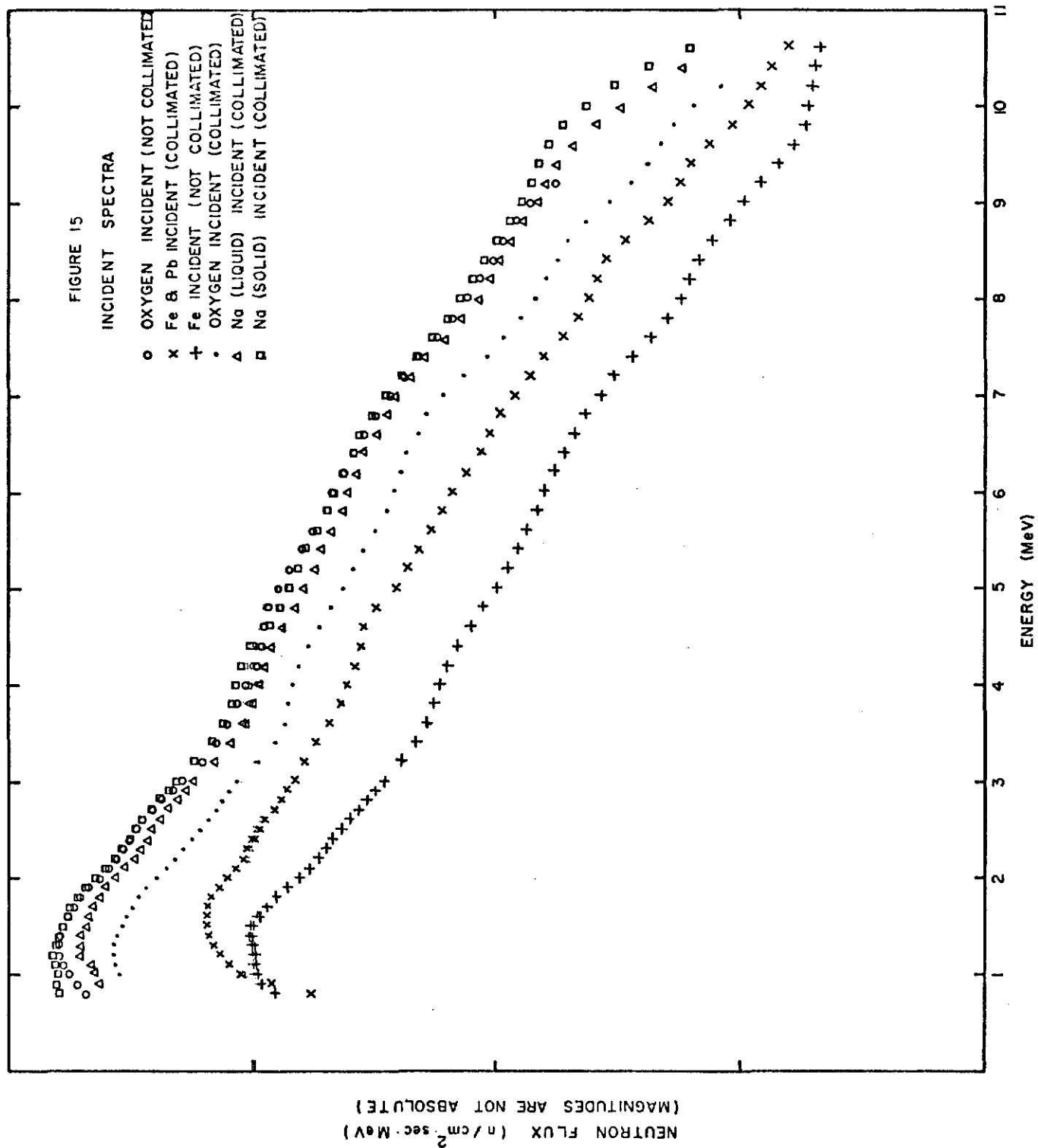
Sample	Nominal Size (inches)	Thickness (cm)	N (atom density) (atoms/cm ³)
Oxygen	2 1/4 x 2 1/4 x 36	91.28	.0403 x 10 ²⁴ *
Fe	2 x 2 x 6	15.24	.0849 x 10 ²⁴
Pb	3 1/2 dia x 9 1/4	23.49	.033 x 10 ²⁴
Na (solid)	2 1/2 x 2 1/2 x 36	91.60	.02541 x 10 ²⁴
Na (liquid)	2 1/2 x 2 1/2 x 36	91.60	.02389 x 10 ²⁴ **

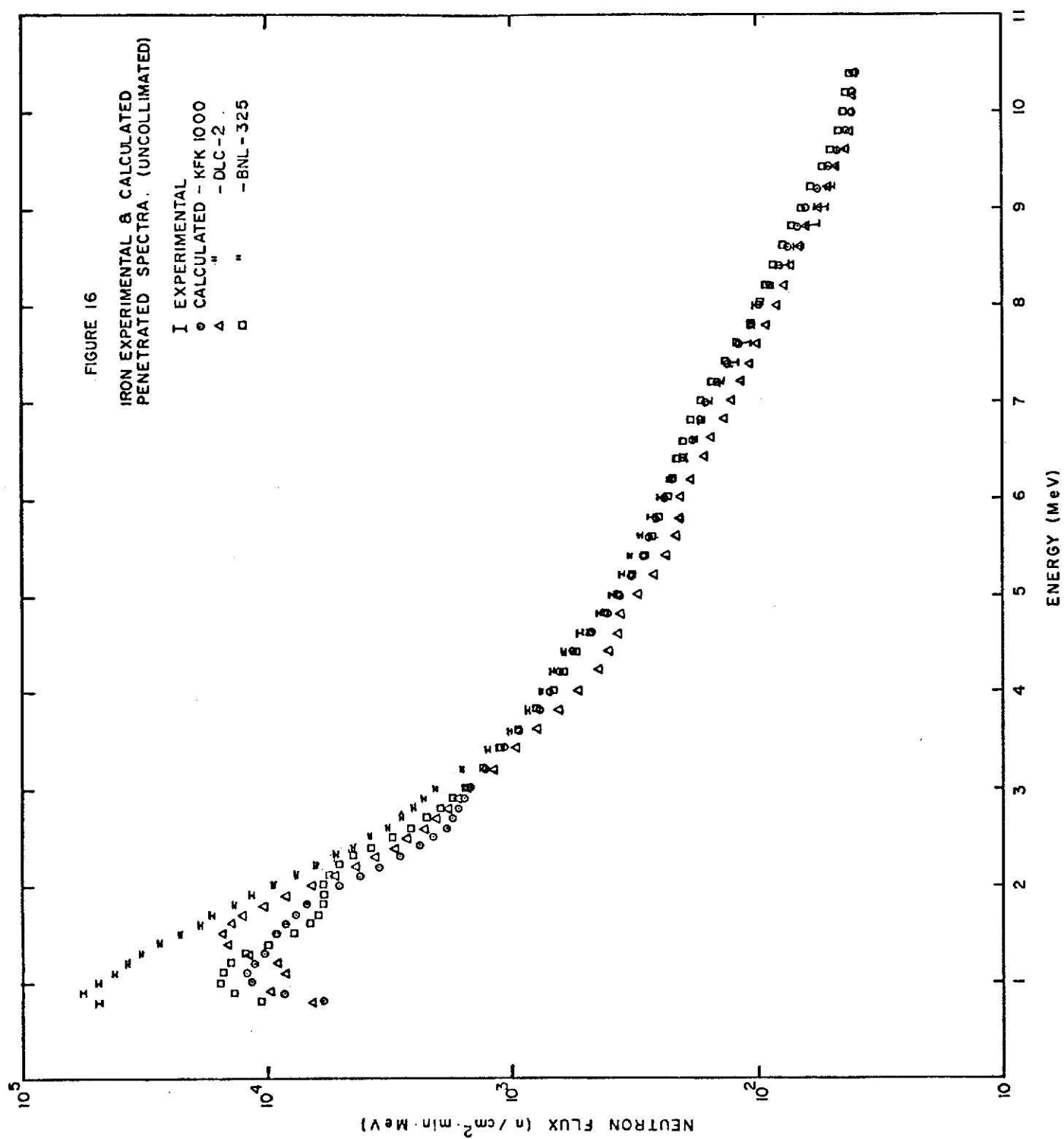
*Corrected to account for void space caused by boiling

**At 165°C (taken from Smithalls²⁵)









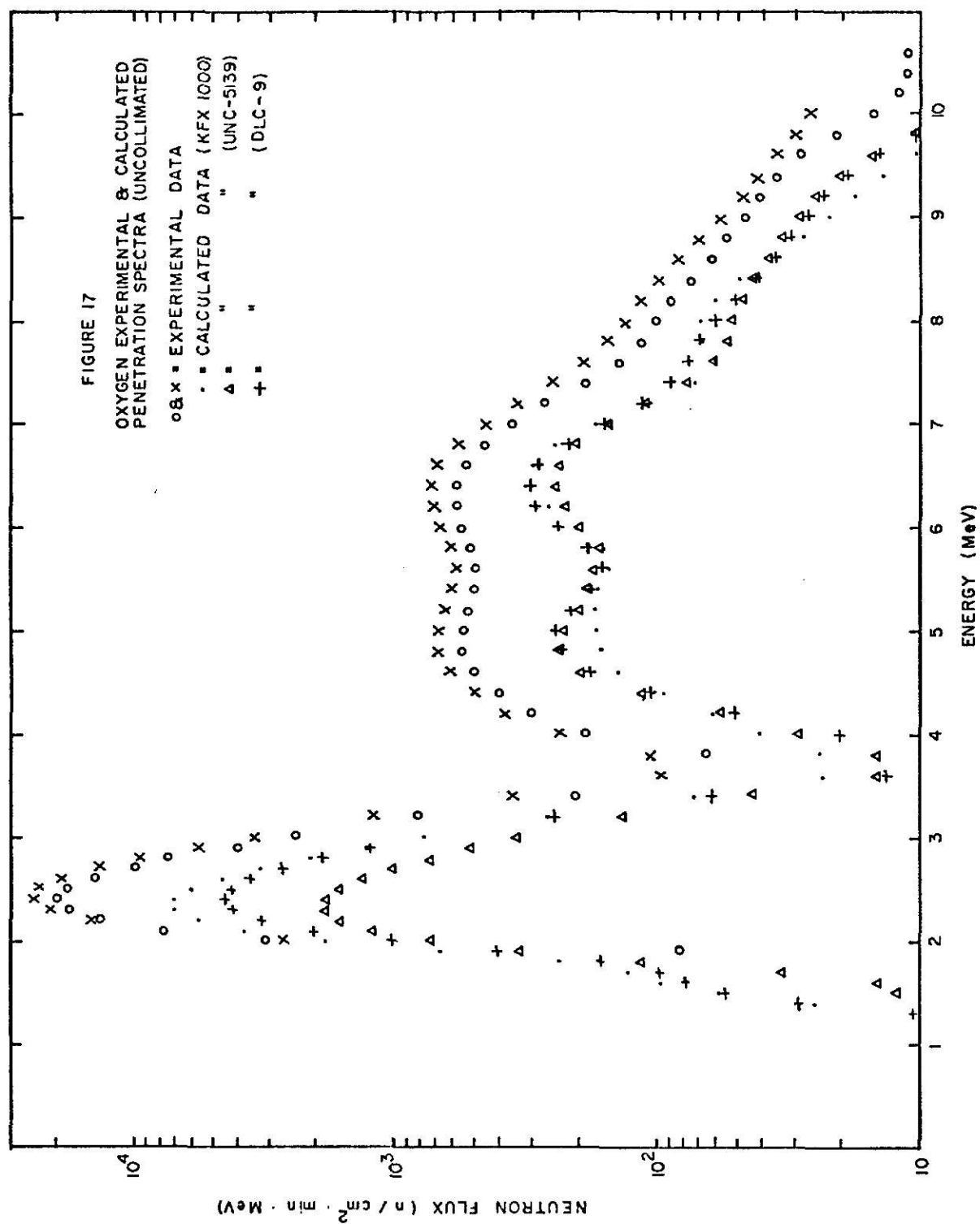
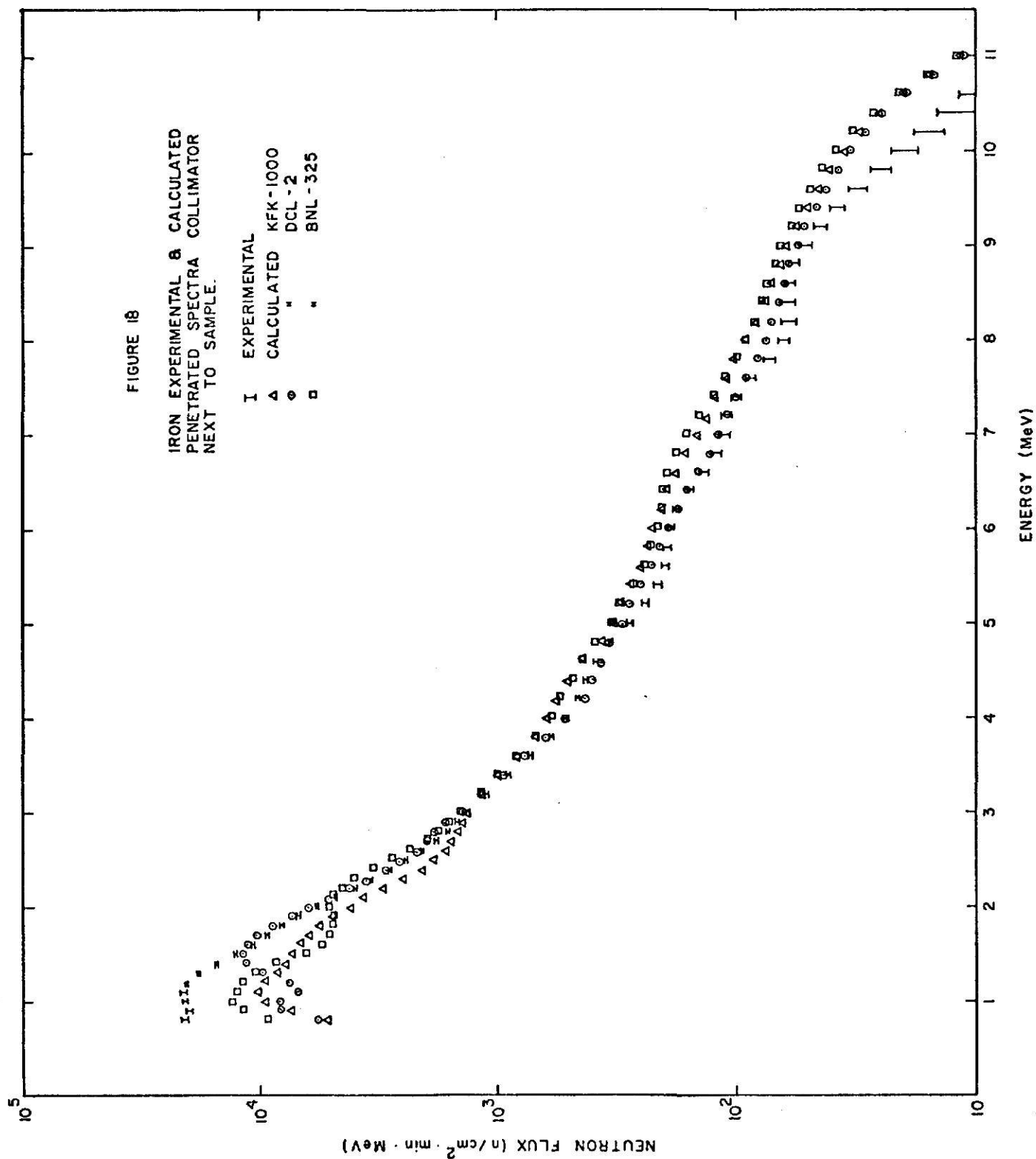
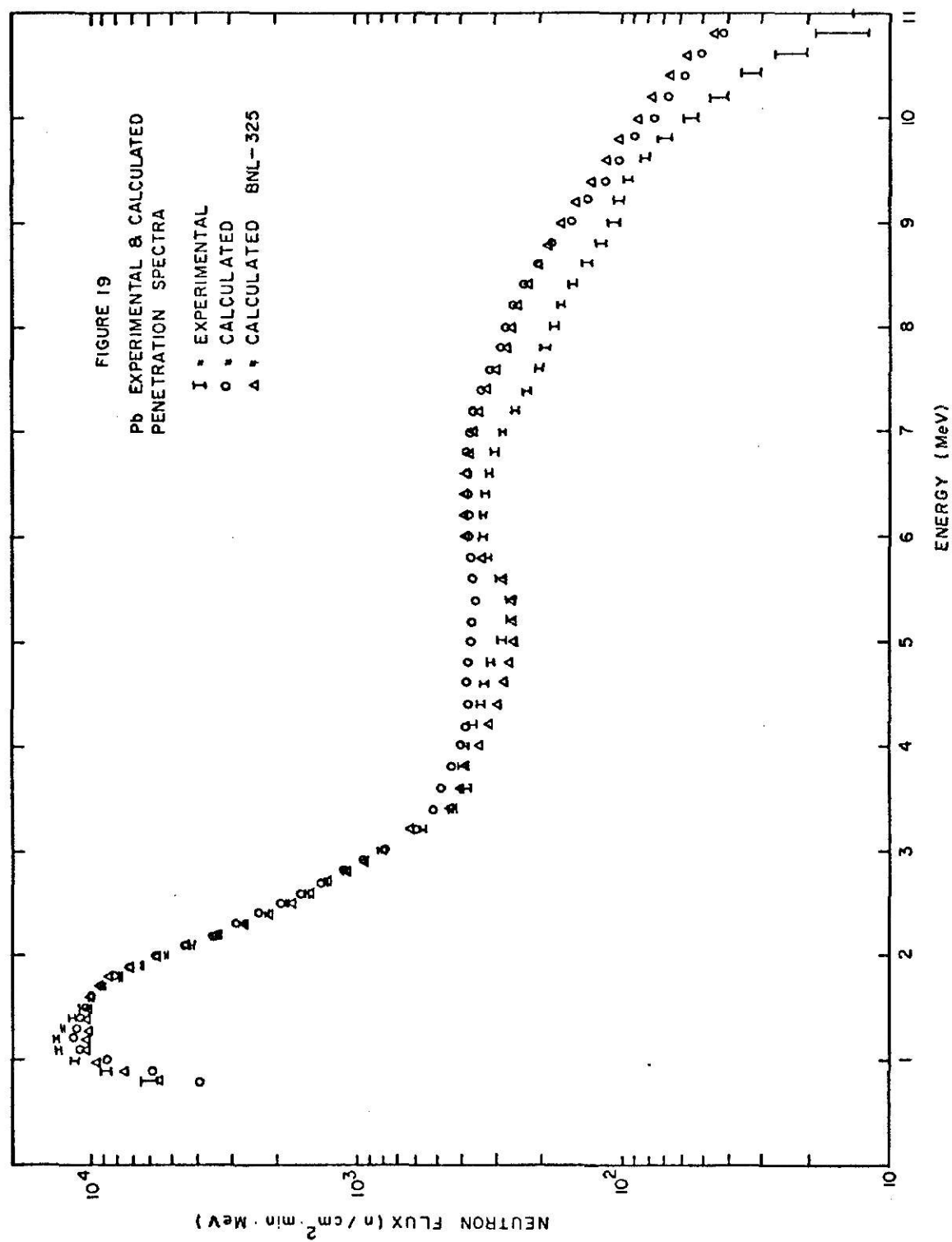


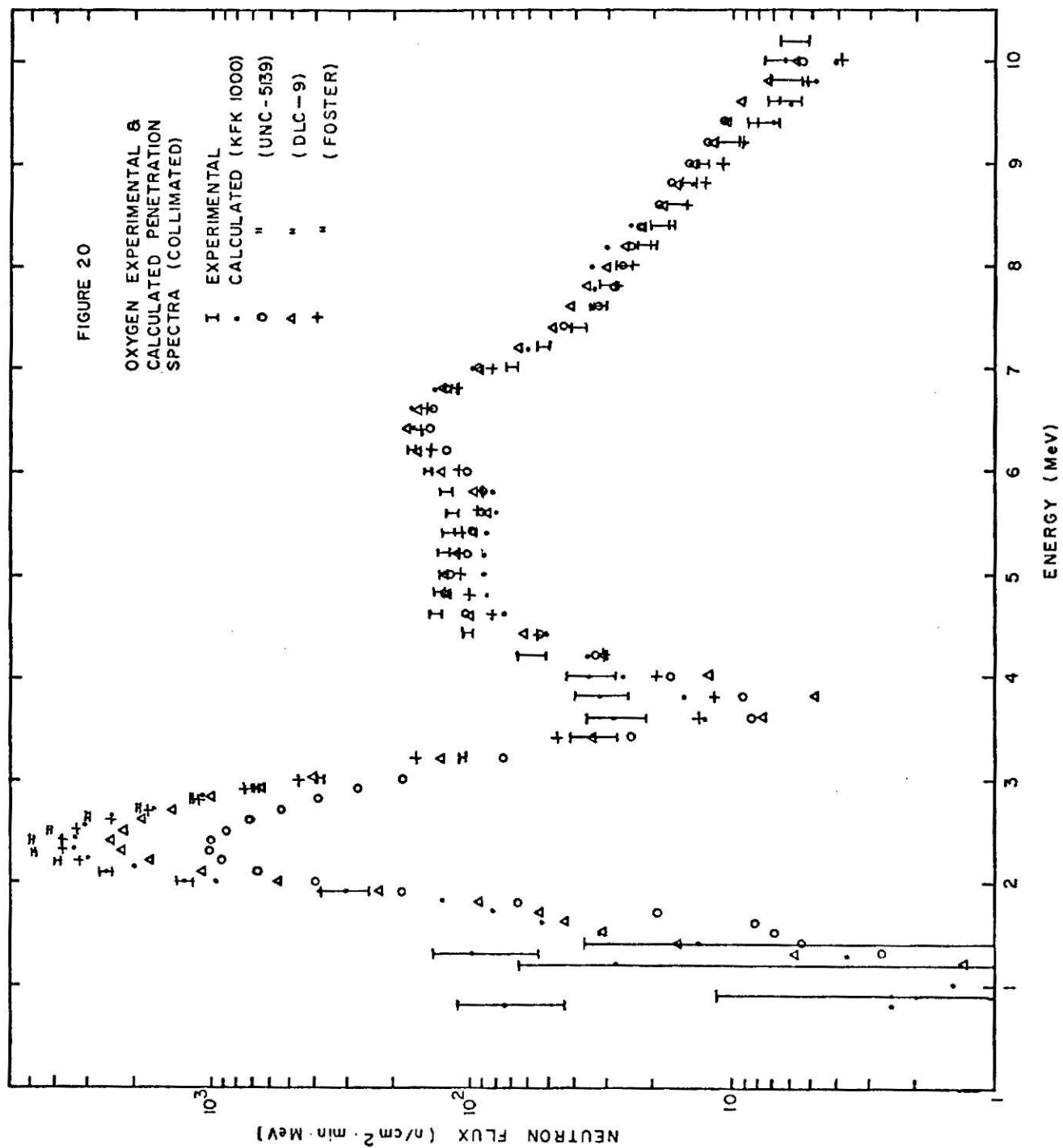
FIGURE 18

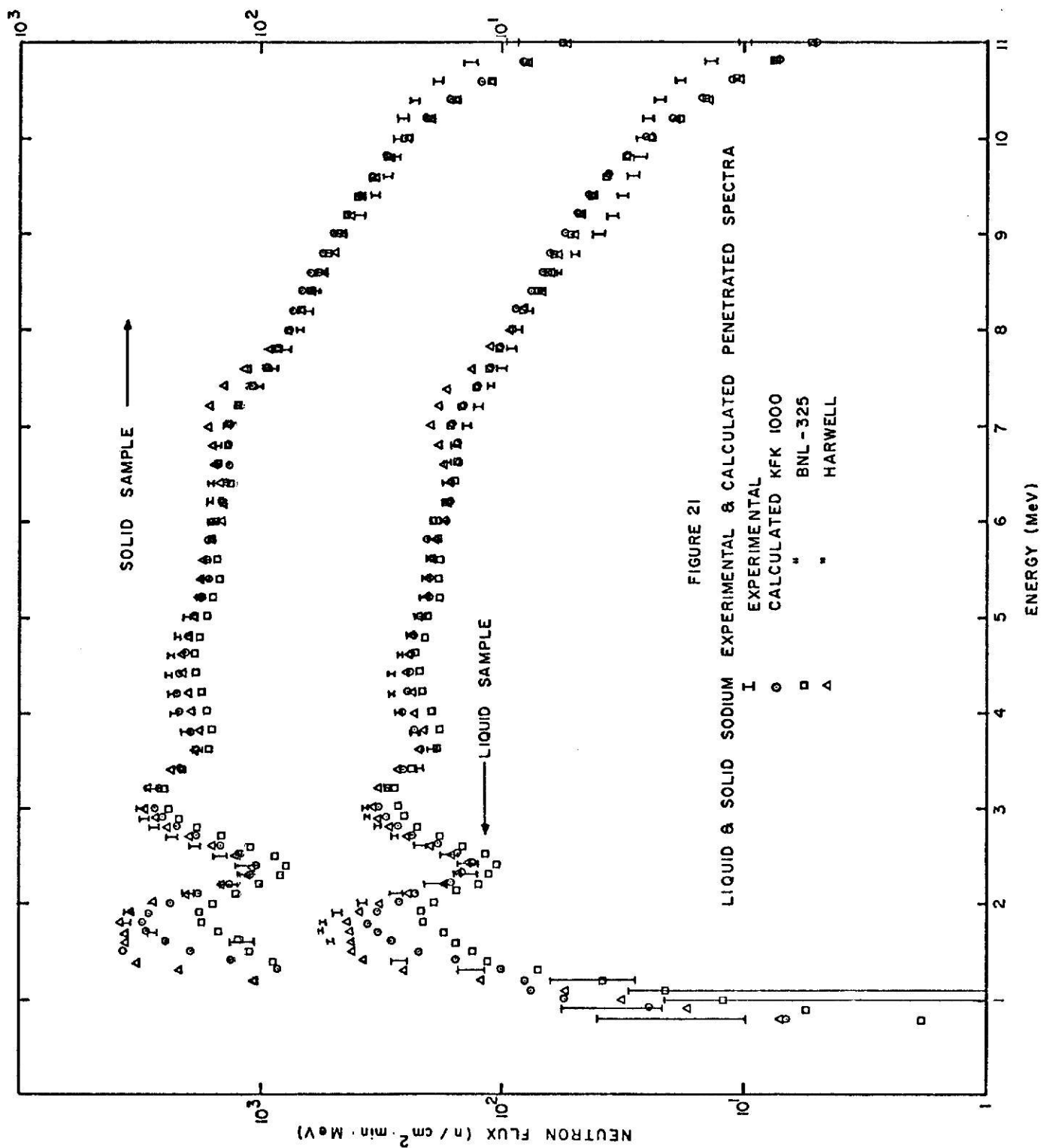
IRON EXPERIMENTAL & CALCULATED
PENETRATED SPECTRA COLLIMATOR
NEXT TO SAMPLE.

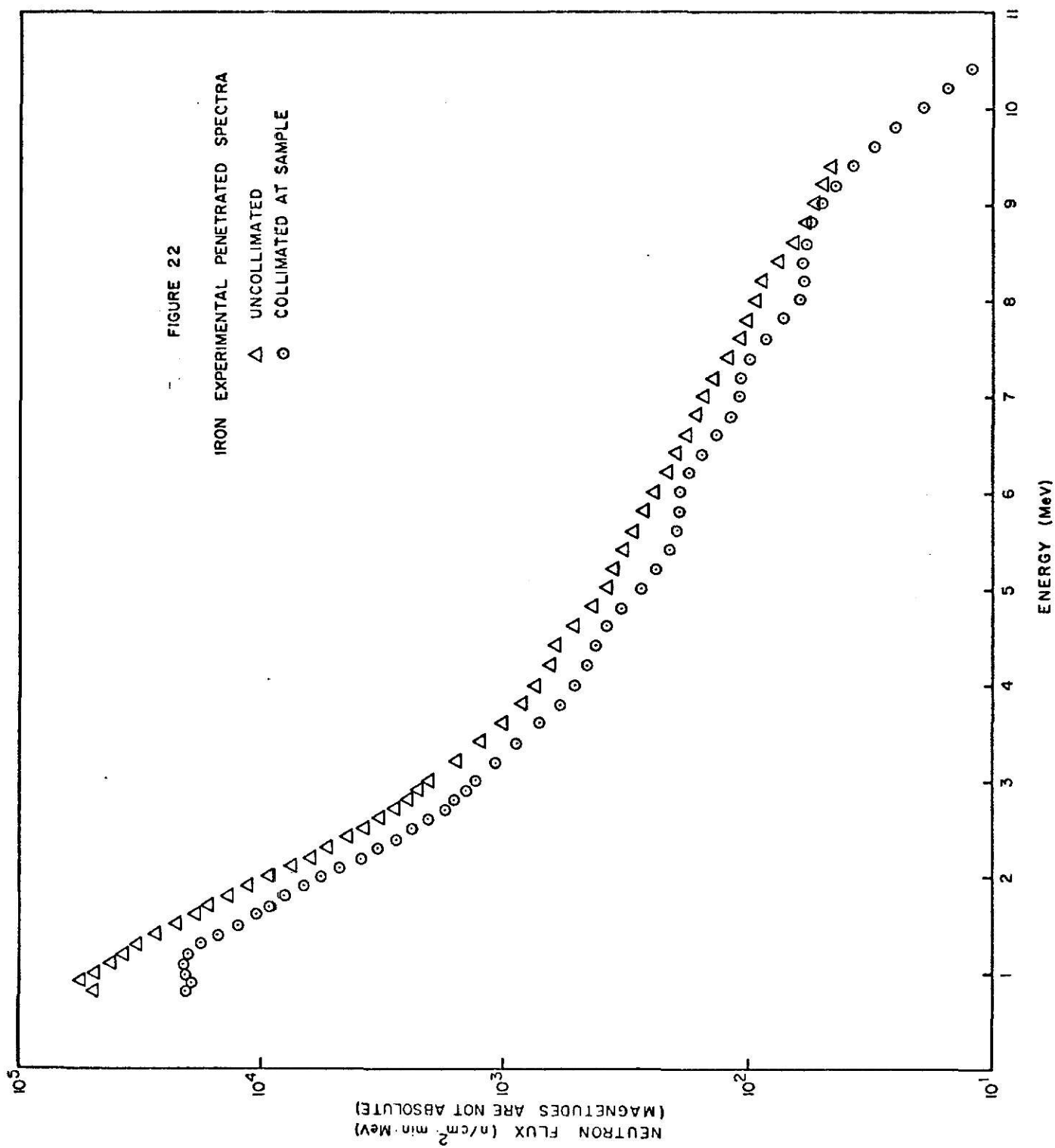
I	EXPERIMENTAL	
Δ	CALCULATED	KFK-1000
○	"	DCL-2
□	"	BNL-325











7.0 CONCLUSIONS

7.1 Detector Resolution

As can be seen from Fig. 12, there is reasonable agreement between the two experimental resolution data. Simons' data set shows an unusual effect in that the resolution begins to decrease at approximately 7.5 MeV. This is considered to be an error in his data since there would seem to be no physical phenomenon which would produce this effect. Verbinski's data set does not show this effect in this region and is probably more representative of the actual resolution of the NE-213 detector. However, there is an inflection point in Verbinski's data at 3 MeV which is questionable. The point at 2.3 MeV seems to be in error, causing the resolution in this region to be poorer than that reported by Simons.

In order to check the resolution of the detector system, oxygen was chosen for a penetration measurement. The large minima in the cross-section at 2.35 MeV produces an almost mono-energetic peak at this energy. Therefore, the width of this peak is a good measure of the resolution of the detector. Figure 14 shows a comparison between the experimentally measured and the calculated transmitted spectra for oxygen using the KFK-1000² cross-section data (since this data set seems to best predict the transmitted spectrum in the 2.35 MeV region as shown in Fig. 20) and the Verbinski resolution data. Figure 14 also shows the comparison between the two spectra when the Verbinski resolution was improved by 25% (multiplying the FWHM by 75%). This latter calculation was used for the following reasons:

- 1) Verbinski's resolution data were taken on another NE-213 detector system at ORNL which does not necessarily have the same resolution as the KSU NE-213 detector, but should have a similar shape as a function of energy.
- 2) Simons' data show a better resolution in the 2.35 MeV region although the resolution at higher energies is in question.

- 3) Measurements of Na^{22} and Co^{60} spectra taken at ORNL and Kansas State University show that the KSU system appears to have at least as good, if not better, resolution.
- 4) The use of Verbinski's resolution data (unchanged) in the calculated transmitted spectrum shows poorer resolution in the 2.35 MeV region than does the experimental measurement. Furthermore, by improving the resolution by 25%, good agreement is found between the experimental and calculated results.

It was concluded that, although the calculated transmitted spectrum is not extremely sensitive to the resolution, improving Verbinski's resolution by 25% best describes the KSU NE-213 system resolution for this calculation and was therefore used on all subsequent calculations. The comparison between the calculated and experimental transmitted spectra for the other materials used in this experiment supports this assumption.

7.2 Energy Calibration

The 2.35 MeV peak in the transmitted oxygen spectrum also provides a check on the energy calibration. As can be seen, all of the calculated and experimental peaks fall between 2.35 and 2.40 MeV indicating that the energy calibration of the system is very accurate.

7.3 Consistency of Experimental Results

Figure 17 shows two experimentally determined transmitted spectra for oxygen. These runs were made to test the consistency of the experimental results, except for a normalization error, the two runs are identical. The normalization error occurred on this run because sulfur was used as a flux monitor. All subsequent runs used the more reliable nickel foils.

7.4 Forward Scattering Assumptions

As was stated in the theory, the first geometry condition (uncollimated) assumed that any forward scattering at shallow angles would miss the solid

angle subtended by the detector. Figure 17 shows such a run for oxygen. Even though there was a small normalization problem, there was a large discrepancy between the experimental and calculated results throughout the energy range. This discrepancy indicates that the experimental measured cross-section was much less than the published data. This result indicates that many neutrons scattered at shallow angles were reaching the detector. This would cause an increase in the experimental result, as shown, and would therefore make the actual cross-section appear too large. Figure 20 shows the same comparison between experimental and calculated results using the second geometry condition (with the collimator placed in front of the detector). The forward scattering problem was virtually eliminated and good agreement was found between the experimental and calculated results.

The total neutron cross-section predicted by the uncollimated case was about 25% lower than the published data. This error is due to forward scattered neutrons which were reaching the detector, but this forward scattering contribution seems very large. Therefore, a mathematical model was used to predict this discrepancy. DLC-2^4 angular dependent cross-section data set was used with the following assumptions:

- 1: Any neutron that was scattered at an angle less than the solid angle subtended by the detector was assumed to be unscattered, and therefore, part of the original beam.
- 2: Any neutron that was scattered at an angle larger than the solid angle subtended by the detector was assumed to be lost from the beam and would not be scattered back into the detector.
- 3: The probability of neutrons scattering into the solid angle of the detector was equal to the probability of zero angle scattering integrated over the detector solid angle.

Neither of the first two assumptions were entirely valid. Neutrons that were scattered at small angles could be scattered again and miss the detector.

Also, neutrons scattered at large angles could be scattered again back into the solid angle of the detector. However, the discrepancies in these two assumptions tend to cancel each other. Thus, it is possible to predict the transmitted spectrum by:

$$\phi_{\text{trans}} = \phi_I \exp[-(\Sigma_t - \Sigma_{fs})t] \quad (11)$$

where Σ_{fs} is the correction in the total neutron cross-section from forward scattered neutrons which reach the detector. Σ_{fs} was calculated using the DLC-2 data and the solid angle of the detector, and the results are shown in Fig. 23. This calculation did not even start to describe the experimentally measured forward scattering contribution. The calculation gave a Σ_t correction of about .01% (see Fig. 23) compared to 25% in the experiment. It is realized that the assumptions made were not completely accurate; however, several orders of magnitude difference between the experimentally measured deviation and the calculated correction are involved. It appears unlikely that refinement of the assumptions would lead to significant improvement of the calculation. Therefore one is led to the conclusion that significant errors may exist in the DLC-2 shallow angle scattering data.

The DLC-2 cross-section data set was first checked against a theoretical minimum cross-section based on the optical model. The Wick's Limit²⁷ gives the minimum zero angle scattering probability by the following equation:

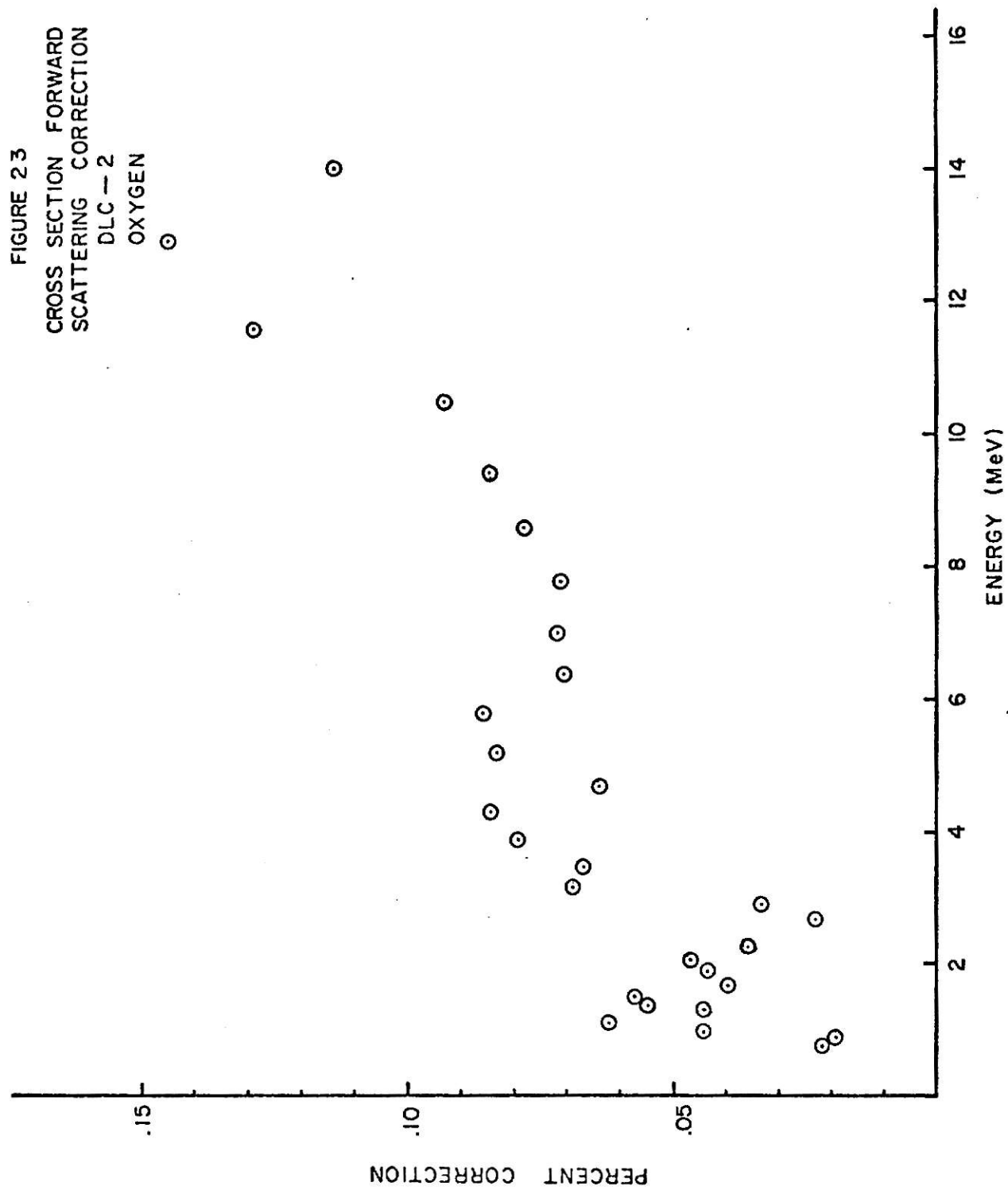
$$\left. \frac{d\sigma}{d(\cos \phi)} \right|_{0^\circ} \geq \frac{k^2}{8\pi} \sigma_{\text{TOT}}^2 \quad (12)$$

$$\text{where } k^2 = \frac{2\mu E}{h^2}$$

θ = scattering angle in center of mass system

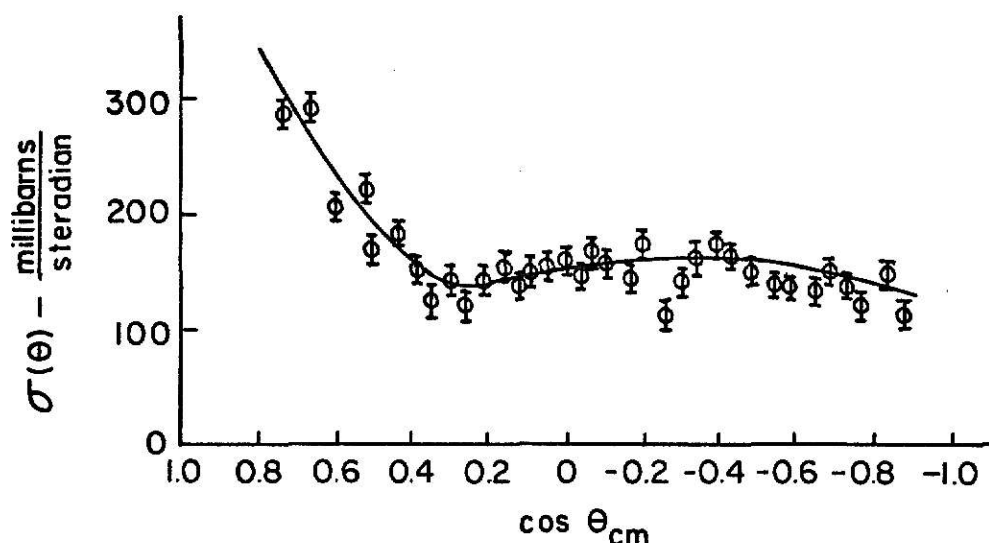
$$\text{and } \mu = \frac{m \cdot M}{m + M}$$

and m, M = masses of the neutron and oxygen atom



This equation was used to check the DLC-2 data at several energies, and the data do indeed satisfy the theoretical minimum. However, this does not indicate that the actual forward scattering probability is not much greater than indicated by the Wick's minimum limit.

If it is assumed that the data taken in this experiment are correct, then there must be an explanation for the large errors in published forward scattering data. It is noted in looking at published data that the differential angular cross-section as a function on angle is not reported between 0° and approximately 30° . For example, the following figure shows such a plot for oxygen at 3.91 MeV taken from BNL-400.¹⁰



Experimental cross section data can not be taken any closer to the zero angle than 30° because of interference between the neutrons scattered at small angles and the uncollided, transmitted flux. Therefore, the zero angle forward scattering probability is determined by exponential extrapolation of the data from 30° back to 0° . The measurements made in this report indicate that the actual forward scattering probability approaches a δ function, i.e., it is very sharply peaked at the zero angle. The error found in published data

is due to a lack of experimental data in this region. Forward scattering probability at small angles is rarely measured. For many materials the error between the extrapolated zero angle scattering probability and the actual may be small, but for oxygen it appears that the extrapolated data are in serious error.

7.5 Multiple Scattering Assumptions

Figure 22 shows a comparison between two iron penetration spectra, one uncollimated and one collimated at the sample. In this example, the effect of multiple scattered neutrons on the penetration data can be seen. A fraction of the incident neutrons were apparently scattered several times in the sample and emerged from the sample in a direction that would intercept the detector. This effect can be seen by the smoothing of the data and in the buildup in the low energy end for the uncollimated case (see Fig. 22). However, the magnitude of the discrepancy caused by multiple scattering of neutrons is much less than that caused by shallow angle scattering of neutrons as can be seen by comparison of Figs. 16 and 18. The uncollimated data points were slightly above the calculated and the collimated were slightly below, but the difference is small. Again, if a true measure of the total neutron cross-section was to be made, the collimator would be used.

7.6 Evaluation of Published Data

The cross section data sets used to obtain the calculated transmitted spectra to be compared with the measurements came from a variety of sources and methods. The KFK-1000² data and the data of Foster⁷ and Langsford¹⁴ were taken using an accelerator and time light measurements. The BNL-325¹¹ data set is a compilation of data from many sources and the best line is drawn through all of the combined data. The UNC-5139²⁰ data set is a

combination of experimental data and theoretical calculations. The DLC⁵ data set is grouped cross-section data from the ENDF/B⁶ file compiled with the ORNL code SUPERTOG²⁹ using 1/E spectrum weighting.

7.6.1 Iron (Fig. 18) - All data show good agreement except for energies at about 1.7 MeV or below. Errors in the cross-section compared to the measurements range from approximately 10% to 15% at 1.3 MeV. The DLC-2 data set shows the best agreement with the experimental result (except in the low energy region), although the errors are small for all three data sets. The error above 9.5 MeV is probably due to poor statistics in the experimental spectrum.

7.6.2 Lead (Fig. 19) - Good agreement is found with both data sets. The largest error at 5.7 MeV is only about 4% which is probably within the statistics of the experiment. The BNL data set seems to be best up to 6 MeV, after which both data sets differ from the experimental.

7.6.3 Oxygen (Fig. 20) - In general, much of the data do not adequately describe the depth of the minima at 2.35 MeV. At this point, the calculation based on the Foster data is within 8% of the experimentally measured cross-section data while UNC-5139 is in error by 40%. There is also some problem with most of the data at 4.7 MeV. The best data set over the entire spectrum is the DLC-9 data, except in the 2.35 MeV region. The discrepancy in this region would be expected since the cross-section has been averaged over some energy width and therefore underestimates the depth of the minima.

7.6.4 Sodium (Fig. 21) - Good agreement is found for most of the data for both samples. The experimental data points for the liquid sample tend to be slightly above the calculated as compared to the solid sample. However, the two experimental spectra agree within 3% and the error is probably due to an error in the density calculation for the liquid sample. The comparison

between these two sets of data shows that the experiment is sensitive to density changes as should be noted. The change in the density from the solid to the liquid sample was 6.4% which resulted in an increase in the calculated transmitted flux by approximately 45% at 3 MeV. As can be seen in Fig. 21 this change in the calculated transmitted spectrum due to the density change in the sample was also measured in the experimental transmitted flux since the experimental and calculated results show good agreement.

The BNL data sets show large errors from 5 MeV down, with a cross-section error of 10% at 1.8 MeV. Langsford shows a discrepancy at 7.3 MeV which does not appear in other data nor in the experimental result. An unfolding problem occurred with the solid sample below about 1.6 MeV and the data below this point are in error. The fluctuations in the experimental results in the higher energy region are probably statistical in nature and should be disregarded.

8.0 SUGGESTIONS FOR FURTHER STUDY

Now that the experimental procedure has been established, the evaluation of total neutron cross-sections for many materials can be quickly and accurately completed. Possibly the most accurate results would be obtained by using two collimators; one at the sample and one at the detector. This would eliminate both multiple and shallow angle scatters. However, it would be difficult to align both collimators with the equipment now available and single collimation at the detector or at the sample does give adequate results.

In order to study the forward scattering vs. multiple scattering phenomenon several penetration spectra could be taken with varying sample thicknesses and without collimation. If the measured result produced the same error in the total cross-section for all thicknesses, then it could be concluded that forward scattering was contributing a great deal to the measured transmitted spectra. However, if the total cross-section error increased with increasing thicknesses it could be concluded that multiple scattering was contributing to the measured spectra. In this experiment the contribution from forward scattered neutrons would always be present, however, it would be constant for all thicknesses. The contribution from multiple scattering, on the other hand, would increase with increasing thickness. The larger thicknesses would have a greater probability for multiple scattering and some of these neutrons would reach the detector. For small thicknesses (approximately 1 mean free path) the probability of multiple scattering is small, and any contribution to the uncollided flux would be from forward scattering only.

If the experiment outlined in the previous paragraph proves conclusively that there is a large contribution to the uncollided flux from

forward scattering neutrons in the uncollimated geometry, as has been indicated by the data taken at this time, then additional measurements of the actual forward scattering probability should be made. First, a more exact formulation of the actual contribution to the uncollided flux from shallow angle scattering near 0° should be derived based on available angular dependent cross section data. This would be a more precise analysis than was used in deriving equation 11, and would take into account the effects of multiple shallow angle scatters in thicker samples, the physical size of the sample, etc. Measurements could then be made, possibly using several different sized collimators. The use of several collimators would make it possible to check the reliability of the experiment and to gain knowledge of the variation in differential scattering probability with angle for angles very close to the 0° angle. As the solid angle subtended by the detector is increased, the number of neutrons detected is a measure of the forward scattering probability over that particular solid angle. The resultant total cross-section discrepancies would be due to forward scattering and could be used to calculate the differential scattering probability near the 0° angle using the formulation derived.

9.0 ACKNOWLEDGEMENTS

The author wishes to express his sincerest gratitude to Dr. Walter Meyer for all of his help and advice throughout the course of this study. Special thanks must be extended to the Department of Nuclear Engineering, the Atomic Energy Commission Fellowship program, and the Atomic Energy Commission Division of Research for their financial support. Also, a note of thanks is extended to Dr. Hermann J. Donnert, Dr. J. K. Shultis, J. W. Thiesing and all others of the Department of Nuclear Engineering who gave their assistance. Finally, a special thank you is given to my wife, Kaye, for her encouragement and support.

10.0 REFERENCES

1. Burris, W. R., "Status of FERDOR Neutron Unscrambling with NE-213 Response Matrix," Intra Laboratory Correspondence, Oak Ridge National Laboratory, Oak Ridge, Tennessee (November 2, 1967).
2. Cierjacks, S., P. Forti, D. Kopsch, L. Kropp, J. Nebe, and H. Unseld, "High Resolution Total Neutron Cross-Sections Between 0.5 - 0.30 MeV," KFK-1000, Institut fur Angewandte Kernphysik, Karlsruhe (June, 1968).
3. Clifford, C. E., E. A. Straker, et al., "Measurements of the Spectra of Uncollided Fission Neutrons Transmitted Through Thick Samples of Nitrogen, Oxygen, Carbon, and Lead: Investigation of the Minimum Total Cross Section," Nucl. Sci. Eng., 27, 299 (1967).
4. DLC-2B, Code Name: Neutron--99 Group Cross-Section, Radiation Shielding Institute Center (July 1, 1969).
5. DLC-9, Code Name: FARS Data 122 Group (104 Neutron, 18 Gamma), Radiation Shielding Institute Center (June 11, 1969).
6. Evaluated Nuclear Data File of the National Neutron Cross Section Center, Brookhaven National Laboratory.
7. Foster, D. G., Oxygen Total Neutron Cross-Section Data, Battelle Northwest (May, 1967).
8. Foster, D. G., and D. W. Glasgow, "Method for Measuring Total Cross-Sections with Neutrons Having Energies from 2.5 to 15 MeV," Nuclear Instruments and Methods, Vol. 36 (January, 1965).
9. Glastone, Samuel, and Alexander Sesonske, Nuclear Reactor Engineering, D. Van Nostrand Co., Inc., Princeton, N. J. (1967).
10. Goldberg, Murrey D., Victoria M. May and John R. Stehn, "Angular Distributions in Neutron-Induced Reactions," BNL 400 (Physics-TID-4500), Brookhaven National Laboratory, National Bureau of Standards, Springfield, Virginia (February 1963).
11. Goldberg, Murrey D., Said F. Mughabghab, et al., "Neutron Cross-Sections," BNL-325, Supplement No. 2 (Physics-TID-4500), Brookhaven National Laboratory, National Bureau of Standards, Springfield, Virginia (February 1967).
12. Handling Metallic Sodium on a Plant Scale, U. S. Industrial Chemicals Co., New York (1959).
13. Jackson, Carey B., Ed., Liquid Metals Handbook, Sodium (NaK) Supplement, U. S. Government Printing Office, Washington D. C. (1955).
14. Langsford, "International Conference on the Study of Nuclear Structure with Neutron Antwerp," (July, 1965).

15. Meyer, Walter, and C. Michael Estes, Private Communication - Unpublished data (April, 1971).
16. Meyer, W., J. W. Thiesing, and C. M. Estes, "Intercalibration of the KSU NE-213 Fast-Neutron Spectrometer System," Technical Progress Report to Division of Research USAEC (AEC Contract No. AT(11-1) 2049), COO-2049-3 Nuclear Engineering, Kansas State University (December 1970).
17. Neal, M. A. and A. E. Miller, Liquid Metals Engineering Center, Canoga Park, California, USAEC, Personal Letter (July 1970).
18. Noffke, Harold of Air Products and Chemicals, Inc., Kansas City, Missouri, Personal Interview (May 8, 1970).
19. "Operation Procedure, Wichita No. 2050-103: Liquid Oxygen," Boeing Company Manual, Wichita, Kansas (April 23, 1968).
20. Ray, J. H., G. Grochowski and E. S. Troubetzkoy, "Neutron Cross Sections of Nitrogen, Oxygen, Aluminum, Silicon, Iron, Deuterium, and Beryllium," UNC-5139, United Nuclear Corporation, Elmsfor, New York (1965).
21. "Safety-Gram, No. 54-c: Liquid Oxygen," Air Products and Chemicals, Inc., Kansas City, Missouri (January 31, 1967).
22. Schwartz, R. B., National Bureau of Standards, Private Communication - Unpublished data (July 1970).
23. Simons, G. G., "Development, Calibration and Utilization of the KSU Fast Neutron Spectrometer System," a Ph.D. Dissertation, Kansas State University (1968).
24. Sitting, Marshall, Sodium--Its Manufacture, Properties, and Uses, Reinhold Publishing Corp., New York, N. Y. (1956).
25. Smithalls, Metals Reference Book, Butterworths, London, England (1967).
26. Straker, E. A., "Experimental Evaluation of Minima in Total Neutron Cross Sections of Several Shielding Materials," ORNL TM-2242, Oak Ridge National Laboratory, Oak Ridge, Tennessee (June 6, 1968).
27. Wick, G. C., Atti Acad. d'Ital., 13, 1203 (1943).
28. Wilk, I. J., "Dangers due to Increased Flammability of Materials in Oxygen-Enriched Atmospheres," Journal of Chemical Education (July 1968).
29. Wright, R. Q., J. L. Lucius, N. M. Greene, and C. W. Craven, "SUPERTO: A Program to Generate Fine Group Constants and P Scattering Matrices Form ENDF/B," ORNL-TM-2679 (1969).

APPENDIX A

COMPUTER PROGRAMS

CALFLUX

NE213RES

POLYFIT

APPENDIX A
COMPUTER PROGRAMS
CALFLUX

This program calculates the transmitted neutron spectrum through samples and smooths the results with the NE-213 resolution function as given by Equation 10 on page 6. After reading all of the input data, the program establishes a cross-section data point or incident spectrum data point for each energy that appears in either the cross-section or incident spectrum library by calling subroutine ENGRID. The program then begins to calculate the transmitted flux at given energies starting with 0.8 MeV in 0.1 MeV intervals to 3.0 MeV, and then in 0.2 MeV intervals (same energy intervals as the FERDOR output). For each energy the FWHM of the resolution function is calculated, and the actual integration is carried out over some energy width calculated by multiplying constant (PFWHM) times the FWHM. (The contribution to the area under a gaussian curve is small past approximately two times the FWHM from the center of the peak.) The contribution to the transmitted flux from each energy interval over the width of the integration is calculated and summed. The energy intervals are for each E_i to E_{i+1} as established by the subroutine ENGRID.

Only one problem was encountered with this procedure. When large positive slopes were present in the cross-section data, the arguments of Equation 10 became such that the value of the error function (erf) was very close to 1.0. Thus, when the difference between two error functions were taken, the result was set equal to zero by the computer. At the same time, the constants that were being multiplied by this difference became very large; however, the product calculated by the computer was always zero. To overcome this problem, the program tests the value of the difference term,

and if it becomes very small the program calls the subroutine ROMBRG which numerically finds the value of the integral between these two energy points.

Output from CALFLUX includes the physical constants for the sample used and a plot of the input cross-section library and incident spectrum library. The resultant calculated flux is listed and also plotted along with the experimentally measured transmitted flux.

INPUT

Card	Format		
1	8F10.4	1) T	= Sample thickness (cm)
		2) RHO	= Molecular Density (atom/cc) $\times 10^{24}$
2	8F10.4	1) WIDTH	= A multiplication constant times the FWHM at which the resolution gaussian will be truncated
3	8F10.4	1) XNORM	= normalization factor between the incident and penetration integrated flux
4	8F10.4	1) PFWHM	= the percentage of calcu- lated FWHM used for the resolution function
5	8F10.4	1) EMAX	= Maximum energy to which the program will calculate the transmitted spectrum
6	I3	1) NXSECT	= number of points in the cross-section library
7 (Deck)	8F10.4	1) EX(I)	= energy of the <u>ith</u> cross- section data point (MeV)
		2) XSECT(I)	= the <u>ith</u> cross-section (barns)
		3) EX(I+1)	= energy...
		⋮	
		8) XSECT(I+3)	= cross-section...

Card	Format		
8	I3	1) NA	= number of incident spectrum library points
9 (Deck)	(FERDOR output Format)	1) ES(I)	= energy of the <u>i</u> th incident spectrum data point (eV)
		2) SPCT(I)	= the <u>i</u> th incident spectrum point ($\text{n/cm}^2 \cdot \text{min} \cdot \text{MeV}$)
10	I3	1) NE	= number of penetration spectrum library points
11 (Deck)	(FERDOR output Format)	1) EE(I)	= energy of the <u>i</u> th penetration spectrum data point (eV)
		2) SPCTE(I)	= the <u>i</u> th penetration spectrum point ($\text{n/cm}^2 \cdot \text{min} \cdot \text{MeV}$)

NOTE:

- 1) The library cross-section must extend from .01 to 15 MeV and must exceed the incident spectrum library at both lower and upper energies.
- 2) The maximum energy in the incident and penetration spectrum library must exceed EMAX.

CALFLUX Listing

FORTRAN IV G LEVEL 18

MAIN

DATE = 71109

22/14/21

```

C      THIS PROGRAM CALCULATES TRANSMITTED NEUTRON SPECTRUM
C      THROUGH SAMPLES AND SMOOTHS THE RESULTS WITH THE
C      NE 213 RESOLUTION FUNCTION
C
C      THE LIBRARY CROSS-SECTION MUST EXTEND FROM .01 TO 15 MEV
C      AND MUST EXCEED THE SPECTRUM LIBRARY AT BOTH LOWER AND UPPER ENERGIES
C
C      T = THICKNESS OF SAMPLE (CM)
C      RHO = MOLECULAR DENSITY (ATOMS/CC) X 10**24
C      XNORM = NORMALIZATION FACTOR BETWEEN REACTOR POWER LEVELS FOR
C      INCIDENT AND TRANSMITTED SPECTRA MEASUREMENTS
C      NSECT = NUMBER OF ENTRIES IN LIBRARY CROSS-SECTION
C      EX(I),XS(I) = ENERGY AND CORRESPONDING CROSS-SECTION IN
C      CROSS-SECTION LIBRARY (MEV,BARNS)
C      WIDTH = A MULTIPLICATION CONSTANT TIMES THE FWHM AT WHICH THE
C      RESOLUTION GAUSSIAN WILL BE TRUNCATED
C      PFWHM = THE PERCENTAGE OF CALCULATED FWHM USED FOR RESOLUTION FUNCTION
C      WE(I),WSECT(I) = ENERGY AND CORRESPONDING INCIDENT SPECTRUM FROM
C      FROM FERDOR CODE AND MUST EXCEED EMAX
C      WEE(I),WSPECTE(I) = ENERGY AND CORRESPONDING EXPERIMENTAL
C      SPECTRUM FROM FERDOR CODE AND MUST EXCEED EMAX
C      EMAX = MAXIMUM ENERGY TO WHICH THE PROGRAM WILL CALCULATE THE
C      TRANSMITTED FLUX
C
0001      IMPLICIT REAL*8 (A-H,O-V,X-Z)
0002      DOUBLE PRECISION DLOG,CEXP,DERF,DABS
0003      EXTERNAL FCN
0004      DIMENSION SPCT(75),EE(75),SPCTE(75),X(150),P(150),ENE(75),FL(75)
0005      COMMON /HOLD1/ EX(100),XS(100),ES(75),SPECTL(75)
0006      COMMON /HOLD2/ E(150),XSECT(150),FLUL(150)
0007      COMMON /HOLD3/ ENERGY,BD,NLO
0008      CALL ERRSET (208,50,1,C,0,0)
0009      900 FORMAT (I3)
0010      901 FORMAT (8F10.4)
0011      902 FORMAT (8X,E10.3,3X,E10.3)
0012      910 FORMAT (11H1,'THIS PROGRAM CALCULATES A SMOOTHED TRANSMITTED SPECTRUM
          FROM TABULATED DATA USING THE RESOLUTION FUNCTION OF THE NE 213
          1',/,40X,'USING THE FOLLOWING PARAMETERS:',/,,,/)
0013      911 FORMAT ('0 THE RESOLUTION HAS BEEN TRUNCATED AT',F6.3,'TIMES THE
          1FWHM OF THE GAUSSIAN')
0014      913 FORMAT('0 THE SAMPLE THICKNESS IS T = ',F10.3,' CM, AND THE MOLEC
          ULAR DENSITY IS RHO = ',D10.3,' X 10**24 MOLECULES/CC',/,,,' THE
          2NORMALIZATION FACTOR IS XNORM = ',F10.3)
0015      914 FORMAT ('1','THE CALCULATED, SMOOTHED TRANSMITTED SPECTRA IS: ',/
          1,5X,'ENERGY',/X,'FLUX TRANSMITTED')
0016      915 FORMAT (5X,F5.1,10X,D12.5)
0017      916 FORMAT (5X,F5.1,10X,D12.5,' POSSIBLE ERROR BECAUSE GAUSSIAN RESOLU
          TION CURVE IS BEING TRUNCATED AT .01 MEV')
0018      917 FORMAT (' PROGRAM HAS BEEN TERMINATED BECAUSE UPPER LIMIT OF INTE
          GRATION EXCEEDS CROSS-SECTION LIBRARY')
0019      919 FORMAT ('1 PLOT OF LOG(FLUX) VS ENERGY',/,,,' ENERGY CAL. F
          LUX EXP. FLUX + = CALCULATED * = EXPERIMENTAL')
0020      920 FORMAT ('1 THE INPUT CROSS-SECTION LIBRARY IS AS FOLLOWS:',/,6X,'
          1ENERGY',3X,'CROSS-SECTION')
0021      921 FORMAT ('1 THE INPUT SPECTRUM IS AS FOLLOWS:',/,6X,'ENERGY',3X,'L
          OCG(SPECTRUM)')

```

FORTRAN IV G LEVEL 18

MAIN

DATE = 71109

22/14/21

```

0022      922 FORMAT ('0 THE FWHM HAS BEEN MULTIPLIED BY ',F6.3)
0023      PI = 3.141592653
0024      READ 901,T,RHO
0025      READ 901,WIDTH
0026      READ 901,XNORM
0027      READ 901,PFWHM
0028      READ 901,EMAX
0029      READ 900,NXSECT
0030      DO 1 I=1,NXSECT,4
0031      1 READ 901,EX(I),XS(I),EX(I+1),XS(I+1),EX(I+2),XS(I+2),EX(I+3),XS(I+
        13)
0032      READ 900,NA
0033      DO 20 I=1,NA
0034      READ 902,ES(I), SPCT(I)
0035      ES(I) = ES(I)*0.1D-05
0036      20 SPCT(I) = DLOG(SPCT(I))
0037      READ 900,NE
0038      DO 42 I=1,NE
0039      42 READ 902, EE(I), SPCTE(I)
0040      DO 44 I=1,NE
0041      IF (SPCTE(I) .LE. 0.000) SPCTE(I) = SPCTE(NE)
0042      44 SPCTE(I) = DLOG(SPCTE(I))
0043      PRINT 910
0044      PRINT 913,T,RHO,XNORM
0045      PRINT 911,WIDTH
0046      PRINT 922,PFWHM
0047      CALL ENGRID (NXSECT,NA,NG)
0048      DO 2 I=1,NG
0049      2 XSECT(I) = XSECT(I)*T*RHO
0050      PRINT 920
0051      CALL PLAT2 (EX,XS,NXSECT)
0052      PRINT 921
0053      CALL PLAT2 (ES,SPECTL,NA)
0054      PRINT 914
0055      NGM1 = NG-1
0056      DO 30 I=1,NGM1
0057      DE = E(I+1)-E(I)
0058      X(I) = (XSECT(I+1)-XSECT(I))/DE
0059      30 P(I) = (FLUL(I+1)-FLUL(I))/DE
0060      WMAX = (EMAX-.3D01)/.2D00 + .2301D02
0061      MAXE = IFIX(WMAX)
0062      DO 3 I=1,MAXE
0063      FLUX = 0.0000
0064      NNN = 0
0065      IF (I.GT.22) GO TO 5
0066      4 ENERGY = .7+.1*I
0067      GO TO 6
0068      5 ENERGY = 3.0+.2*(I-23)
0069      6 FWHM = .885250782D00-.148362712D01*ENERGY+.139992319D01*ENERGY**2-
        1.52543823D00*ENERGY**3+.99524739D-01*ENERGY**4-.10331713D-01*ENE
        2RGY**5+.512664175D-03*ENERGY**6-.10426J772D-04*ENERGY**7
0070      FWHM = FWHM*PFWHM
0071      BU = FWHM*FWHM/(0.4D1*C.6931472D0)
0072      AL = 80**5
0073      ELO = ENERGY-FWHM*WIDTH
0074      IF (ELO-0.01) 7,7,8
0075      7 ELO = 0.01
0076      8 EUP = ENERGY+FWHM*WIDTH

```

FORTRAN IV G LEVEL 18

MAIN

DATE = 71109

22/14/21

```

0077      IF (EUP-E(NG)) 9,9,10
0078      9 CONTINUE
0079      DO 22 J=1,NG
0080      IF (ELO .LT. E(J)) GO TO 23
0081      22 CONTINUE
0082      23 K = 0
0083      AB = E(J-1)
0084      E(J-1) = ELO
0085      24 K = K+1
0086      K1 = K-1
0087      NLO = J-1+K1
0088      NUP = J+K1
0089      28 IF (E(NUP) .LT. EUP) GO TO 27
0090      ABC = E(NUP)
0091      E(NUP) = EUP
0092      NNN = 1
0093      27 YLO = (E(NLO)-ENERGY+0.5D0*X(NLO)*BO)/AL
0094      DYLO = DERF(YLO)
0095      YUP = (E(NUP)-ENERGY+0.5D0*X(NLO)*BO)/AL
0096      DYUP = DERF(YUP)
0097      ZLO = YLO-P(NLO)*AL/0.2D01
0098      DZLO = DERF(ZLO)
0099      ZUP = YUP-P(NUP)*AL/0.2D01
0100      DZUP = DERF(ZUP)
0101      CONST = X(NLO)*(E(NLO)-ENERGY)-XSECT(NLO)+0.25*X(NLO)**2*BO
0102      DDY = DYUP-DYLO
0103      IF (DABS(DDY) .LE. 0.1D-13) GO TO 40
0104      FLUX1 = DEXP(FLUL(NLO)+CONST)*DDY
0105      DDZ = DZUP-DZLO
0106      IF (DABS(DDZ) .LE. 0.1D-13) GO TO 40
0107      FLUX2 = DEXP(CONST+P(NLO)*(ENERGY-E(NLO))-X(NLO)*P(NLO)*BO/0.2D01-
      IP(NLO)*P(NLO)*BO/J.4D01)*DDZ
0108      GO TO 52
0109      40 FLUX1 = 0.0D00
0110      E11 = E(NLO)
0111      E22 = E(NLO+1)
0112      EPS = .1D-01
0113      MRON = 5
0114      NRON = 0
0115      FLUX2 = .2D01*ROMERG(E11,E22,EPS,MRON,NRON,FCN)/((BO*PI)**.5)
0116      52 FLUX = FLUX+0.5D00*(FLUX1+FLUX2)
0117      IF (K .EQ. 1) E(NLO) = AB
0118      IF (NNN .EQ. 1) GO TO 31
0119      GO TO 24
0120      31 E(NUP) = ABC
0121      FLUX = FLUX *XNORM
0122      ENE(1) = ENERGY
0123      FL(1) = DLOG(FLUX)
0124      IF (FLO .EQ. .01) GO TO 12
0125      PRINT 915,ENERGY,FLUX
0126      GO TO 3
0127      12 PRINT 916,ENERGY,FLUX
0128      3 CONTINUE
0129      PRINT 919
0130      CALL PLAT3 (ENE,FL,SPCTE,MAXE)
0131      GO TO 11
0132      10 PRINT 917
0133      11 STOP

```

FORTRAN IV G LEVEL 1R

ENGRID

DATE = 71109

22/14/21

```

0001      SUBROUTINE ENGRID (NXSECT,NA,NG)
0002      IMPLICIT REAL*8 (A-H,O-Z)
0003      DOUBLE PRECISION DLOG,DEXP,DABS
0004      COMMON /HOLD1/ EX(100),XS(100),ES(75),SPECTL(75)
0005      COMMON /HOLD2/ E(150),XSECT(150),FLUL(150)
0006      FLUL(1) = DLOG(DEXP(SPECTL(1))/0.2001)
0007      E(1) = EX(1)
0008      XSECT(1) = XS(1)
0009      I=1
0010      K = 1
0011      J = 1
0012      I1 = 1
0013      J1 = 0
0014      1 I = I+I1
0015      J = J+J1
0016      K = K+1
0017      IF ((EX(I)-0.10-05) .GT. ES(J)) GO TO 10
0018      IF (DABS(EX(I)-ES(J)) .LT. 0.10-05) GO TO 11
0019      E(K) = EX(I)
0020      J1 = 0
0021      I1 = 1
0022      XSECT(K) = XS(I)
0023      FLUL(K) = ((SPECTL(J)-FLUL(K-1))*(E(K)-E(K-1))/(ES(J)-E(K-1)))+FLUL
0024      1(K-1)
0025      GO TO 12
0026      10 E(K) = ES(J)
0027      J1 = 1
0028      I1 = 0
0029      FLUL(K) = SPECTL(J)
0030      XSECT(K) = ((XS(I)-XSECT(K-1))*(E(K)-E(K-1))/(EX(I)-E(K-1)))+XSECT(
0031      1(K-1)
0032      GO TO 12
0033      11 E(K) = ES(J)
0034      J1 = 1
0035      I1 = 1
0036      FLUL(K) = SPECTL(J)
0037      XSECT(K) = XS(I)
0038      12 CONTINUE
0039      IF (J .GE. NA) GO TO 13
0040      GO TO 1
0041      13 K = K+1
0042      I = I+I1
0043      E(K) = EX(I)
0044      XSECT(K) = XS(I)
0045      FLUL(K) = SPECTL(NA)
0046      I1 = 1
0047      IF (I .GE. NXSECT) GO TO 15
0048      GO TO 13
0049      15 NG = K
0050      RETURN
0051      END

```

22/14/21

Address	Instruction	Comment
0001	FUNCTION ROMBERG (A,B,EPS,M,N,FCN)	
0002	IMPLICIT REAL*8(A-H,O-Z)	
	CRUMBERG INTEGRATION	01530001
0003	DIMENSION P(20)	01530005
0004	IF(N.LT.2)GO TO 200	
0005	IF(N.GT.3)GO TO 200	
0006	IF(M-2)199,99,98	01530007
0007	98 M=20	01530008
0008	99 X=A	01530009
0009	MM=M	
0010	NN=N+1	
0011	EP=FCN(X)	01530010
0012	X=FCN(B)	
0013	2001 SUM=(X+EP)*0.500	
0014	M=2	
0015	2007 AEP=DABS(EP)	
0016	2008 AX=DABS(X)	
0017	2009 ASUM=(AEP+AX)*0.500	
0018	FMAX=AEP	
0019	IF(FMAX.GE.AX)GO TO 100	
0020	FMAX=AX	
0021	100 I=1	
0022	NC=1	
0023	H=B-A	
0024	S1=H*SUM	
0025	P(1)=S1	
0026	AS1=H*ASUM	
0027	2002 X=A-H*0.500	01530018
0028	GO TO 102 J=1,NC	
0029	X=X+H	01530021
0030	M=M+1	
0031	EP=FCN(X)	
0032	2010 AEP=DABS(EP)	
0033	IF(FMAX.GE.AEP)GO TO 101	
0034	FMAX=AEP	
0035	101 SUM=SUM+EP	
0036	102 ASUM=ASUM+EP	
0037	2003 S2=H*SUM*0.500	01530023
0038	2011 AS2=H*ASUM*0.500	
0039	K=1	01530025
0040	GO TO 105	01530026
0041	2012 EP=DABS(S2-S1)	
0042	2013 AX=DABS(S2)	
0043	GO TO (110,2004,111,112),NN	
0044	110 CEP=AX	
0045	GO TO 113	
0046	2004 DEP=1.000	
0047	GO TO 113	
0048	111 DEP=AS2	
0049	GO TO 113	
0050	112 DEP=FMAX	
0051	113 I=EP-EPS*DEP	
0052	IF(I)107,107,103	01530029
0053	103 IF(I-PM)2005,108,2005	
0054	2005 H=H*0.500	01530031
0055	S1=S2	01530033
0056	AS1=AS2	
0057	P(K)=S2	01530034

FORTRAN IV G LEVEL 18

RUMBRG

DATE = 71109

22/14/21

0058	I=I+1	01530045
0059	NC=2*NC	
0060	GO TO 2002	01530037
0061	105 IF (K.GT.1) GO TO 2012	
0062	J=2*K	
0063	C=2**J	01530040
0064	T=S2	01530041
0065	2006 S2=(C*S2-P(K))/(1-1.00C)	01530042
0066	P(K)=T	01530044
0067	K=K+1	01530045
0068	GO TO 105	01530046
0069	108 PRINT 1,I	01530047
0070	1 FORMAT(' M EXCEEDED I= ',I2)	01530048
0071	107 RUMBRG=S2	01530049
0072	EPS=EP/DEP	
0073	GO TO 120	
0074	200 PRINT 2,N	
0075	2 FORMAT(' ERROR RETURN N= ',I2)	
0076	120 RETURN	
0077	END	


```

FORTRAN IV G LEVEL 18          FCN          DATE = 71109          22/14/21

0001      FUNCTION FCN(X)
0002      IMPLICIT REAL*8 (A-H,O-Z)
0003      DOUBLE PRECISION DEXP
0004      COMMON /HOLD2/ E(150),XSECT(150),FLUL(150)
0005      COMMON /HOLD3/ ENERGY,B0,NLO
0006      FLUXL = FLUL(NLO)+((FLUL(NLO+1)-FLUL(NLO))*(X-E(NLO)))/(E(NLO+1)-E
0007      (NLO))
0007      XS = XSECT(NLO)+((XSECT(NLO+1)-XSECT(NLO))*(X-E(NLO)))/(E(NLO+1)-
0008      E(NLO))
0008      FCN = DEXP(FLUXL-XS)*DEXP(-(ENERGY-X)**2/B0)
0009      RETURN
0010      END

```

FORTTRAN IV G LEVEL 18

PLAT2

DATE = 71109

22/14/21

```
0001      SUBROUTINE PLAT2(Z,Y,N)
C
C          PLOTTING SUBROUTINE PLAT2
0002      IMPLICIT REAL*8 (A-H,U-W,Y-Z)
0003      INTEGER XX
0004      DIMENSION XX(120),Z(N),Y(N),NN(2)
0005      DATA NN/1H ,1H*/
0006      YMAX = -1.E50
0007      YMIN = 1.E50
0008      DO 3 I=1,N
0009        IF(Y(I) - YMAX) 5,5,4
0010        4 YMAX = Y(I)
0011        5 IF (YMIN - Y(I)) 3,3,6
0012        6 YMIN = Y(I)
0013        3 CONTINUE
0014        RANGE = YMAX - YMIN
0015        DIV = RANGE/100.
0016        PRINT 30,DIV
0017        30 FORMAT(1H ,25X,' THE SCALE OF THIS GRAPH IS 1 DIVISION =' ,D12.5,'U
INTS'//,29X,'123456789012345678901234567890123456789012345678901234567890123456789012345678901234567890123456789012345678901234567890123456789012345678901')
0018        CO 1 J=1,120
0019        1 XX(J) = NN(1)
0020        IX = 1
0021        CO 2 I=1,N
0022        XX(IX) = NN(1)
0023        X = 1.0+(99./RANGE)*(Y(I)-YMIN)
0024        IX = IFIX(X)
0025        XX(IX) = NN(2)
0026        IF (I .EQ. 1) GO TO 8
0027        IF((Z(I)-Z(I-1)).GT. .15D00) GO TO 7
0028        8 PRINT 20,Z(I),Y(I),(XX(J),J=1,101)
0029        20 FORMAT (1H ,2012.4,'----',101A1)
0030        GO TO 2
0031        7 IF(Z(I)-Z(I-1) .GT. .25) GO TO 9
0032        PRINT 10,Z(I),Y(I),(XX(J),J=1,101)
0033        10 FORMAT (1H0,2012.4,'----',101A1)
0034        GO TO 2
0035        9 PRINT 40,Z(I),Y(I),(XX(J),J=1,101)
0036        40 FORMAT (1H-,2012.4,'----',101A1)
0037        2 CONTINUE
0038        RETURN
0039        END
```

FORTRAN IV G LEVEL 18

PLAT3

DATE = 71109

22/14/21

```

0001      SUBROUTINE PLAT3(Z,Y,W,N)
      C
      C      PLOTTING SUBROUTINE PLAT3
      C
      C      THIS SUBROUTINE PLOTS ON THE ORDINATE TWO VARIABLES (Y & W)
      C      VERSES THE VARIABLE Z ON THE ABSISSA.
      C
0002      IMPLICIT REAL*8 (A-H,O-W,Y-Z)
0003      DOUBLE PRECISION DEXP
0004      INTEGER XX,XX2
0005      DIMENSION XX(120),XX2(120),Z(N),Y(N),W(N),NN(3)
0006      DATA NN/1H,1H+,1H*/
0007      YMAX = -1.E50
0008      YMIN = 1.E50
0009      DO 3 I=1,N
0010          IF(Y(I) - YMAX) 5,5,4
0011      4 YMAX = Y(I)
0012      5 IF (YMIN - Y(I)) 3,3,6
0013      6 YMIN = Y(I)
0014      3 CONTINUE
0015      DO 14 I=1,N
0016          IF(W(I)-YMAX) 12,12,13
0017      13 YMAX = W(I)
0018      12 IF(YMIN-W(I)) 14,14,15
0019      15 YMIN = W(I)
0020      14 CONTINUE
0021      RANGE = YMAX - YMIN
0022      DIV = RANGE/100.
0023      PRINT 30,DIV
0024      30 FORMAT(1H,25X,' THE SCALE OF THIS GRAPH IS 1 DIVISION =',E12.5,'U
      INITS'//,31X,'12345678901234567890123456789012345678901234567890123
      2456789012345678901234567890123456789012345678901')
      DO 1 J=1,120
0025      1 XX(J) = NN(1)
0026      IX = 1
0027      IX2 = 1
0028      DO 2 I=1,N
0029          XX(IX) = NN(1)
0030          XX(IX2) = NN(1)
0031          X = 1.0+(99./RANGE)*(Y(I)-YMIN)
0032          X2 = 1.0+(99./RANGE)*(W(I)-YMIN)
0033          IX = IFIX(X)
0034          IX2 = IFIX(X2)
0035          XX(IX) = NN(2)
0036          IF (IX .NE. IX2) XX(IX2) = NN(3)
0037          Y(I) = DEXP(Y(I))
0038          W(I) = DEXP(W(I))
0039          IF (I .EQ. 1) GO TO 8
0040          IF((Z(I)-Z(I-1)) .GE. .15000) GO TO 9
0041      8 PRINT 20,Z(I),Y(I),W(I),(XX(J),J=1,101)
0042      20 FORMAT (1H,3E9.2,'---',101A1)
0043      21 FORMAT (1H+,30X,101A1)
0044      GO TO 2
0045      9 PRINT 10,Z(I),Y(I),W(I),(XX(J),J=1,101)
0046      10 FORMAT (1H0,3E9.2,'---',101A1)
0047      2 CONTINUE
0048      RETURN
0049      END
0050

```

Sample Input Data - CALFLUX

15.24	.08497						
1.5							
30.826							
0.75							
11.0							
40							
0.01	5.00	0.40	5.00	0.50	4.00	0.63	2.50
0.80	4.00	0.90	2.80	1.00	2.40	1.10	2.80
1.20	2.50	1.30	3.40	1.38	2.50	1.44	3.70
1.50	2.00	1.56	3.80	1.60	3.00	2.00	3.00
2.10	3.50	2.20	3.20	2.40	3.40	2.55	4.20
2.65	3.40	3.00	3.30	3.20	3.70	3.30	3.10
3.50	3.60	3.60	3.50	4.10	3.70	4.20	3.20
4.30	3.70	4.40	3.40	4.50	3.80	5.00	3.70
7.00	3.60	4.20	3.30	8.30	3.50	8.70	3.20
8.80	3.30	12.0	2.80	14.0	2.60	15.0	2.50
65							
1	0.800E 06	0.701E 04					
2	0.600E 06	0.785E 04					
3	0.100E 07	0.802E 04					
4	0.110E 07	0.813E 04					
5	0.120E 07	0.848E 04					
6	0.130E 07	0.838E 04					
7	0.140E 07	0.813E 04					
8	0.150E 07	0.781E 04					
9	0.160E 07	0.742E 04					
10	0.170E 07	0.714E 04					
11	0.180E 07	0.660E 04					
12	0.190E 07	0.618E 04					
13	0.200E 07	0.566E 04					
14	0.210E 07	0.518E 04					
15	0.220E 07	0.476E 04					
16	0.230E 07	0.443E 04					
17	0.240E 07	0.413E 04					
18	0.250E 07	0.387E 04					
19	0.260E 07	0.360E 04					
20	0.270E 07	0.334E 04					
21	0.280E 07	0.307E 04					
22	0.290E 07	0.283E 04					
23	0.300E 07	0.261E 04					
24	0.320E 07	0.223E 04					
25	0.340E 07	0.191E 04					
26	0.360E 07	0.165E 04					
27	0.380E 07	0.156E 04					
28	0.400E 07	0.148E 04					
29	0.420E 07	0.141E 04					
30	0.440E 07	0.130E 04					
31	0.460E 07	0.110E 04					

32	0.480E	07	0.105E	04
33	0.500E	07	0.025E	03
34	0.520E	07	0.835E	03
35	0.540E	07	0.773E	03
36	0.560E	07	0.707E	03
37	0.580E	07	0.641E	03
38	0.600E	07	0.600E	03
39	0.620E	07	0.572E	03
40	0.640E	07	0.528E	03
41	0.660E	07	0.468E	03
42	0.680E	07	0.408E	03
43	0.700E	07	0.352E	03
44	0.720E	07	0.302E	03
45	0.740E	07	0.257E	03
46	0.760E	07	0.210E	03
47	0.780E	07	0.180E	03
48	0.800E	07	0.165E	03
49	0.820E	07	0.140E	03
50	0.840E	07	0.127E	03
51	0.860E	07	0.124E	03
52	0.880E	07	0.110E	03
53	0.900E	07	0.961E	02
54	0.920E	07	0.836E	02
55	0.940E	07	0.726E	02
56	0.960E	07	0.628E	02
57	0.980E	07	0.530E	02
58	0.100E	08	0.453E	02
59	0.102E	08	0.366E	02
60	0.104E	08	0.276E	02
61	0.106E	08	0.192E	02
62	0.108E	08	0.124E	02
63	0.110E	08	0.804E	01
64	0.112E	08	0.585E	01
65	0.114E	08	0.506E	01

65

1	0.800E	06	0.208E	05
2	0.900E	06	0.198E	05
3	0.100E	07	0.205E	05
4	0.110E	07	0.215E	05
5	0.120E	07	0.205E	05
6	0.130E	07	0.180E	05
7	0.140E	07	0.152E	05
8	0.150E	07	0.127E	05
9	0.160E	07	0.107E	05
10	0.170E	07	0.032E	04
11	0.180E	07	0.811E	04
12	0.190E	07	0.691E	04
13	0.200E	07	0.576E	04
14	0.210E	07	0.476E	04

15	0.220E 07	0.207E 04
16	0.220E 07	0.226E 04
17	0.240E 07	0.284E 04
18	0.250E 07	0.241E 04
19	0.260E 07	0.207E 04
20	0.270E 07	0.182E 04
21	0.280E 07	0.163E 04
22	0.290E 07	0.148E 04
23	0.300E 07	0.134E 04
24	0.320E 07	0.111E 04
25	0.340E 07	0.897E 03
26	0.360E 07	0.722E 03
27	0.380E 07	0.597E 03
28	0.400E 07	0.515E 03
29	0.420E 07	0.465E 03
30	0.440E 07	0.428E 03
31	0.460E 07	0.389E 03
32	0.480E 07	0.338E 03
33	0.500E 07	0.285E 03
34	0.520E 07	0.243E 03
35	0.540E 07	0.216E 03
36	0.560E 07	0.203E 03
37	0.580E 07	0.196E 03
38	0.600E 07	0.190E 03
39	0.620E 07	0.178E 03
40	0.640E 07	0.158E 03
41	0.660E 07	0.135E 03
42	0.680E 07	0.120E 03
43	0.700E 07	0.114E 03
44	0.720E 07	0.109E 03
45	0.740E 07	0.100E 03
46	0.760E 07	0.867E 02
47	0.780E 07	0.735E 02
48	0.800E 07	0.645E 02
49	0.820E 07	0.612E 02
50	0.840E 07	0.611E 02
51	0.860E 07	0.606E 02
52	0.880E 07	0.575E 02
53	0.900E 07	0.520E 02
54	0.920E 07	0.452E 02
55	0.940E 07	0.381E 02
56	0.960E 07	0.312E 02
57	0.980E 07	0.251E 02
58	0.100E 08	0.200E 02
59	0.102E 08	0.158E 02
60	0.104E 08	0.123E 02
61	0.106E 08	0.929E 01
62	0.108E 08	0.694E 01
63	0.110E 08	0.532E 01
64	0.112E 08	0.442E 01
65	0.114E 08	0.408E 01

CALFLUX Sample Output

THIS PROGRAM CALCULATES A SMOOTHED TRANSMITTED SPECTRUM FROM TABULATED DATA USING THE RESOLUTION FUNCTION OF THE REF 2.3
USING THE FOLLOWING PARAMETERS:

THE SAMPLE THICKNESS IS T = 91.280 CM, AND THE MOLECULAR DENSITY IS RHO = C.403D-01 X 10**24 MOLECULES/CC

THE NORMALIZATION FACTOR IS XNORM = 25.694

THE RESOLUTION HAS BEEN TRUNCATED AT 1.500TIMES THE FWHM OF THE GAUSSIAN

THE FWHM HAS BEEN MULTIPLIED BY 0.750

THE CALCULATED, SMOOTHED TRANSMITTED SPECTRA IS:

ENERGY	FLUX TRANSMITTED
0.8	0.259010 01
0.9	0.256180 01
1.0	0.145410 01
1.1	0.716730 00
1.2	0.900500 00
1.3	0.377750 01
1.4	0.139190 02
1.5	0.330040 02
1.6	0.542280 02
1.7	0.723830 02
1.8	0.132630 03
1.9	0.370940 03
2.0	0.993240 03
2.1	0.272110 04
2.2	0.311190 04
2.3	0.378750 04
2.4	0.377720 04
2.5	0.326080 04
2.6	0.249120 04
2.7	0.172700 04
2.8	0.112020 04
2.9	0.693750 03
3.0	0.417690 03
3.2	0.141500 03
3.4	0.405110 02
3.6	0.133300 02
3.8	0.147600 02
4.0	0.251670 02
4.2	0.368990 02
4.4	0.546380 02
4.6	0.779380 02
4.8	0.910850 02
5.0	0.918580 02
5.2	0.933080 02
5.4	0.911210 02
5.6	0.825820 02
5.8	0.861460 02
6.0	0.111530 03
6.2	0.149610 03
6.4	0.178340 03
6.6	0.177990 03
6.8	0.146750 03
7.0	0.122270 03
7.2	0.633860 02
7.4	0.407120 02
7.6	0.337650 02
7.8	0.349330 02
8.0	0.355560 02
8.2	0.318580 02
8.4	0.253850 02
8.6	0.190870 02
8.8	0.144280 02
9.0	0.113170 02
9.2	0.919160 01
9.4	0.758840 01
9.6	0.626570 01
9.8	0.517800 01

NE213RES

This program determines the resolution of the NE-213 detection system from the measured and unfolded responses to the monoenergetic neutrons. The code is based upon the expressions derived in Appendix B for gaussian resolution fitting using weighted least squares. Input to the program includes the upper and lower bounds of each point in the unfolded spectrum over which the gaussian is to be fit. Output includes the FWHM and the standard deviation on this value along with the comparison between the actual data and the calculated data based on the gaussian fit. The matrix inversion required in the calculation is done by the subroutine MATINV.

INPUT

Card	Format	
1	I10	1) NDS = Number of data sets to be analyzed
2	F10.0,I10	1) ENEUT = Nominal energy of the monoenergetic neutrons
		2) NDP = Number of data points in this set to be fit to the gaussian
3 (Deck)	8F10.0	1) EN(I) = Energies in the unfolded spectrum (MeV)
		:
4 (Deck)	8F10.0	1) PLO(I) = Lower bound of each point in the unfolded spectrum
		:
5 (Deck)	8F10.0	1) PUP(I) = Upper bound of each point in the unfolded spectrum
		:

NE213RES Listing

```

FORTRAN IV G LEVEL 18          MAIN          DATE = 71109          22/12/23

C**** THIS PROGRAM DETERMINES THE RESOLUTION OF A DETECTION SYSTEM FROM
C**** THE MEASURED AND UNFOLDED RESPONSES TO THE MONOENERGETIC NEUTRONS
0C01      IMPLICIT REAL*8 (A-H,O-Z)
0C02      DOUBLE PRECISION DLOG,DEXP
0C03      DIMENSION Y(25),EN(25),A(3,3),B(3),VAR(25),PLO(25),PUP(25)
          L,HIDUM(3,1)
0C04      1 FORMAT(8F10.0)
0005      2 FORMAT(110)
0C06      3 FORMAT(F11.0,110)
0C07      4 FORMAT(/4X,27H EXPERIMENTAL NEUTRON ENERGY,5X,F5.2,2X,3HMEV)
0008      5 FORMAT(/4X,17H UNFOLDED ENERGIES)
0C09      6 FORMAT(1X,12F10.1)
0010      7 FORMAT(5X,17H UNFOLDED SPECTRUM)
0C11      8 FORMAT(5X,9H VARIANCES)
0C12      9 FORMAT(/4X,12H PEAK ENERGY=,F5.2,1X,3HMEV,3X,4H+OR-,F5.2,4H MEV)
0013      10 FORMAT(/4X,3H PEAK HT=,F10.0,3X,4H+OR-,F10.0)
0C14      11 FORMAT(/4X,20H FULL WIDTH HALF MAX=,F6.3,4H MEV,3X,4H+OR-,F6.3,
          14H MEV/)
0C15      556 FORMAT(1H0,20H NORMALIZED PEAK HT.=,D15.6,1X,11H N/CM-CM-SEC)
0C16      557 FORMAT(1H0,3H HD=,D15.6,1X,7H MEV-MEV)
C**** NDS IS THE NUMBER OF DATA SETS TO BE ANALYZED
0C17      READ(1,2)NDS
0018      DO 100 K=1,NDS

C
C**** ENEUT IS THE NOMINAL ENERGY OF THE MONOENERGETIC NEUTRONS
C**** NDP IS THE NUMBER OF DATA POINTS IN THIS SET
C
0019      READ(1,3)ENEUT,NDP
0C20      DO 20 II=1,NDP,8
0021      20 READ(1,1){EN(II-1+I),I=1,8}

C
C**** EN(I) ARE THE ENERGIES IN MEV IN THE UNFOLDED SPECTRUM
C
0C22      DO 21 II=1,NDP,8
0023      21 READ(1,1){PLO(II-1+I),I=1,8}
0C24      DO 22 II=1,NDP,8
0025      22 READ(1,1){PUP(II-1+I),I=1,8}
0026      DO 321 I=1,NDP
0027      PLO(I)=PLO(I)*10000.
0028      321 PUP(I)=PUP(I)*10000.

C
C**** PLO AND PUP ARE THE LOWER AND UPPER BOUNDS OF EACH POINT ON THE
C UNFOLDED SPECTRUM
C
0029      DO 200 I=1,NDP
0030      Y(I)=(PLO(I)+PUP(I))/2.
0031      200 VAR(I)=((PUP(I)-PLO(I))/2.)**2
0032      DO 101 I=1,3
0033      B(I)=0.
0034      DO 101 J=1,3
0035      101 A(I,J)=0.
0036      DO 102 I=1,NDP
0037      RATIO=Y(I)*Y(I)/VAR(I)
0038      A(1,3)=A(1,3)+RATIO
0039      A(2,3)=A(2,3)+RATIO*EN(I)
0040      A(3,2)=A(3,2)+RATIO*EN(I)*EN(I)
0041      A(2,1)=A(2,1)+RATIO*(LN(I)**3)
0042      A(1,1)=A(1,1)+RATIO*(EN(I)**4)

```

FORTRAN IV G LEVEL 18

MAIN

DATE = 71109

22/12/23

```

0043      B(1) = B(1)*RATIO*DLOG(Y(1))*EN(1)*EN(1)
0044      B(2) = B(2)*RATIO*DLOG(Y(1))*EN(1)
0045      102 B(3) = B(3)*RATIO*DLOG(Y(1))
0046      A(3,2)=A(2,3)
0047      A(3,1)=A(2,2)
0048      A(1,3)=A(2,2)
0049      A(1,2)=A(2,1)
0050      DO 176 I=1,3
0051      176 BNUM(I,1)=B(I)
0052      N1 = 1
0053      N3 = 3
0054      CALL MATINV(A,N3,BNUM,N1,DETERM,N3)
0055      DO 177 I=1,3
0056      177 B(1)=BNUM(I,1)
0057      BO=-1./B(1)
0058      EQ=BO*B(2)/2.
0059      YC = HEXP(B(3)+EQ*EQ/BO)
0060      DUM = DLOG(.2D01)
0061      FWHM = 2.*(BO*DUM)**.5
0062      VARBO=A(1,1)/(B(1)*B(1))
0063      SDVBO = VARBO**.5
0064      VAREQ=(B(2)*B(2)*VARBO+BO*BO*A(2,2))/4.
0065      SDVEQ = VAREQ**.5
0066      VARYC=YC*YC*(A(3,3)+4.*EQ*EQ*VAREQ/(BO*BO)+(VARBO*(EQ**4)))/
      I(BO**4))
0067      SDVYC = VARYC**.5
0068      VARFW=VARBO*DUM/BO
0069      SDVFW = VARFW**.5
0070      PI=3.1415927
0071      YNORM = 1./(BO*PI)**.5
0072      WRITE(3,4)ENEUT
0073      WRITE(3,5)
0074      WRITE(3,6)(EN(I),I=1,NCP)
0075      WRITE(3,7)
0076      WRITE(3,6)(Y(I),I=1,NDP)
0077      WRITE(3,8)
0078      WRITE(3,6)(VAR(I),I=1,NDP)
0079      WRITE(3,9)EQ,SDVEQ
0080      WRITE(3,10)YC,SDVYC
0081      WRITE(3,556)YNORM
0082      WRITE(3,557)BO
0083      100 WRITE(3,11)FWHM,SDVFW
0084      STOP
0085      END

```

FORTRAN IV G LEVEL 18

MATINV

DATE = 71109

22/12/23

```

0001      SUBROUTINE MATINV (A,N,B,M,DETERM,NMAX)
      C
      C      MATRIX INVERSION WITH ACCOMPANYING SOLUTION OF LINEAR EQUATIONS
      C      A INPUT-COEFFICIENT MATRIX
      C      RETURN-INVERSE MATRIX
      C      N NUMBER OF EQUATIONS
      C      B INPUT-RIGHT HAND SIDE VECTOR(S)
      C      RETURN-SOLUTION VECTOR(S)
      C      M NUMBER OF RIGHT HAND SIDE VECTOR(S)
      C      DETERM RETURN-DETERMINATE OF A
      C      NMAX MAXIMUM NUMBER OF EQUATIONS AS DIMENSIONED IN MAIN PROGRAM
      C
      C**** REMOVE NEXT STATEMENT IN SINGLE PRECISION VERSION
0002      IMPLICIT REAL*8 (A-H,O-Z)
0003      REAL*4 PIVOT
0004      DOUBLE PRECISION DABS
0005      DIMENSION A(NMAX,NMAX),B(NMAX,1)
0006      COMMON /F402/ PIVOT(100), INDEX(100)
      C
      C      INITIALIZE DETERMINANT AND PIVOT ELEMENT ARRAY
      C
0007      DETERM=1.0
0008      DO 20 I=1,N
0009      PIVOT(I)=0.0
0010      20 CONTINUE
      C
      C      PERFORM SUCCESSIVE PIVOT OPERATIONS (GRAND LOOP)
      C
0011      DO 550 I=1,N
      C
      C      SEARCH FOR PIVOT ELEMENT AND EXTEND DETERMINANT PARTIAL PRODUCT
      C
0012      AMAX=0.0
0013      DO 105 J=1,N
0014      IF (PIVOT(J).NE.0.0) GO TO 105
0015      DO 100 K=1,N
0016      IF (PIVOT(K).NE.0.0) GO TO 100
0017      TEMP=DABS(A(J,K))
0018      IF (TEMP.LT.AMAX) GO TO 100
0019      IROW=J
0020      ICOLUM=K
0021      AMAX=TEMP
0022      100 CONTINUE
0023      105 CONTINUE
0024      INDEX(I)=4096*IROW+ICOLUM
0025      J=IROW
0026      AMAX=A(J,ICOLUM)
0027      DETERM=AMAX*DETERM
      C
      C      RETURN IF MATRIX IS SINGULAR (ZERO PIVOT) AFTER COLUMN INTERCHANGE
      C
0028      IF (DETERM.EQ.0.0) GO TO 600
      C
0029      PIVOT(ICOLUM)=AMAX
      C
      C      INTERCHANGE ROWS TO PUT PIVOT ELEMENT ON DIAGONAL
      C
0030      IF (IROW.EQ.ICOLUM) GO TO 260

```

FORTRAN IV G LEVEL 18

MATINV

DATE = 71109

22/12/23

```

0031      DETERM=-DETERM
0032      DO 200 K=1,N
0033      SWAP=A(J,K)
0034      A(J,K)=A(ICOLUM,K)
0035      A(ICOLUM,K)=SWAP
0036      200 CONTINUE
0037      IF (M.LE.0) GO TO 260
0038      DO 250 K=1,M
0039      SWAP=B(J,K)
0040      B(J,K)=B(ICOLUM,K)
0041      B(ICOLUM,K)=SWAP
0042      250 CONTINUE
C
C      DIVIDE PIVOT ROW BY PIVOT ELEMENT
C
0043      260 K=ICOLUM
0044      A(ICOLUM,K)=1.0
0045      DO 350 K=1,N
0046      A(ICOLUM,K)=A(ICOLUM,K)/AMAX
0047      350 CONTINUE
0048      IF (M.LE.0) GO TO 380
0049      DO 370 K=1,M
0050      B(ICOLUM,K)=B(ICOLUM,K)/AMAX
0051      370 CONTINUE
C
C      REDUCE NON-PIVOT ROWS
C
0052      380 DO 550 J=1,N
0053      IF (J.EQ.ICOLUM) GO TO 550
0054      T=A(J,ICOLUM)
0055      A(J,ICOLUM)=0.0
0056      DO 450 K=1,N
0057      A(J,K)=A(J,K)-A(ICOLUM,K)*T
0058      450 CONTINUE
0059      IF (M.LE.0) GO TO 550
0060      DO 500 K=1,M
0061      B(J,K)=B(J,K)-B(ICOLUM,K)*T
0062      500 CONTINUE
0063      550 CONTINUE
C
C      INTERCHANGE COLUMNS AFTER ALL PIVOT OPERATIONS HAVE BEEN PERFORMED
C
0064      600 DO 710 I=1,N
0065      I1=N+1-I
0066      K=INDEX(I1)/4096
0067      ICOLUM=INDEX(I1)-4096*K
0068      IF (K.EQ.ICOLUM) GO TO 710
0069      DO 705 J=1,N
0070      SWAP=A(J,K)
0071      A(J,K)=A(J,ICOLUM)
0072      A(J,ICOLUM)=SWAP
0073      705 CONTINUE
0074      710 CONTINUE
C
0075      RETURN
0076      END

```


Sample Input Data - NE213RES

1							
.90	9						
0.7	0.8	0.9	1.0	1.1	1.2	1.3	1.4
1.5							
016	8015	12454	10040	5530	2057	578	124
22							
208	6290	12742	11190	5682	2096	607	140
25							

POLYFIT

This program fits a given resolution function to a polynomial of degree m by a weighted least squares procedure. The program was written to perform the calculations derived in Appendix B on polynomial fitting. Input to the program includes the upper and lower bounds on the resolution data to be fitted. Output includes the variance of the m th order polynomial fit, the coefficients of the fit, and a comparison between the input values and the values calculated by the polynomial. Again, the matrix inversion required by the calculation is done by the subroutine MATINV.

INPUT

Card	Format		
1	I3	1) N	= number of data points to be fit
2 (Deck)	3F10.4	1) E(I)	= Energy of the i th data point (MeV)
		2) SPCT(I)	= The FWHM at energy i (MeV)
		3) SDEV(I)	= The standard deviation of the FWHM at energy i
3	I10	1) NA	= Number of fits to be attempted
4	I10	1) M	= Order of the approximation for the first fit
5	I10	1) M	= Order of the approximation for the second fit
.	.	.	
.	.	.	
.	.	.	
.	.	1) M	= Order of the approximation for the NA fit

POLYFIT Listing

FORTRAN IV G LEVEL 18

MAIN

DATE = 71109

22/07/41

```

C**** THIS PROGRAM FITS A GIVEN RESOLUTION FUNCTION TO A POLYNOMIAL OF
C**** DEGREE M BY A WEIGHTED LEAST SQUARES PROCEDURE.
0001      IMPLICIT REAL*8 (A-H,O-Z)
0002      DIMENSION E(100),PLO(100),PUP(100),SPCT(100),VAR(100),SDEV(100),
          1CSPECT(100),A(15,15),B(15,1),C(15),SDEVC(15)
0003      1 FORMAT(11I3)
0004      2 FORMAT(13)
0005      3 FORMAT(3F10.4)
0006      4 FORMAT(172HORDER OF APPROXIMATION TOO LARGE FOR THE NUMBER OF DATA
          1POINTS AVAILABLE)
0007      5 FORMAT(6X,23HORDER OF APPROXIMATION=,13)
0008      6 FORMAT(11X,6HEENERGY,6X,14HINPUT FWHM      ,4X,7HSTD DEV,6X,
          114HCALC. FWHM      /)
0009      7 FORMAT(6X,4D17.6)
0010      8 FORMAT(176X,2BHRESULTS OF LEAST SQUARES FIT//)
0011      9 FORMAT(6X,11HCoefficient,15X,5HVALUE,9X,7HSTD DEV/)
0012     10 FORMAT(11X,11C,I2,12X,2D17.9//)
0013     14 FORMAT(176X,2HVARIANCE OF THE FIT=,D15.6//)
0014     15 FORMAT(4F10.4)

C
C**** N=NUMBER OF DATA POINTS
C**** NA=NUMBER OF APPROXIMATIONS USED
C**** M=ORDER OF APPROXIMATION
C**** PLO,PUP=LOWER AND UPPER BOUNDS OF THE SPECTRUM
C**** E=ENERGY
C
0015      READ 2,N
0016      DO 100 I=1,N
0017      READ 3,E(I),SPCT(I),SDEV(I)
0018     100 VAR(I)=(SDEV(I))**2.
0019      READ 1,NA
0020      DO 101 K=1,NA
0021      READ 1,M
0022      IF(N.LT.(M+1))GO TO 102
0023      M1=M+1
0024      DO 103 I=1,M1
0025      B(I,1)=0.
0026      DO 103 J=1,M1
0027     103 A(I,J)=0.
0028      DO 104 J=1,M1
0029      I=1
0030      NP=1-1+J-1
0031      DO 104 L=1,N
0032     104 A(I,J)=A(I,J)+(E(L)**NP)/VAR(L)
0033      DO 105 I=2,M1
0034      J=M+1
0035      NP=1-1+J-1
0036      DO 105 L=1,N
0037     105 A(I,J)=A(I,J)+(E(L)**NP)/VAR(L)
0038      DO 106 I=1,M1
0039      DO 106 L=1,N
0040     106 B(I,1)=B(I,1)+SPCT(L)*(E(L))**(1-1)/VAR(L)
0041      DO 107 I=2,M1
0042      DO 107 J=2,M1
0043     107 A(I,J-1)=A(I-1,J)
0044      CALL MATINV(A,M1      ,B,1,DETERM,15)
0045      DO 108 I=1,M1
0046      C(I)=B(I,1)

```

FORTRAN IV G LEVEL 18

MAIN

DATE = 71109

22/07/41

```

0047      108 SDEV(I)=DSQR(A(I,I))
0048      DO 109 J=1,N
0049      109 CSPCT(J)=0.
0050      DO 110 J=1,N
0051      DO 110 I=1,M1
0052      110 CSPCT(J)=CSPCT(J)+C(I)*(E(J)**(I-1))
0053      DEV=0.
0054      DO 111 I=1,N
0055      111 DELV=DEV+((CSPCT(I)-SPCT(I))**2)/(0.5*FLUAT(N-M-1))
0056      PRINT 5,M
0057      PRINT 8
0058      PRINT 9
0059      DO 113 I=1,M1
0060      113 PRINT 10,I,C(I),SDEV(I)
0061      PRINT 6
0062      DO 112 I=1,N
0063      112 PRINT 7,E(I),SPCT(I),SDEV(I),CSPCT(I)
0064      PRINT 14,DEV
0065      GO TO 101
0066      102 PRINT 4
0067      101 CONTINUE
0068      STOP
0069      END

```

FORTRAN IV G LEVEL 18

MATINV

DATE = 71109

22/07/41

```

0001      SUBROUTINE MATINV (A,N,B,M,DETERM,NMAX)
      C
      C      MATRIX INVERSION WITH ACCOMPANYING SOLUTION OF LINEAR EQUATIONS
      C      A   INPUT-COEFFICIENT MATRIX
      C      RETURN-INVERSE MATRIX
      C      N   NUMBER OF EQUATIONS
      C      B   INPUT-RIGHT HAND SIDE VECTOR(S)
      C      RETURN-SOLUTION VECTOR(S)
      C      M   NUMBER OF RIGHT HAND SIDE VECTOR(S)
      C      DETERM RETURN-DETERMINATE OF A
      C      NMAX MAXIMUM NUMBER OF EQUATIONS AS DIMENSIONED IN MAIN PROGRAM
      C
      C**** REMOVE NEXT STATEMENT IN SINGLE PRECISION VERSION
0002      IMPLICIT REAL*8 (A-H,O-Z)
0003      REAL*4 PIVOT
0004      DIMENSION A(NMAX,NMAX),B(NMAX,1)
0005      COMMON /F402/ PIVOT(100), INDEX(100)
      C
      C      INITIALIZE DETERMINANT AND PIVOT ELEMENT ARRAY
      C
0006      DETERM=1.0
0007      DO 20 I=1,N
0008      PIVOT(I)=0.0
0009      20 CONTINUE
      C
      C      PERFORM SUCCESSIVE PIVCT OPERATIONS (GRAND LOOP)
      C
0010      DO 550 I=1,N
      C
      C      SEARCH FOR PIVOT ELEMENT AND EXTEND DETERMINANT PARTIAL PRODUCT
      C
0011      AMAX=0.0
0012      DO 105 J=1,N
0013      IF (PIVOT(J).NE.0.0) GO TO 135
0014      DO 100 K=1,N
0015      IF (PIVOT(K).NE.0.0) GO TO 100
0016      TEMP=DABS(A(J,K))
0017      IF (TEMP.LT.AMAX) GO TO 100
0018      IROW=J
0019      ICOLUM=K
0020      AMAX=TEMP
0021      100 CONTINUE
0022      105 CONTINUE
0023      INDEX(I)=4096*IROW+ICOLUM
0024      J=IROW
0025      AMAX=A(J,ICOLUM)
0026      DETERM=AMAX*DETERM
      C
      C      RETURN IF MATRIX IS SINGULAR (ZERO PIVOT) AFTER COLUMN INTERCHANGE
      C
0027      IF (DETERM.EQ.0.0) GO TO 550
      C
0028      PIVOT(ICOLUM)=AMAX
      C
      C      INTERCHANGE ROWS TO PUT PIVOT ELEMENT ON DIAGONAL
      C
0029      IF (IROW.EQ.ICOLUM) GO TO 260
0030      DETERM=-DETERM

```

```

FORTRAN IV C LEVEL 18          MATINV          DATE = 71109          22/07/41

0031      DO 200 K=1,N
0032      SWAP=A(J,K)
0033      A(J,K)=A(ICOLUMN,K)
0034      A(ICOLUMN,K)=SWAP
0035      200 CONTINUE
0036      IF (M.LE.0) GO TO 260
0037      DO 250 K=1,M
0038      SWAP=B(J,K)
0039      B(J,K)=B(ICOLUMN,K)
0040      B(ICOLUMN,K)=SWAP
0041      250 CONTINUE
C
C      DIVIDE PIVOT ROW BY PIVOT ELEMENT
C
0042      260 K=ICOLUMN
0043      A(ICOLUMN,K)=1.0
0044      DO 350 K=1,N
0045      A(ICOLUMN,K)=A(ICOLUMN,K)/AMAX
0046      350 CONTINUE
0047      IF (M.LE.0) GO TO 380
0048      DO 370 K=1,M
0049      B(ICOLUMN,K)=B(ICOLUMN,K)/AMAX
0050      370 CONTINUE
C
C      REDUCE NON-PIVOT ROWS
C
0051      380 DO 550 J=1,N
0052      IF (J.EQ.ICOLUMN) GO TO 550
0053      T=A( J,ICOLUMN)
0054      A( J,ICOLUMN)=0.0
0055      DO 450 K=1,N
0056      A( J,K)=A( J,K)-A(ICOLUMN,K)*T
0057      450 CONTINUE
0058      IF (M.LE.0) GO TO 550
0059      DO 500 K=1,M
0060      B( J,K)=B( J,K)-B(ICOLUMN,K)*T
0061      500 CONTINUE
0062      550 CONTINUE
C
C      INTERCHANGE COLUMNS AFTER ALL PIVOT OPERATIONS HAVE BEEN PERFORMED
C
0063      600 DO 710 I=1,N
0064      I1=N+1-I
0065      K=INDEX(I1)/4096
0066      ICOLUM=INDEX(I1)-4096*K
0067      IF (K.EQ.ICOLUMN) GO TO 710
0068      DO 705 J=1,N
0069      SWAP=A(J,K)
0070      A(J,K)=A(J,ICOLUMN)
0071      A(J,ICOLUMN)=SWAP
0072      705 CONTINUE
0073      710 CONTINUE
C
0074      RETURN
0075      END

```

Sample Input Data - POLYFIT

21

1.0	0.462	.025
1.2	0.427	.019
1.5	0.529	.012
1.6	0.490	.022
1.7	0.487	.022
1.8	0.541	.018
2.0	0.527	.022
2.1	0.577	.015
2.4	0.560	.017
2.7	0.521	.029
3.0	0.673	.009
3.2	0.622	.021
3.6	0.648	.009
3.9	0.678	.010
4.2	1.010	.014
4.6	0.896	.010
4.9	0.886	.007
6.0	1.119	.014
7.0	1.329	.006
8.0	1.316	.008
9.0	1.000	.009

5

6

7

8

9

10

APPENDIX B

DERIVATIONS

TRANSMITTED FLUX INTEGRAL

GAUSSIAN RESOLUTION FITTING

POLYNOMIAL FITTING

APPENDIX B

DERIVATIONS

TRANSMITTED FLUX INTEGRAL

$$\phi_{\text{trans}}(E) = \int_0^\infty \phi_I(E') e^{-\Sigma(E')t} R(E, E') dE' \quad (1)$$

$$\text{where } R(E, E') = y_0(E) \exp\left(\frac{-(E' - E)^2}{b_0(E)}\right) \quad (2)$$

$$\therefore \phi_{\text{trans}}(E) = \int_0^\infty \phi_I(E') \exp(-\Sigma(E')t) y_0(E) \exp\left(\frac{(E' - E)^2}{b_0(E)}\right) dE' \quad (3)$$

Assume $\log[\phi_I(E')]$ is linear between discrete energy points; between E_i and E_{i+1} :

$$\phi_I(E') = \phi_I^i + \exp\left(\left(\frac{\ln\phi_I^{i+1} - \ln\phi_I^i}{E_{i+1} - E_i}\right)(E' - E_i)\right)$$

where ϕ_I^i = incident flux at E_i

$$\text{now let } P_i = \left(\frac{\ln\phi_I^{i+1} - \ln\phi_I^i}{E_{i+1} - E_i}\right)$$

$$\begin{aligned} \therefore \phi_I(E') &= \phi_I^i + \exp[(P_i)(E' - E_i)] \\ &= \phi_I^i + \exp(P_i E') \exp(-P_i E_i) \end{aligned} \quad (4)$$

Assume $\Sigma(E')$ is linear between discrete energy points; between E_i and E_{i+1} :

$$\Sigma(E')t = \Sigma_i t + \left(\frac{\Sigma_{i+1} - \Sigma_i}{E_{i+1} - E_i}\right)(E' - E_i)t$$

where Σ_i = cross-section at E_i

$$\text{now let } X_i = \left(\frac{\Sigma_{i+1} - \Sigma_i}{E_{i+1} - E_i}\right)t$$

$$\text{and } S_i = \Sigma_i t$$

$$\therefore \Sigma(E')t = S_i - X_i(E' - E_i)$$

$$\therefore \exp[-\Sigma(E')t] = \exp(-S_i + X_i E_i) \exp(-X_i E') \quad (5)$$

$$\text{Also, } \exp\left[-\frac{(E' - E)^2}{b_o}\right] = \exp\left[-\frac{E^2}{b_o}\right] \exp\left[-\frac{E'^2}{b_o} + \frac{2E'E}{b_o}\right] \quad (6)$$

$$y_o = \frac{1}{\sqrt{b_o \pi}} = \text{normalization factor for gaussian} \quad (7)$$

Now, if there exists a ϕ_I^i and Σ_i for each E_i , the integral of equation (3) can be integrated piecewise:

$$\begin{aligned} \phi_{\text{trans}}(E) = & \int_0^{E_1} [] dE' + \int_{E_1}^{E_2} [] dE' + \dots + \int_{E_i}^{E_{i+1}} [] dE' \\ & + \dots + \int_{E_n}^{\infty} [] dE' \end{aligned} \quad (8)$$

$$\text{or } \phi_{\text{trans}}(E) = \sum_{i=0}^{\infty} \int_{E_i}^{E_{i+1}} [] dE' \quad (9)$$

$$\text{where } [] = \phi_I(E') \exp[-\Sigma(E')t] y_o(E) \exp\left[-\frac{(E' - E)^2}{b_o(E)}\right] \quad (10)$$

Now, substituting equation (4), (5), (6), and (7) into (10), each term of equation (9) will be:

$$\begin{aligned} & \int_{E_i}^{E_{i+1}} \left\{ \phi_I^i + \exp(P_i E') \exp(-P_i E_i) \right\} \left\{ \exp(-S_i + X_i E_i) \exp(-X_i E') \right\} \left\{ \frac{1}{b_o \pi} \right\} \\ & \left\{ \exp\left(-\frac{E^2}{b_o}\right) \exp\left(-\frac{E'^2}{b_o} + \frac{2E'E}{b_o}\right) \right\} dE' \\ & = \frac{1}{\sqrt{b_o \pi}} \exp(-S_i + X_i E_i - \frac{E^2}{b_o}) \int_{E_i}^{E_{i+1}} \left\{ \phi_I^i + \exp(P_i E') \exp(-P_i E_i) \right\} \\ & \left\{ \exp\left(-\frac{E'^2}{b_o} + \frac{2E'E}{b_o} - X_i E'\right) \right\} dE' \end{aligned} \quad (11)$$

$$\text{let } C_i = \frac{1}{\sqrt{b_o \pi}} \exp(-S_i + X_i E_i - \frac{E^2}{b_o}) \quad (12)$$

$$= C_i \phi_i \int_{E_i}^{E_{i+1}} \exp(-\frac{E'^2}{b_o} + \frac{2E'E}{b_o} - X_i E') dE' \\ + C_i \exp(-P_i E_i) \int_{E_i}^{E_{i+1}} \exp(-\frac{E'^2}{b_o} + \frac{2EE'}{b_o} - X_i E' + P_i E') dE' \quad (13)$$

These two integrals are of the form:

$$\int_{x_1}^{x_2} e^{-(ax^2 + 2bx + c)} dx = \frac{1}{\sqrt{a}} \left(\frac{b^2 - ac}{a} \right) \int_{y_1}^{y_2} e^{-y^2} dy \quad (14)$$

$$\text{where } y = \sqrt{a} \left(x + \frac{b}{a} \right)$$

$$\text{Note } \int_{y_1}^{y_2} e^{-y^2} dy = \frac{\sqrt{\pi}}{2} [\text{erf}(y_2) - \text{erf}(y_1)]$$

$$\text{For first integral } a = \frac{1}{b_o}, b = \left(\frac{X_i}{2} - \frac{E}{b_o} \right), c = 0, y_i = \frac{1}{\sqrt{b_o}} \left(E_i - E + \frac{X_i b_o}{2} \right)$$

Now, substituting these constants into (14), and combining (13) and (14)

$$\therefore \text{ first integral} = \frac{\phi_i}{2} \exp \left(\frac{X_i^2 b_o}{4} + X_i (E_i - E) - S_i \right) [\text{erf}(y_{i+1}) - \text{erf}(y_i)] \quad (15)$$

For second integral

$$a = \frac{1}{b_o}, b = \frac{X_i}{2} - \frac{E}{b_o} - \frac{P_i}{2}, c=0, z_i = \frac{1}{\sqrt{b_o}} \left(E_i - E + \frac{X_i b_o}{2} - \frac{P_i b_o}{2} \right)$$

Substituting these constants into (14) and combining (13) and (14)

second integral =

$$\frac{1}{2} \exp \left(\frac{X_i^2}{4} b_o + X_i (E_i - E) + P_i (E - E_i) - \frac{X_i P_i b_o}{2} - \frac{P_i^2}{4} b_o - S_i \right)$$

Adding (15) and (16), equation (11) is now equal to:

$$\begin{aligned} & \left[\frac{1}{2} \exp \left(\frac{X_i^2}{4} b_o + X_i (E_i - E) - S_i \right) \right] \left[\phi_I^i (\operatorname{erf}(y_{i+1}) - \operatorname{erf}(y_i)) \right. \\ & \left. + \exp \left[P_i (E - E_i) - \frac{X_i P_i b_o}{2} - \frac{P_i^2}{4} b_o \right] (\operatorname{erf}(Z_{i+1}) - \operatorname{erf}(Z_i)) \right] \quad (17) \end{aligned}$$

$$\therefore \phi_{\text{trans}}(E) =$$

$$\begin{aligned} & \sum_{i=1}^{\infty} \left\{ \left[\frac{1}{2} \exp \left(\frac{X_i^2}{4} b_o + X_i (E_i - E) - S_i \right) \right] \left[\phi_I^i (\operatorname{erf}(y_{i+1}) - \operatorname{erf}(y_i)) \right. \right. \\ & \left. \left. + \exp \left(P_i (E - E_i) - \frac{X_i P_i b_o}{2} - \frac{P_i^2}{4} b_o \right) (\operatorname{erf}(Z_{i+1}) - \operatorname{erf}(Z_i)) \right] \right\} \quad (18) \end{aligned}$$

where ϕ_I^i = incident flux at E_i

Σ_i = cross-section at E_i

$S_i = \Sigma_i t$

$X_i = (\Sigma_{i+1} - \Sigma_i) / (E_{i+1} - E_i)$

$P_i = (\ln \phi_I^{i+1} - \ln \phi_I^i) / (E_{i+1} - E_i)$

$y_i = \frac{1}{\sqrt{b_o}} (E_i - E + \frac{X_i b_o}{2})$

$Z_i = \frac{1}{\sqrt{b_o}} (E_i - E + \frac{X_i b_o}{2} - \frac{P_i b_o}{2})$

b_o = function of the resolution = $\frac{(\text{FWHM})^2}{4 \cdot \ln 2}$

GAUSSIAN RESOLUTION FITTING

Using Weighted Least Squares

Gaussian:

$$y_i = y_o e^{\frac{-(x_i - x_o)^2}{b_o}} \quad (1)$$

Definition: FWHM

$$\frac{1}{2} y_o = y_o \exp\left(\frac{-(x - x_o)^2}{b_o}\right)$$

$$\ln y_o = \ln 2 = \ln y_o - \frac{(x - x_o)^2}{b_o}$$

$$\ln 2 = \frac{(x - x_o)^2}{b_o}$$

$$(x - x_o)^2 = b_o \cdot \ln 2$$

$$x - x_o = (b_o \ln 2)^{\frac{1}{2}}$$

$$\text{Now,} \quad \text{FWHM} = 2(x - x_o) = 2(b_o \ln 2)^{\frac{1}{2}} \quad (2)$$

$$\text{also,} \quad b_o = \frac{(\text{FWHM})^2}{4 \ln 2} \quad (3)$$

Determine y_o so total area under Gaussian is equal to 1

$$1 = \int_0^{\infty} y_o \exp\left(\frac{-(x_i - x_o)^2}{b_o}\right) dx_i \approx y_o \int_{-\infty}^{\infty} \exp\left(\frac{-(x_i - x_o)^2}{b_o}\right) dx_i \quad (4)$$

since the gaussian curves are on the positive real axis, and at some distance from the origin.

$$\text{Let } z = x_i - x_o, \quad dx_i = dz$$

$$\therefore \approx y_o \int_{-\infty}^{\infty} e^{-z^2/b_o} dz = y_o \left\{ 2 \int_0^{\infty} e^{-z^2/b_o} dz \right\} \quad (5)$$

$$\int_0^{\infty} e^{-z^2/b_o} dz = \sqrt{b_o} \int_0^{\infty} e^{-z^2} dz = \sqrt{b_o} \frac{\pi}{2} [\operatorname{erf}(z)]_0^{\infty}$$

$$\therefore \int_0^{\infty} e^{-z^2/b_o} dz = \frac{\sqrt{b_o \pi}}{2} (1 - 0) = \frac{\sqrt{b_o \pi}}{2} \quad (6)$$

$$\therefore 1 = 2y_o \frac{\sqrt{b_o \pi}}{2}$$

or $y_o = \frac{1}{\sqrt{b_o \pi}} \quad \text{Normalized} \quad (7)$

Using Weighted Least Squares

Taking the $\ln(\quad)$ of equation 1.

$$\ln y_i = \ln y_o - \frac{(x_i - x_o)^2}{b_o} \quad (8)$$

$$\text{let } z_i = \ln y_i$$

$$\therefore \sigma_{z_i}^2 = \left(\frac{\delta z_i}{\delta y_i} \right)^2 \sigma_{y_i}^2 = \left(\frac{1}{y_i} \right)^2 \sigma_{y_i}^2 = \frac{\delta y_i^2}{y_i^2}$$

Thus, weight the function z_i by $\frac{1}{\sigma_{z_i}^2} = \frac{y_i^2}{\sigma_{y_i}^2}$

$$\therefore W = \begin{pmatrix} \frac{y_1^2}{\sigma_{y_1}^2} & 0 & 0 & \cdot \\ 0 & \frac{y_2^2}{\sigma_{y_2}^2} & \cdot & \cdot \\ 0 & 0 & \cdot & \frac{y_n^2}{\sigma_{y_n}^2} \end{pmatrix} \quad (9)$$

Now, using equation 8

$$\ln y_i = \ln y_o - \frac{x_i^2}{b_o} + \frac{2x_i x_o}{b_o} - \frac{x_o^2}{b_o} \quad (10)$$

Let $\ln y_o - \frac{x_o^2}{b_o} = s_3$ (11)

$$\frac{2x_o}{b_o} = s_2 \quad (12)$$

$$- \frac{1}{b_o} = s_1 \quad (13)$$

Thus

$$\begin{pmatrix} x_1^2 & x_1 & 1 \\ x_2^2 & x_2 & 1 \\ \vdots & \vdots & \vdots \\ x_n^2 & x_n & 1 \end{pmatrix} \begin{pmatrix} s_1 \\ s_2 \\ s_3 \end{pmatrix} = \begin{pmatrix} z_1 \\ z_2 \\ \vdots \\ z_n \end{pmatrix} \quad (14)$$

This is of the form: $A \cdot X = B$

For least square solution: $A^T A \cdot X = A^T B$

Now, applying weighting function:

$$W A^T A \cdot X = W A^T B \quad (15)$$

Since W is a diagonal matrix, equation 15 can be written as:

$$A^T W A X = A^T W B$$

or $X = (A^T W A)^{-1} A^T W B \quad (16)$

Defining the term of equation 16:

$$A^T = \begin{pmatrix} x_1^2 & x_2^2 & \dots & x_n^2 \\ x_1 & x_2 & \dots & x_n \\ 1 & 1 & \dots & 1 \end{pmatrix}$$

$$W A = \begin{pmatrix} \frac{x_1^2 y_1^2}{\sigma y_1^2} & \frac{x_1 y_1^2}{\sigma y_1^2} & \frac{y_1^2}{\sigma y_1^2} \\ \frac{x_2^2 y_2^2}{\sigma y_2^2} & \frac{x_2 y_2^2}{\sigma y_2^2} & \frac{y_2^2}{\sigma y_2^2} \\ \vdots & \vdots & \vdots \\ \frac{x_n^2 y_n^2}{\sigma y_n^2} & \frac{x_n y_n^2}{\sigma y_n^2} & \frac{y_n^2}{\sigma y_n^2} \end{pmatrix}$$

$$A^T W A = \begin{pmatrix} \sum_{i=1}^n \frac{x_i^4 y_i^2}{\sigma y_i^2} & \sum_{i=1}^n \frac{x_i^3 y_i^2}{\sigma y_i^2} & \sum_{i=1}^n \frac{x_i^2 y_i^2}{\sigma y_i^2} \\ \sum_{i=1}^n \frac{x_i^3 y_i^2}{\sigma y_i^2} & \sum_{i=1}^n \frac{x_i^2 y_i^2}{\sigma y_i^2} & \sum_{i=1}^n \frac{x_i y_i^2}{\sigma y_i^2} \\ \sum_{i=1}^n \frac{x_i^2 y_i^2}{\sigma y_i^2} & \sum_{i=1}^n \frac{x_i y_i^2}{\sigma y_i^2} & \sum_{i=1}^n \frac{y_i^2}{\sigma y_i^2} \end{pmatrix}$$

$$W B = \begin{pmatrix} \frac{y_1^2}{\sigma y_1^2} z_1 \\ \frac{y_2^2}{\sigma y_2^2} z_2 \\ \vdots \\ \frac{y_n^2}{\sigma y_n^2} z_n \end{pmatrix} \quad A^T W B = \begin{pmatrix} \sum_{i=1}^n \frac{x_i^2 y_i^2}{\sigma y_i^2} z_i \\ \sum_{i=1}^n \frac{x_i y_i^2}{\sigma y_i^2} z_i \\ \sum_{i=1}^n \frac{y_i^2}{\sigma y_i^2} z_i \end{pmatrix}$$

Substituting these quantities into equation 16, get solution of the form:

$$X = \begin{pmatrix} S_1 \\ S_2 \\ S_3 \end{pmatrix}$$

where S_1 , S_2 and S_3 are given by equations 11, 12, and 13.

Also

$$\sigma_{S_1}^2 = (A^T W A)^{-1}_{11}$$

$$\sigma_{S_2}^2 = (A^T W A)^{-1}_{22}$$

$$\sigma_{S_3}^2 = (A^T W A)^{-1}_{33}$$

Therefore:

$$b_o = -\frac{1}{S_1}$$

$$\text{and } \sigma_{b_o}^2 = \left(\frac{\partial b_o}{\partial S_1} \right)^2 \sigma_{S_1}^2 = \frac{1}{S_1^2} \sigma_{S_1}^2$$

$$x_o = \frac{b_o S_2}{2}$$

$$\text{and } \sigma_{x_o}^2 = \left(\frac{\partial x_o}{\partial b_o} \right)^2 \sigma_{b_o}^2 + \left(\frac{\partial x_o}{\partial S_2} \right)^2 \sigma_{S_2}^2 = \frac{S_2^2}{4} \sigma_{b_o}^2 + \frac{b_o^2}{4} \sigma_{S_2}^2$$

$$\ln y_o = S_3 + \frac{x_o^2}{b_o}$$

$$\sigma_{y_o}^2 = \left(\frac{\partial y_o}{\partial S_3} \right)^2 \sigma_{S_3}^2 + \left(\frac{\partial y_o}{\partial x_o} \right)^2 \sigma_{x_o}^2 + \left(\frac{\partial y_o}{\partial b_o} \right)^2 \sigma_{b_o}^2$$

$$= \left(e^{S_3 + \frac{x_o^2}{b_o}} \right)^2 \sigma_{S_3}^2 + \left(\frac{2x_o}{b_o} e^{S_3 + \frac{x_o^2}{b_o}} \right)^2 \sigma_{x_o}^2 + \left(-\frac{x_o^2}{b_o^2} e^{S_3 + \frac{x_o^2}{b_o}} \right)^2 \sigma_{b_o}^2$$

Note, exponentials may get large, causing overflows on the computer

Therefore, let $z = \ln y_o = S_3 + \frac{x_o^2}{b_o}$

$$\begin{aligned}
\sigma_3^2 &= \left(\frac{1}{y_o}\right) \sigma_{y_o}^2 = \left(\frac{\partial z}{\partial S_3}\right) \sigma_{S_3}^2 + \left(\frac{\partial z}{\partial x_o}\right)^2 \sigma_{x_o}^2 + \left(\frac{\partial z}{\partial b_o}\right)^2 \sigma_{b_o}^2 \\
&= \sigma_{S_3}^2 + \left(\frac{2x_o}{b_o}\right)^2 \sigma_{x_o}^2 + \left(-\frac{x_o^2}{b_o}\right)^2 \sigma_{b_o}^2 \\
\therefore \sigma_{y_o}^2 &= y_o^2 \left(\sigma_{S_3}^2 + \frac{4x_o^2}{b_o^2} \sigma_{x_o}^2 + \frac{x_o^4}{b_o^4} \sigma_{b_o}^2 \right)
\end{aligned}$$

POLYNOMIAL FITTING

Using Weighted Least Squares

The method used for this problem is the same as that used for the gaussian fitting problem. In this case, data is fit to a polynomial of degrees m :

$$y_i = a_0 + a_1 x_i + a_2 x_i^2 + a_3 x_i^3 + \dots + a_m x_i^m \quad (1)$$

For this function, the weighting function W is the variance of y_i , that is:

$$W = \begin{pmatrix} \frac{1}{\sigma_{y_1}^2} & \cdot & \cdot & 0 \\ \cdot & \frac{1}{\sigma_{y_2}^2} & \cdot & \cdot \\ 0 & \cdot & \frac{1}{\sigma_{y_n}^2} & \cdot \end{pmatrix} \quad (2)$$

Rewriting equation 1:

$$\begin{pmatrix} 1 & x_1 & x_1^2 & \dots & x_1^m \\ 1 & x_2 & x_2^2 & \dots & x_2^m \\ \cdot & \cdot & \cdot & \dots & \cdot \\ 1 & x_n & x_n^2 & \dots & x_n^m \end{pmatrix} \begin{pmatrix} a_0 \\ a_1 \\ a_2 \\ \cdot \\ a_m \end{pmatrix} = \begin{pmatrix} y_1 \\ y_2 \\ y_3 \\ \cdot \\ y_n \end{pmatrix} \quad (3)$$

This is of the form $A \cdot X = B$

If $n > m$, which is normally the case, the set of equations in equation 3 is over determined, and the least squares solution is:

$$A^T A X = A^T B$$

Now, applying the weighting function W and rearranging as before:

$$X = (A^T W A)^{-1} A^T W B \quad (4)$$

This is the same equation as used in the gaussian fitting problem, where A and B are defined by equation 3, and

$$A^T = \begin{pmatrix} 1 & 1 & \cdots & 1 \\ x_1 & x_2 & \cdots & x_n \\ x_1^2 & x_2^2 & \cdots & x_n^2 \\ \cdot & \cdot & \cdots & \cdot \\ x_1^m & x_2^m & \cdots & x_n^m \end{pmatrix}$$

$$WA = \begin{pmatrix} \frac{1}{\sigma_{y_1}^2} & \frac{x_1}{\sigma_{y_1}^2} & \cdots & \frac{x_1^m}{\sigma_{y_1}^2} \\ \frac{1}{\sigma_{y_2}^2} & \frac{x_2}{\sigma_{y_2}^2} & \cdots & \frac{x_2^m}{\sigma_{y_2}^2} \\ \cdot & \cdot & \cdots & \cdot \\ \frac{1}{\sigma_{y_n}^2} & \frac{x_n}{\sigma_{y_n}^2} & \cdots & \frac{x_n^m}{\sigma_{y_n}^2} \end{pmatrix}$$

$$A^T WA = \begin{pmatrix} \sum_{i=1}^n \frac{1}{\sigma_{y_i}^2} & \sum_{i=1}^n \frac{x_i}{\sigma_{y_i}^2} & \cdots & \sum_{i=1}^n \frac{x_i^m}{\sigma_{y_i}^2} \\ \sum_{i=1}^n \frac{x_i}{\sigma_{y_i}^2} & \sum_{i=1}^n \frac{x_i^2}{\sigma_{y_i}^2} & \cdots & \sum_{i=1}^n \frac{x_i^{m+1}}{\sigma_{y_i}^2} \\ \cdot & \cdot & \cdots & \cdot \\ \sum_{i=1}^n \frac{x_i^m}{\sigma_{y_i}^2} & \sum_{i=1}^n \frac{x_i^{m+1}}{\sigma_{y_i}^2} & \cdots & \sum_{i=1}^n \frac{x_i^{m+m}}{\sigma_{y_i}^2} \end{pmatrix}$$

$$WB = \begin{pmatrix} \frac{y_1}{\sigma_{y_1}^2} \\ \frac{y_2}{\sigma_{y_2}^2} \\ \vdots \\ \frac{y_n}{\sigma_{y_n}^2} \end{pmatrix} \quad A^T WB = \begin{pmatrix} \sum_{i=1}^n \frac{y_i}{\sigma_{y_i}^2} \\ \sum_{i=1}^n \frac{x_i y_i}{\sigma_{y_i}^2} \\ \vdots \\ \sum_{i=1}^n \frac{x_i^m y_i}{\sigma_{y_i}^2} \end{pmatrix}$$

Substituting these quantities into equation (4), the solution is of the term

$$X = \begin{pmatrix} a_0 \\ a_1 \\ a_2 \\ \vdots \\ a_m \end{pmatrix} \quad \text{where the } a_i \text{'s are the coefficients of the polynomial of degree } m.$$

APPENDIX C

SAMPLE CONTAINERS

OXYGEN SAMPLE CONTAINER DESIGN

LIQUID SODIUM SAMPLE CONTAINER DESIGN

APPENDIX C

SAMPLE CONTAINERS

OXYGEN SAMPLE CONTAINER DESIGN

A rectangular tank was the sample (liquid oxygen) vessel and had an inner box of 2" x 2" x 36", an outer box of 4" x 4" x 40", and the void in between was filled with Vermiculite insulating material. A double walled cylinder (1 1/2" I.D., 3 1/2" O.D., 8" high) acted as a vent at the top of the oxygen reservoir. The inner pipe extended 12" beyond the double walled cylinder for venting purposes. The entire insulating chamber was sealed to prevent exposure to the liquid oxygen.

Due to the flammable and sometimes explosive nature of materials in the presence of high concentrations of oxygen, several precautions were necessary. The sample tank was cleaned several times both inside and out during construction with trichlorethylene to remove any contamination, especially oil, and was checked using a black light. The insulating material, Vermiculite, is known for its inert properties, but a further check was made to determine if oxygen is absorbed to a great extent by the material. The Vermiculite was also "outgassed" at 600°F for several hours to remove contaminants. All equipment was grounded so that static electricity would not cause a spark. The venting tube on top of the sample tank had a "goose-neck" shape to prevent foreign material from falling into the oxygen reservoir. The venting tube was large enough to reduce the number of fillings necessary during an experiment. Evaporation of O_2 was estimated to be ≈ 500 liters/hr of gas (≈ 6 liters/hr liquid) which was dispersed into the volume of the reactor bay. This created a rise of .005%/hour in oxygen concentration in the bay. Total increase in oxygen concentration during a single experiment was less than .01% since the initial filling of the sample

was carried out outside the reactor bay; thus, the large evolution of gaseous oxygen associated with "cooling down" of the sample tank took place out of doors.

As a final precaution, before any large volumes of oxygen were introduced into the bay, a small sample (≈ 0.5 liter) of liquid oxygen in an aluminum dewar was placed in the neutron beam from the reactor to insure that no unforeseen reactions would take place.

LIQUID SODIUM SAMPLE CONTAINER DESIGN

Due to the high chemical reactivity of sodium, especially with water, several precautions were taken to insure that the sodium was kept under an inert atmosphere. To achieve this, a double walled stainless steel container of 1/16" stock was used. The inner container, 2" x 2" x 36" long, held the sodium and was heated with resistance heating wire. A funnel shaped reservoir provided an expansion chamber for the sodium as it was heated. The outer container was 4" x 6" x 40", with the void between the inner and outer chamber being filled with Vermiculite for insulation to a depth of 4". The top two inches of the void were filled with an inert gas (nitrogen) which was constantly passed over the sodium, and maintained at a pressure of approximately 2 psi gage. Directly over the sodium expansion chamber, the outer chamber had a removable section so that calcium carbonate could be added in case of fire at the sodium interface. Exposure of the sodium to the neutron beam resulted in a radiation hazard with the formation of ≈ 15 millicuries of Na^{24} , which resulted in a dose rate of ≈ 15 mr/hr. at 1 foot. Therefore, the sample had to be stored in a dry, shielded area until the Na^{24} decayed.

THE EVALUATION OF MINIMA IN TOTAL NEUTRON CROSS-SECTION
BY TRANSMISSION OF FISSION SPECTRA THROUGH THICK SAMPLES

by

WILLIAM HOWARD MILLER

B.S., Kansas State University, 1970

AN ABSTRACT OF A MASTER'S THESIS

submitted in partial fulfillment of the

requirements for the degree

MASTER OF SCIENCE

Department of Nuclear Engineering

KANSAS STATE UNIVERSITY
Manhattan, Kansas

1971

ABSTRACT

An evaluation of minima in total neutron cross-sections was performed for several materials by comparing an experimentally measured transmitted spectrum with the corresponding calculated result. Published cross-section data were evaluated for iron, lead, liquid oxygen, and solid and liquid sodium. Since thick samples (three or more mean free paths thick) were used, the analysis was very sensitive to minima in the cross-section.

The incident neutron spectrum was obtained from the Triga Mark II reactor and was detected using an NE-213 liquid scintillator spectrometer system. Computer codes were used to unfold the raw data and to calculate the transmitted spectrum (which was a function of published cross-section data, the measured incident flux on the sample and the resolution of the detector). The results of this study demonstrate the usefulness of this technique in evaluating total neutron cross-section.

Several experimental geometry conditions were used in this work to obtain valid results and to study the effects of forward scattering and multiple scattering in the thick samples. The results showed that there is a question as to the accuracy of published angular cross-section data near the zero scattering angle.